Design of Resilient Controllers for Buildings Energy Management

Jesse James Arthur Prince Agbodjan

DOCTORAT BRETAGNE LOIRE MATHSTIC

CentraleSupélec

THÈSE DE DOCTORAT DE

CENTRALESUPELEC

ÉCOLE DOCTORALE N° 601
Mathématiques et Sciences et Technologies de l'Information et de la Communication
Spécialité : *Automatique, Productique, Robotique*

Par

Jesse-James A. PRINCE AGBODJAN

Design of resilient controllers for Buildings Energy Management

Thèse présentée et soutenue à Rennes, le mardi 11 mai 2021
Unité de recherche : Institut d'Électronique et des Technologies du numÉrique (IETR)
Thèse N° : 2021CSUP0003

Rapporteurs avant soutenance :

Didier THEILLIOL	Professeur, Université de Lorraine
Ionela PRODAN	Maître de conférence, Grenoble INP

Composition du Jury :

Président :	Eric BIDEAUX	Professeur, INSA Lyon
Examinateurs :	Didier THEILLIOL	Professeur, Université de Lorraine
	Eric BIDEAUX	Professeur, INSA Lyon
	Hervé GUÉGUEN	Professeur, CentraleSupélec
	Ionela PRODAN	Maître de conférences, Grenoble INP
	Pierre HAESSIG	Maître de conférences, CentraleSupélec
	Romain BOURDAIS	Maître de conférences, CentraleSupélec
Dir. de thèse :	Hervé GUÉGUEN	Professeur, CentraleSupélec

Table of Contents

Acknowledgement **7**

Notation **10**

List of Acronyms **13**

List of Figures **17**

List of Tables **18**

1 Introduction **19**

1.1 Context 19

1.2 Motivation and contribution 21

1.3 Outline of the thesis 23

1.4 Publications 25

I Background **27**

2 Introduction to MPC in building control and reliability theory **29**

2.1 Model Predictive Control (MPC) 30

2.1.1 MPC Strategy 30

2.1.2 Traditional and Economic MPC 36

2.1.3 MPC in Buildings: main variants 37

2.2 Introduction to Reliability theory 39

2.2.1 Measures of reliability 40

2.2.2 Bathtub curve 43

2.2.3 The Bernoulli and Geometric distribution 44

2.3 Conclusion 46

3 Description of the solar home **47**
3.1 Introduction . . . 47
3.2 Model of the solar home . . . 48
3.2.1 Solar home's components . . . 48
3.2.2 Dataset of the solar home . . . 51
3.2.3 Sizing of components . . . 52
3.3 Rule based controller for HEMS in absence of outage . . . 58
3.4 Conclusion . . . 59

II Resilient HEMS **63**

4 Deterministic discrete Rare event **65**
4.1 Introduction . . . 65
4.2 Existing methods strategies . . . 66
4.3 Control goals . . . 70
4.4 Classic MPC . . . 70
4.4.1 Main objectives . . . 70
4.4.2 Auxiliary objective . . . 71
4.4.3 Global Objective . . . 71
4.5 The Resilient MPC . . . 74
4.5.1 Global objective . . . 75
4.6 Comparison metrics . . . 76
4.7 Simulation and results . . . 77
4.7.1 Simulation settings . . . 77
4.7.2 Simulation results . . . 79
4.8 Conclusion . . . 88

5 Stochastic discrete rare event **89**
5.1 Introduction . . . 90
5.2 Problem statement . . . 91
5.2.1 System description . . . 91
5.2.2 Problem formulation . . . 92
5.2.3 Decision structure . . . 93
5.3 State of the art of resolution methods . . . 95

5.3.1 Robust Optimization . . . 95
5.3.2 Stochastic programming . . . 96
5.4 Stochastic Discrete Constraint Model Predictive Controller (Stochastic Discrete Constraint Model Predictive Controller (SDCMPC)) . . . 102
5.4.1 Relaxed constrained . . . 102
5.4.2 Deterministic equivalent problem . . . 103
5.4.3 Important remarks . . . 105
5.5 Model of the grid behavior . . . 105
5.5.1 Markov Chain . . . 105
5.6 Application . . . 107
5.6.1 Optimization variables . . . 107
5.6.2 Simulation settings . . . 108
5.6.3 Extreme failure rate . . . 108
5.6.4 Varying the failure and repair rate . . . 114
5.6.5 Varying the failure, repair rate and c_1 . . . 117
5.6.6 SDCMPC vs. MSP wait and see . . . 117
5.7 Conclusion . . . 121

Conclusion **123**

III Appendices 127

Appendices **128**

A Résumé étendu en français **128**
A.1 Introduction . . . 128
A.2 Introduction du MPC et de la sûreté de fonctionnement . . . 129
A.2.1 Commande prédictive . . . 129
A.2.2 Commande prédictive dans le bâtiment . . . 132
A.2.3 Introduction à la sûreté de fonctionnement . . . 133
A.3 Description de la maison solaire . . . 136
A.3.1 Modèle du bâtiment solaire . . . 137
A.3.2 Dimensionnent des éléments . . . 139
A.4 Contrôleur énergétique résilient : Panne déterministe . . . 141
A.4.1 Objectifs de contrôle . . . 142

A.4.2 Contrôleur classique prédictif 142
A.4.3 Contrôleur résilient prédictif 143
A.4.4 Métriques de comparaison 144
A.4.5 Simulations et résultats 145
A.5 Contrôleur énergétique stochastique : Panne probabiliste 150
A.5.1 Énoncé du problème 150
A.5.2 Formulation du problème 151
A.5.3 Contrôleur prédictif à contraintes stochastiques discrètes 152
A.5.4 Modélisation de l'état du réseau électrique 155
A.5.5 Cas d'application 156
A.6 Conclusion 161

B Coding **162**

Bibliography **163**

ACKNOWLEDGEMENT

I am very grateful to God for without his grace, blessings, keeping me physically and mentally well, I would not be where I am today.

This thesis wouldn't have started and reached an end without my amazing three supervisors, professor Hervé GUÉGUEN, Romain BOURDAIS and Pierre HAESSIG. Thank you for providing me with guidance and support throughout the years. Most importantly, thank you for giving me the freedom I needed without putting pressure on me when I was sometimes behind schedule. Thank you, Hervé, to provide an excellent working environment and bring so many exciting and diverse people together. Thank you, Romain, for always been there to help me refocus on what is essential and deepened my understanding of the thesis's subject. Thank you also for all the music-related talks and especially for helping me learn a lot about guitars. Unfortunately, I have chosen to lean to play the piano during these three years. Still, I can assure you that the guitar knowledge will come in handy very soon. A special thank you to Pierre, whom I worked with the most. Thank you for the long hours of discussion about the thesis and all the other domains in which you have tremendous knowledge. I am very grateful for having been your first PhD student.

My works with three people have steered me toward the research domain and I would like to thank you all. First Veronique EGLIN and Stephane BRES my co-supervisors during my internship at LIRIS and Carolina ALBEA SÁNCHEZ my supervisors during my internship at LAAS.

What made my PhD journey really enjoyably and exciting was the fantastic group of inspiring people in the AUT team of CentraleSupelec IETR besides my supervisors. They are not only inspiring in a scientific sense but merely great people. My thanks go to Nabil and Stanislav for accepting to follow me as members of the "Comité de Suivi Individual " during these three years and for all their pieces of advice; to Marie-Anne for all the interesting talk. I also would like to thank the PhD students that I shared the office with, Amanda, Xiang, Rafael, and Zhigang for all the good moments we have spent together talking about our work and all other sorts of things. I consider these experiences

invaluable and unforgettable.

I want to thank all my family in France, especially my cousin's and my ant's. Stephane, I came here and since the day you have welcomed me at the airport, you have opened your house's door to me, and you have been both like an elder brother and father. A special thank you to your wife Joella, who now I consider as my elder sister from another mother. This says a lot about our relationship. You are a wonderful human being besides being an excellent cook. I also thank my lovely niece Shadé and Noah, that I have seen grown so much, for making my every day at the house very warm and pleasant.

I have come from Paris to Rennes, having no idea what these next three years would be like. Now that I have finished my PhD, I, fortunately, cannot claim that I am Britain. The weather still bothers me, but I would like to thank all the fantastic people I have met here that made my staying unforgettable. Mélania STRATULAT, you are one of those who make me feel like I am not human enough. Your benevolence is clearly something to be inspired by. Thank you for bearing with me because I know I am not the easiest person to be with; you have always been by my side, and I hope that the best is still yet to come for us. Bernyce MOUDOUMA, my first "cadre" friend, we had met when somehow I was feeling a bit down, but you lift me without even realizing it with your strength. Thank you for all the music you helped me discovered and for being such a good friend. Fanny, my vegan friend, thank you for fighting for what you believe in and not caring about whatever I say.

I am grateful for the privilege of having been the treasurer of the " Association des Docteur et Doctorant de l'IETR " and meeting many PhD students from all around the world, who showed me a different perspective on many questions.

I am eternally grateful to my family and friends in Benin and all over the world. In particular, I would like to thank my parents that sacrifice so much to send me to fulfil my study in France far away from them. I only can imagine how difficult it is for them. Calling them to hear their voice and see their faces always gave me faith, love, strength and determination. They have made all this possible, and without their support, I would not be here. My sister and brothers Ronica Orlanne, Ronic Aurel and John-William, I thank you for all your love, kindness, honesty and support. Thank you for giving me the hugest laughs ever every time we talk. You are the best I could ever ask for.

Last, but not least, I would like to thank all My best friends. Patrick TOGBÉ and Richard Da-COSTA, Thank you for being a source of inspiration and supporting me more

and more since we have known one another. Even if the distance and each of us focusing on accomplishing his dreams seems to have weakened or relationship in appearance, nothing could be far from the truth. Every time we get to talk, I am so grateful that it feels like nothing has changed between us, just like we have seen one another the previous day at Zogbohouè. Cadiatou Déborah SAVADOGO, a special thanks to you because we got significantly closer during these last three years. I cannot dare to say that it is due to my efforts. You are a sister, a confident, a support that I needed without realizing it. Thank you for always being there for me even during the period I was not the best imaginable friend you deserve. My youngest aunt Ludmilla Emelline MITO who thinks of herself as older than me to give me pieces of advice; I am in great debt to you. Mainly because you are the first person to have ever talked to me about "campus France". Thank you for encouraging me to apply (mostly because you knew you would miss me so much if you came here alone). My dear Hellade SEMANOU, I am so grateful for all the confidence you have put in me by making me your first son's godfather. Waliou ABOUDOU, I cannot thank you enough for the sleepless nights we had together, each of us working on his projects and all the pep talks. Juste S., Samson G. and all the others, you all have a special place in my heart.

NOTATION

Throughout the thesis, scalars and vectors are denoted with lower cases letters ($a, b, ..., \alpha, \beta, ...$), matrices are denoted with upper case letters ($A, B, ..., A, B$), and constraint and number sets are denoted with upper case blackboard bold letters ($\mathbb{X}, \mathbb{U}, ..., \mathbb{N}, \mathbb{R}$) for.

General operators and relations

$\mid$	such that
$\in$	is element of (belongs to)
$\forall$	for all
$\exists$	there exists

Sets, Spaces and Set Operators

$\{\cdot, \ldots\}$	set or sequence
$\setminus$	set difference
$\mathbb{R}$	set of real numbers
$\mathbb{R}_{0+}$	set of non-negative real numbers
$\mathbb{R}^n$	space of n-dimensional (column) vector with real entries
$\mathbb{R}^{n \times m}$	space of n by m matrices with real entries
$\mathbb{N}$	natural numbers (non negative integers)
$\mathbb{N}_j^k$	set of consecutive non-negative integers {j, . . . , k }
$\{n : j : m\}$	Set of element ranging from n to m with step j
card $\{E\}$	cardinal (number of elements) of the set E
$\times$	cartesiant product, $\mathbb{X} \times \mathbb{Y} = \{(x, y) \,\mid\, x \in \mathbb{X},\, y \in \mathbb{Y}\}$
$\subset$	strict subset

Probability Theory

Pr[·]	probability measure
E[·]	expectation with respect to probability measure Pr

Systems and Control Theory

n_x	number of states, $n_x \in \mathbb{N}_+$
n_u	number of inputs, $n_u \in \mathbb{N}_+$
x	state, $x \in \mathbb{R}^{n_x}$
u	Control inputs, $u \in \mathbb{R}^{n_u}$

List of Acronyms

BEMS	Building Energy Management System.
CC	Chance Constraints.
CDF	Cumulative Distribution Function.
CMPC	Classical Model Predictive Controller.
EMPC	Economic Model Predictive Control.
GPO	Grid Power Outage.
HEMS	Home Energy management System.
HVAC	Heating Ventilation and Air Conditioning.
LQG	Linear Quadratic Gaussian.
LQR	Linear Quadratic Regulator.
MC	Markov Chain.
MPC	Model Predictive Control.
MPPT	Maximum Power Point Tracking.
MSP	Multistage Stochastic Programming.
PEVs	Plug-in Electric Vehicles.
PGPO	Planned Grid Power Outage.
PHEV	Plug-in Hybrid Electric Vehicle.
PHEVs	Plug-in Hybrid Electric Vehicles.
PV	Photovoltaic.
r.v	random variable.
RBC-R	Rule Based Controller with Reserve.

RBPSC-R	Rule Based Power Save Controller with Reserve.
REE	Rare and Extreme Event.
ReMPC	Resilient MPC.
RMPC	Robust MPC.
RO	Robust Optimization.
SDCMPC	Stochastic Discrete Constraint Model Predictive Controller.
SMPC	Stochastic MPC.
UGPO	Unplanned Grid Power Outage.
V2H	Vehicle to Home.
Vs2Hs	Vehicles to Homes.

List of Figures

1.1 Florida grid power outages resulting from hurricanes Irma and wilma . . . 20
1.2 Illustration of a system theoretical resilience curves during a disruptive event . . . 20

2.1 MPC scheme for the control of a system . . . 31
2.2 Sliding or receding horizon principle . . . 32
2.3 Overview of the main equipment controlled in the single-zone approach . . . 38
2.4 Overview of the main equipment considered in each zone of the multi-zone controlled approach . . . 38
2.5 State variable and time to failure of a item . . . 40
2.6 Relation between $F(t)$, $R(t)$ and $f(t)$ for a normal distribution . . . 43
2.7 Bathtub curve . . . 44
2.8 Reliability functions of a geometric distribution . . . 45

3.1 Power flow model of a solar home . . . 48
3.2 Evolution of the electricity's price for a day . . . 49
3.3 Load demand and solar production for 8 days of the training test. . . . 52
3.4 Effect of the solar home's components sizing on its energy consumption from the electrical grid. . . . 53
3.5 Solar production of client number 60 for the test set, year 2010-2011. . . . 54
3.6 Solar production of client number 60 for the test set, year 2012-2013. . . . 55
3.7 Investment cost depending on the sizing of the solar home components . . . 57
3.8 Global cost depending on the sizing of the solar home components with an energy cost of 0.2€/kWh . . . 58
3.9 Flowchart algorithm of a Rule-based controller for HEMS. . . . 60
3.10 Flowchart algorithm of the Rule-based controller simulation for HEMS. . . . 61

4.1 Prevision on the grid state for planned and unplanned GPO . . . 67
4.2 Relation between P_l^*, P_s P^c, P_s^c . . . 75
4.3 Load satisfaction levels and their corresponding load satisfaction ratios. . . . 77

4.4 Evolution of the electricity's price for a simulation day 78
4.5 GPO period within the test set. 79
4.6 Evolution of the decision variables and energy within the storage for four days without a Grid Power Outage (GPO) for both the CMPC and ReMPC 80
4.7 Behaviour of Classical Model Predictive Controller (CMPC) and Resilient MPC (ReMPC) in case of an unplanned GPO 82
4.8 Behaviour of CMPC and ReMPC in case of an planned GPO 83

5.1 A simple example of a scenario tree 98
5.2 Multistage Stochastic Programming Wait and See 98
5.3 Multistage Stochastic Programming Here and Now 99
5.4 Multistage Stochastic Programming Here and Now with recourse 99
5.5 Markov chain model of the electricity grid 106
5.6 Low prob of failure, no outage 110
5.7 Low prob of failure, with outage 110
5.8 High prob of failure, no outage 111
5.9 High prob of failure, with outage 111
5.10 Variation of the energy in the storage function of the MPC horizon with a high failure rate 112
5.11 Variation of the grid and shedded energy function of the repair and failure rate 113
5.12 Zoom on Zone 2 and 4 of figures 5.11 114
5.13 Monthly energy drawn from the grid function of λ, μ and c_1 115
5.14 Cut in the energy drawn from the grid at $\mu = 5.10^{-4}$ and $\mu = 5.10^{-1}$ . . . 116
5.15 SDCMPC vs. MSPWS: Computing time and memory estimate usage . . . 118
5.16 Example of one simulation scenario 119
5.17 Reconstructed optimization cost rearranged in ascending order of the results obtained by the SDCMPC with an horizon of 7.5 hour 121

A.1 Méthodologie de la commande prédictive 130
A.2 Principe de l'horizon glissant 131
A.3 Relation entre les fonctions $F(t), R(t)$ et $z(t)$ pour une $f(t)$ loi normale $\mu = 3.5$ et de $\sigma^2 = 1$ 135
A.4 Courbe en baignoire 135
A.5 Modèle en flux de la maison solaire 137

A.6 Coût Global dimensionnement 140
A.7 Prévision de l'état du réseau électrique dans le cas des pannes planifiées et non planifiées 141
A.8 Les Mois de simulation et les jours de pannes 146
A.9 ReMPC vs CMPC : Panne planifiée 147
A.10 ReMPC vs CMPC : Panne non planifiée 147
A.11 Chaîne de Markov modélisant l'état du réseau électrique 155
A.12 SDCMPC : taux de défaillance faible $\lambda = 10^{-15}$ 156
A.13 SDCMPC : taux de défaillance élevé $\lambda = 0.99$ 156
A.14 Évolution de l'utilisation de la mémoire RAM et du temps de calcul en fonction de l'horizon de prédiction 158
A.15 Exemple d'un scénario de simulation de Monté Carlo 159
A.16 Performances des contrôleurs en fonction du scénario de Monté carlo 160

List of Tables

2.1 Common types of cost function 35
2.2 Common types of constraints 36
2.3 Relationship between $F(t)$, $f(t)$, $R(t)$ and $z(t)$ 44

3.1 Sizing parameters of the solar home 57

4.1 Main features of works on HEMS resilience 69
4.2 Performances of the CMPC and the ReMPC for planned and unplanned GPOs 85
4.3 Performances of the RBC-R and RBCPS-R controllers for Unplanneds GPOs 86
4.4 ReMPC with storage reserve performances: Unplanned GPO 87

5.1 Controller Performances for both Low and High failure rate 109
5.2 Stochastic Controller Performances for a Monte Carlo simulation of 10 days in Closed loop with a prediction horizon of 7.5 hours for SDCMPC and MSPWS and 24 hours for SDCMPC2 120

A.1 Types de contraintes 133
A.2 Relation mathématique entre $F(t)$, $f(t)$, $R(t)$ et $z(t)$ 135
A.3 Performances du ReMPC et du RBCPS-R 148
A.4 Performances du SDCMPC pour les taux de défaillances faible et élevé . . 157
A.5 Performances des contrôleurs pour 100 simulations de monté carlo 160

Chapter 1

Introduction

You know you're in trouble when people stop listening to sad music, because the moment people stop listening to sad music, they don't want to know anymore. They are turning themselves off. [a]

a. Thom Yorke

Contents

1.1 Context **19**

1.2 Motivation and contribution **21**

1.3 Outline of the thesis **23**

1.4 Publications **25**

1.1 Context

Extreme weather events with links to climate change are getting worse while becoming more frequent worldwide. In the United States, hurricanes, heat waves and forest fires are occurring more often [Wal+14]. The loss of electricity supply for long periods is among the many consequences of these natural disasters. For instance, in Puerto Rico, the months-long blackout after hurricane Maria [spe18], leading to an estimated death toll in the thousands [Kis+18]. In Florida, after Hurricane Irma, nearly two-thirds of electricity customers were cut off power with quasi three million remaining without electricity for four days or more [Adm17] as indicated by Figure 1.1 [1].

Given that the societal effects associated with these natural disasters are extremely costly, efforts are being made to address them as quickly as possible. The most com-

1. Source: U.S. Energy Information Administration based on data from Florida Division of Emergency Management and U.S. Department of Energy Situation Reports

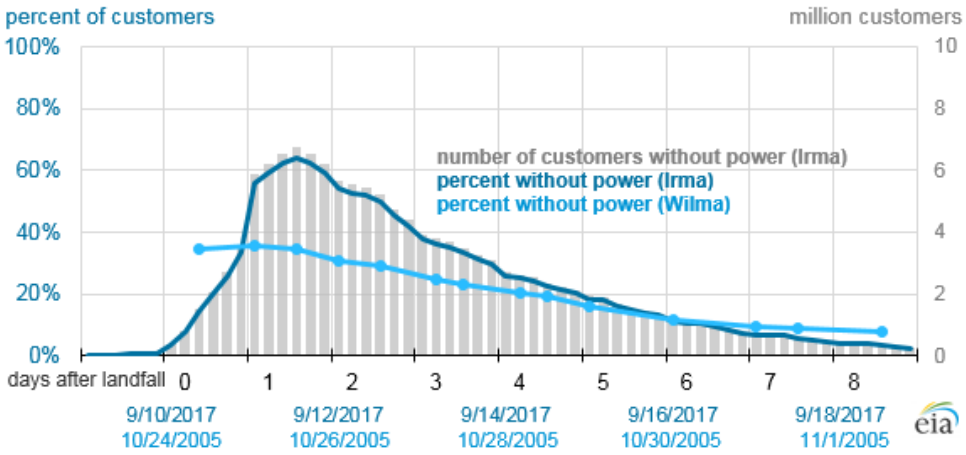

Figure 1.1 – Florida grid power outages resulting from hurricanes Irma and wilma

mon way to achieve these intended results is by resiliency: incorporating it in existing frameworks and designing new frameworks taking it into account.

The term resilience is derived from the domain of physics which defines it as *the ability of something to return to its original size and shape after being compressed or deformed.* A more general definition given in the "U.S. Presidential Policy Directive 21" [The13] is *the ability to prepare for and adapt to changing conditions and withstand and recover rapidly from disruptions. Resilience includes the ability to withstand and recover from deliberate attacks, accidents, or naturally occurring threats or incident.*

From the viewpoint of system engineering, we could reformulate the definition as the ability of a system to prepare and adapt its behaviour before and after the occurrence of stressor events. Figure 1.2 conceptually illustrates three possible resilience curves,

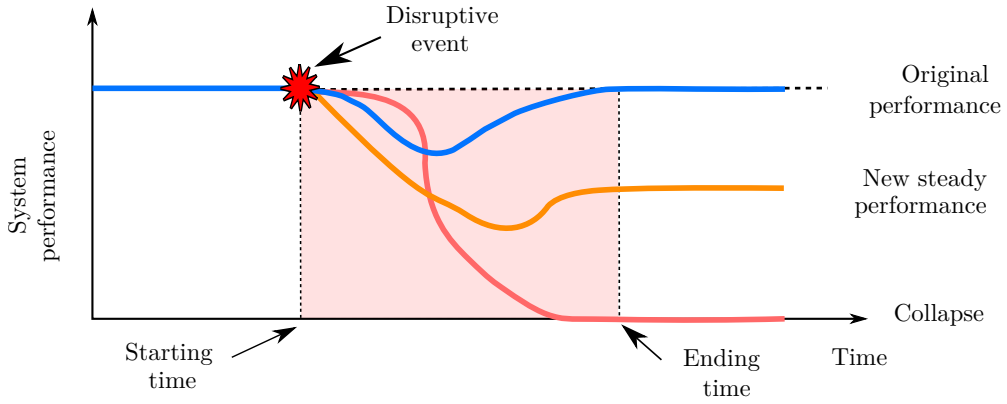

Figure 1.2 – Illustration of a system theoretical resilience curves during a disruptive event

representing the evolution of system performance.

There has been a rush toward the necessity of deeply understanding and designing following resilience guidelines in the research community. Most of these works focus on large scales systems such as interconnected critical Infrastructures, cyber physics systems and system of systems [KC13; FPZ15; RCA16; Mal+17; CRA18] from the global or distribution viewpoint since for these large scale systems an outage direct cost could be estimated up to billions plus invaluable indirect cost [FPZ15].

Although the aim of implementing resilience within these systems is to improve the users' welfare globally; they are often individually left out of the loop. However, given the challenges of global warming, and the advances in home automation technologies, nowadays many buildings are built or and renovated to reduce their dependency from the electrical grid. From 2014 to 2020, the worldwide installed residential photovoltaic capacity has increased from 32 GW to 93 GW with a projected value reaching 173 GW in 2025, and for off-grid locations 2 GW to 6 GW with a projected value reaching 10 GW [Age20]. Therefore, it becomes clear that integrating resilience in these building energetic systems is as essential as the electrical grid infrastructures' resiliency.

1.2 Motivation and contribution

There are many works on Building Energy Management System (BEMS) based on different techniques and algorithms; however, a few focus on resilience. The work we present in this thesis is to answer to the main question, that is:

How to control an energy system to make it resilient to rare and extreme events ?

This question gives rises to several others such as [2]:

- How to model a rare and extreme event?
- How to integrate such an event into the design of a controller?
- Have existing works already tried to answer this question? If yes, how can these existing works be improved?

2. the following questions are not intended to be ordered by priority.

- Does the resulting controller behaves as expected?
- Are existing frameworks such as robust optimization and stochastic programming relevant for rare and extreme event or should other frameworks be investigated?
- etc.

The contributions of this thesis will try to give element of answer to all these previous questions.

The first contribution is to provide a thorough state of the art of existing works that integrate resilience in an energetic system. We focus on BEMS, especially houses', from the user (human) viewpoint since he is the first to feel the rare event's effect, however often neglected in several works that rather zero in on the infrastructures [Xin17; Mal+17].

Based on the first contribution we find out that existing strategies although very interesting are limited in several manners [3]. Mainly they do not fully exploit flexibility and forecasts of the user's demand and supply (i.e., weather predictions for solar and wind-powered energy). About the latter, nowadays, their quality and efficiency have largely increased; hence, their usefulness for building control is no longer to prove. We, therefore, propose the first resilient model predictive controller that fully exploits all the available knowledge. For this first controller, we investigate rare deterministic events that can be categorized into two types: planned and unplanned. By deterministic here, we refer to a known complete information about the rare event [4].

When there is complete information about the occurrence of rare events, we know what strategy to apply. This deterministic vision of the rare event is very interesting because it focuses on the said event's occurrence. However, in reality, rare events by definition occur infrequently with low frequency, i.e., rarely; thus, their probability of occurrence is very low. Modelling the rare event through its probability of occurrence becomes therefore very essential. This is possible with the help of tools from the reliability theory. Therefore, our second contribution is to formalize the problem by providing a unified framework to use tools from reliability theory and predictive control to design a controller that integrates these rare events' probability of occurrence.

In this thesis, we focus on a particular type of rare events that are Grid Power Outage (GPO). Modelling statistically, the GPO leads to integrating discrete stochastic variables into a continuous optimization problem. Especially the stochastic constraints take their

3. See table 4.1 in chapter 4 for more information
4. Refer to definitions 4.1 and 4.2 for more

values within a discrete set. This leads to a well known problem experienced by the multistage stochastic optimization that is, an exponentially growth of the resulting problem's size in consonance with the Model Predictive Control (MPC) horizon and the discrete set cardinality. Therefore, the usefulness of special numerical techniques to solve this problem is obvious. The third contribution is to formally propose a new method that reformulates the discrete stochastic constraints to avoid the exponential growth.

As the fourth contribution, we show the efficiency of the previously proposed method by benchmarking and comparing it with the Multistage Stochastic Programming algorithm in the context of a Building Energy Management System controlling a house.

1.3 Outline of the thesis

The manuscript of the thesis is organized as follows:

Chapter 2

This chapter is set to be a background for the other chapters. We present with some mathematical preliminaries both framework around which the thesis is based: Model Predictive Control and Reliability theory. For the first, we emphasize its usability in Building Energy Management System, and for the second, a general introduction is given.

Chapter 3

This chapter aims to give a concise overview of the building model that we use in this work. As this model will be used later to design resilient predictive controllers, we emphasize its structural components and their sizing based on a given dataset. We finish by presenting an example of a non-resilient rule-based controller that is used to manage the energy flow within the building in the absence of grid power outages. A slightly modified version of this controller is used later in chapter 4 as a baseline of comparison.

Chapter 4

This chapter is concerned with formally introducing the concept of resilience to deterministic events in Building Energy Management System. We present a state of the art of existing strategies and their inconvenience, which motivates the new controller. Based on the well-known classic Predictive controller used in Building Energy Management System, we explicitly state the design of the resilient controller. To prove its added value, we compare its performances to three other controllers presented previously. Given that the chapter is based on our paper written back in 2018, we finish by discussing its relevance compared to four other papers that have been written since.

Chapter 5

The developments in chapter 5 are motivated by the application of deterministic events made in the previous chapter. Here, instead of having perfect information about the rare event which makes it deterministic, we get one step closer to reality by considering rare stochastic events. We present a formalization of the resulting problem that gives rise to discrete stochastic constraints and show its implications. Specifically, a state of the art of existing resolution methods shows that Robust optimization and chance constraints are not well suited for the problem. As for the multistage stochastic Optimization, the combination explosion that incurred due to model predictive control horizon makes it almost impossible to be used passed some point. With the reliability theory's help, we propose a new controller that reformulates the discrete stochastic constraints to offer a solution to the combination explosion. We apply the new controller to the building described in chapter 3 considering an electrical grid provider modelled by a Markov chain.

1.4 Publications

The work presented in this thesis was done in collaboration with my supervisors and is largely based on the publications that are listed bellow:

Chapter 3 is based on the following publication:

1 - Pierre Haessig, Jesse-James Prince Agbodjan, Romain Bourdais and Hervé Guéguen
Gestion d'énergie avec entrées incertaines : Quel algorithme choisir ? Bechmark open source sur une maison solaire
Symposium de Génie Électrique (SGE 2018), Nancy, France 2018

Chapter 4 is based on the following publication:

2 - Jesse-James Prince Agbodjan, Pierre Haessig, Romain Bourdais and Hervé Guéguen
Resilience in energy management system: A study case
IFAC workshop on Control of Smart Grid and Renewable Energy Systems (CSGRES), Jeju, Korea 2019.

Chapter 5 is based on the following publication

3 - Jesse-James Prince Agbodjan, Pierre Haessig, Romain Bourdais and Hervé Guéguen
Stochastic modelled grid outage effect on home Energy Management
IEEE Conference on Control Technology and Applications (CCTA), Montréal, Canada 2020.

4 - Jesse-James Prince Agbodjan, Pierre Haessig, Romain Bourdais and Hervé Guéguen
Integrating stochastic discrete constraints in MPC. Application to Home Energy Management System
IFAC Journal of Systems Control (IN REVIEW).

Part I

Background

Chapter 2

Introduction to MPC in building control and reliability theory

We are confident when the story we tell ourselves comes easily to mind with no contradiction and no competing scenario. But ease and coherence do not guarantee that a belief held with confidence is true. [a]

a. Daniel Kahneman, *Thinking fast and slow*

Contents

2.1 Model Predictive Control (MPC) 30

2.1.1 MPC Strategy 30

2.1.2 Traditional and Economic MPC 36

2.1.3 MPC in Buildings: main variants 37

2.2 Introduction to Reliability theory 39

2.2.1 Measures of reliability 40

2.2.2 Bathtub curve 43

2.2.3 The Bernoulli and Geometric distribution 44

2.3 Conclusion 46

In this chapter, we present key concepts on which the thesis is based. This overview starts with a presentation of the general principle of the predictive control, emphasising its usability in our application, Home Energy management System (HEMS). Then, we offer a brief introduction to some important notions of reliability theory and its main functions.

2.1 Model Predictive Control (MPC)

MPC or interchangeably referred to as *Receding Horizon control* (RHC), *Receding Horizon Predictive control* (RHPC), *Moving Horizon Optimal Control* (MHOC) or *Model-based Predictive Control* (MBPC) is an advanced control methodology that relies on the use of an internal model of the process to control. The term MPC does not designate a specific control strategy but rather an ample range of control methods which make explicit use of a model of the process to obtain the control signal by optimising an objective function [CA07].

The development and application of MPC technology were driven by industry; however, it is important to note that the idea of controlling a system by solving a sequence of open-loop dynamic optimisation problems was not new. [I63] was the first to propose the moving horizon approach (which later became known as the "Open Loop Optimal Feedback" [Dre64; Pap88] which is at the core of all MPC algorithms.

Although very simple to implement and design, MPC algorithms can control large scale systems with multiple control variables. Most importantly, MPC provides a simple method to deal with constraints on inputs and states. These constraints are present in most control engineering applications and represent limitations on actuators and plant states arising from physical, economic, or safety constraints.

2.1.1 MPC Strategy

The methodology of all the controllers included in the MPC family follows the strategy described by Figure 2.1. As necessary ingredients, a discrete *model* of the system is needed

$$x(k+1) = f\Big(k, x(k), u(k)\Big), \tag{2.1}$$

as well as the definition of the constraints,

$$u(k) \in \mathbb{U} \subset \mathbb{R}^{n_u} \tag{2.2}$$

$$x(k) \in \mathbb{X} \subset \mathbb{R}^{n_x} \tag{2.3}$$

where k indexes the discrete current instant, x and u represent the system's state and input. The constraint formulation above made suppose that the state and input's con-

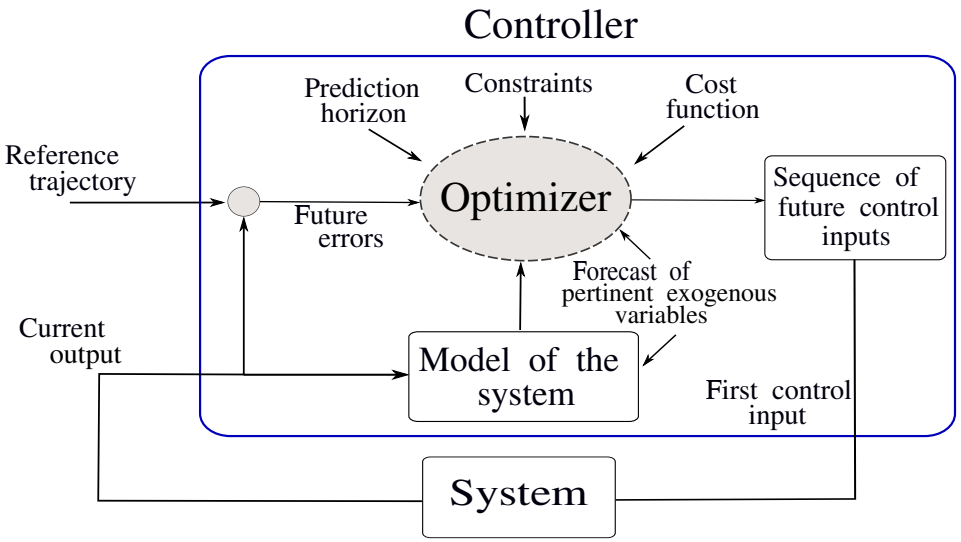

Figure 2.1 – MPC scheme for the control of a system

straints are separated, but they can also be combined as in

$$(u(k), x(k)) \in \mathbb{D} \subset \mathbb{U} \times \mathbb{X}. \tag{2.4}$$

Assumption 2.1. It is assumed that at each instant k the state $x(k)$ can either be measured, observed or estimated.

At each discrete instant k, the system's evolution over a finite prediction horizon H is formulated based on the model, and an optimization problem is solved according to some optimality criterion and subject to the constraints.

In the following, we distinguish between an *actual* variable at instant $k+h$ denoted by some $v(k+h)$, and the *prediction* of the actual variable at instant $k+h$ computed at time k denoted $v(k+h|k)$ with $h \in \mathbb{N}_0^H$. Furthermore, vectors (and matrices) that contain all predictions of a variable along the prediction horizon are denoted with capital letters. As example,

$$V(k) = \begin{bmatrix} v(k|k) \\ v(k+1|k) \\ \vdots \\ v(k+H|k) \end{bmatrix} \tag{2.5}$$

denotes an ordered collection of the vectors $v(k+h|k)$, with $V(k) \in \mathbb{R}^{(H+1)n_v}$.

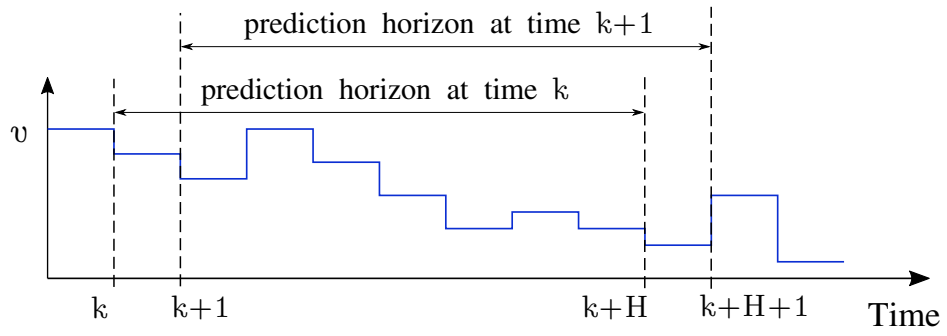

Figure 2.2 – Sliding or receding horizon principle

The solved optimization problem gives as result an optimal trajectory of inputs and states into the future satisfying the dynamics and constraints of the system while optimizing the given criterion. Although the optimal input sequence

$$U^*\Big(k, x(k)\Big) = \begin{bmatrix} u^*(k|k) \\ u^*(k+1|k) \\ \vdots \\ u^*(k+H-1|k) \end{bmatrix} \tag{2.6}$$

is available, solely the first input associated with the first time step, i.e. $u^*(k|k)$ is applied to the system and the rest is discarded.

In order to compensate for modeling errors and/or disturbances, a new measurement is taken at the next time step $k+1$. The whole procedure is repeated with the prediction horizon shifted by one time step. This process of shifting the prediction horizon by one at each new time step as shown by Figure 2.2 is also known as *sliding* or *receding* horizon. This is what introduces feedback to the problem since the new finite optimal control problem solved at the beginning of the next time step is a function of the new state at that point in time and hence of any disturbances that have meanwhile acted on the system. The procedure is summarized in the following algorithm.

Algorithm 1 MPC Algorithm

1: **for** each time step k **do**
2: Get a measurement of the current state $x(k)$;
3: Solve the MPC Problem 2.1 with prediction horizon H to obtain $U^*\Big(k, x(k)\Big)$;
4: apply the first element $u^*(k|k)$ to the system.
5: **end for**

A generic MPC strategy is given by the following finite horizon optimal control problem.

Problem 2.1 (**Generic MPC problem**).

$$J^*\Big(x(k)\Big) = \min_{u(k|k),\ldots,u(k+H-1|k)} \quad \sum_{h=0}^{H-1} l_h\Big(x(k+h|k), u(k+h|k)\Big) + V_f\Big(x(k+H|k)\Big) \tag{2.7a}$$

$$\begin{aligned}
\text{s.t. } & \forall h \in \mathbb{N}_0^{H-1} \\
& u(k+h|k) \in \mathbb{U} && (2.7b)\\
& x(k+h|k) \in \mathbb{X} && (2.7c)\\
& x(k+H|k) \in \mathbb{X}_f && (2.7d)\\
& x(k|k) = x(k) && (2.7e)\\
& x(k+h+1|k) = f\Big(k, x(k+h|k), u(k+h|k)\Big) && (2.7f)
\end{aligned}$$

where (2.7a) is the cost function, (2.7b) the constraints on the the control, (2.7c) the constraints on the states, (2.7d) the terminal constraint on the state, (2.7e) the current state, (2.7f) the system's dynamic, H is the prediction horizon, $h \in \mathbb{N}_0^{H-1}$ is the prediction step, $l_h : \mathbb{R}^{n_x} \times \mathbb{R}^{n_u} \to \mathbb{R}$ is the *stage cost*, $f_k : \mathbb{R}^{n_x} \times \mathbb{R}^{n_u} \to \mathbb{R}^{n_x}$ is the function describing the dynamics of the system's model at instant k and $V_f : \mathbb{R}^{n_x} \to \mathbb{R}$ is the *terminal cost*.

Definition 2.1. *The closed-loop state trajectory is described by*

$$x(k+1) = f\Big(k, x(k), u^*\Big(k|k, (x(k)\Big)\Big) \tag{2.8}$$

where the optimal control input $u^*\Big(k|k, (x(k)\Big)$ is obtained at each time step by solving MPC Problem (2.1)

Defining problem 2.1 and implementing the MPC strategy, come down to:

(i) Choosing a 'good' prediction horizon;

(ii) Finding a model that describes the system;

(iii) Defining a well suited cost function;

(iv) Describing the system's constraints.

In the following, a brief explanation of each of the four components in the above MPC formulation is provided with comments on their significance in building control.

Prediction horizon

The physical systems we consider here are controlled in discrete time. The optimization problem is solved over the prediction horizon H. The latter refers to the length of time for which the MPC problem computes the system output. The time step k is the time during which the control signal remains unchanged. Generally for BEMS, the prediction horizon is 5-48 hours [AJ14] and the time step is between 30 minutes and 3 hours [RH11].

Model of the system

The model of the system plays a decisive role in the MPC strategy. The chosen model must be able to capture well enough the process dynamics to precisely predict the future outputs and at the same time must be simple enough to ensure a reasonable computation time of the optimization process [Prí+13]. Generally, three types of models which review can be found in [LW14], are used in BEMS.

(i) White box model: They are also referred to as forward modeling approaches and are build using the physical principles of the system. To predict whole buildings and their sub-systems behaviours, detailed equations are used to model the building components, sub-systems and systems. Due to the detailed dynamic equations in white-box models, they have the potential to capture the building dynamic, hence are the most suitable for optimization based strategy.

(ii) Black box model: They are often known as data-driven models since they model, based on data the functional relationships between system inputs and system outputs. They mostly rely on statistical analyses and machine learning algorithms to assess and forecast the building energy consumption. A review of these data-driven models can be found in [Bou+19].

(iii) Grey box: Combine both the white box and black box model. A part of the system's dynamic is known, and the other part is modelled with a black box.

Cost function

Generally, the cost function describes a certain desired behaviour which serves two purposes:

- Stability: The cost is chosen such that under some additional assumptions, the optimal cost is a Lyapunov function; hence stability can be guaranteed [May+00].

Table 2.1 – Common types of cost function

Function type	**Mathematical Description**
Quadratic cost	$l_h\Big(x(k+h\|k), u(k+h\|k)\Big) = x(k+h\|k)^T Q x(k+h\|k) + u(k+h\|k)^T R u(k+h\|k)$
	$V_f(x(k+h\|k) = x^T(k+h\|k) P x(k+h\|k)$
Linear norm cost	$l_h\Big(x(k+h\|k), u(k+h\|k)\Big) = \|Qx(k+h\|k)\|_p + \|Ru(k+h\|k)\|_p$
	$V_f(x(k+h\|k) = \|Px(k+h\|k)\|_p, p \in \{1, \infty\}$

- Performance target: The cost specifies a certain preference, i.e., maximizing the user's comfort.

The majority of cost functions that are often used are convex. Some common choices, which are also listed in Table 2.1, are:

- *Quadratic cost.* The weight of the multiplicative factors of the states and the inputs, i.e. the choice of the matrices $Q \succeq 0$ and $R \succ 0$ provides a trade-off between the speed of response (regulation quality) and the cost of control action (input energy). If the system has no constraints, or when they are not active, then for a given Q and R this cost is equivalent to the cost of finite-horizon, discrete-time Linear Quadratic Regulator (LQR)/Linear Quadratic Gaussian (LQG).
- *Linear norm cost.* If the goal is to minimize 'amounts', outliers, or economically motivated signals, then the linear norm cost function is more suitable than the quadratic one. Using a 1-norm is a common choice for minimizing the energy consumption of buildings.

Constraints

The ability to specify constraints in the MPC formulation is the key strength of the MPC approach. Many different types of constraints are used in practice, an overview of common types suitable for building control is given in Table 2.2.

- *Linear constraint.* This is the most common type of constraint and is used to put upper and/or lower bounds on variables. Linear constraints are the easiest to handle when solving optimization problems and can also be used to approximate any convex constraint to an arbitrary degree of accuracy.

Table 2.2 – Common types of constraints. Note that constraints on the state $x(k+h|k)$ are listed here for illustrative purposes, but can also be applied to input u $u(k+h|k)$ or as mixed constraints to both state $x(k+h|k)$ and input $u(k+h|k)$.

Constraint type	**Mathematical Description**
Linear constraint	$Ax(k+h\|k) \leq b$
Convex quadratic constraint	$(x(k+h\|k) - \bar{x})^T Q(x(k+h\|k) - \bar{x}) \leq 1,\ Q \succeq 0$
Stochastic constraint	$A(\boldsymbol{\xi})x(\boldsymbol{\xi}, k+h\|k) \leq b(\boldsymbol{\xi})$
Switched constraint	if *condition* then $A_1 x(k+h\|k) \leq b1$ else $A_2 x(k+h\|k) \leq b_2$
Nonlinear constraint	$h(x(k+h\|k)) \leq 0$

- *Convex quadratic constraint.* This type of constraint is used to bound a variable to lie within an ellipsoid.
- *Stochastic constraint.* When uncertainty arises in the problem, it is the type of constraint that is used. Since an optimization problem can only be solved if all variables are deterministic, a reformulation into a deterministic equivalent problem is performed.
- *Switched constraint.* This type of constraint comprises a set of constraints, where each one is relevant only if a predefined condition is met. It is the type of constraint usually used in hybrid systems, i.e. systems that exhibit both continuous and discrete-time behaviour.
- *Non-linear constraint.* This constraint class comprises any type of constraint that does not fit into the above categories, where $h(x(k+h|k))$ can be any nonlinear function. In general, it is very difficult to handle this type of constraint when solving optimization problems.

2.1.2 Traditional and Economic MPC

Generally, when the scientific community refer to MPC, they directly imply the traditional target-tracking MPC. Its goal is to reach and closely track a set of predefined reference trajectories of some controlled variables. This is done through penalization of the deviation of the system's outputs from the reference trajectories.

In managing real-time process operation, when the emphasis of the control is oriented towards the economic signals, the traditional target-tracking MPC is generally inade-

quate. Mainly because a positive deviation from the target may represent a profit, while a negative deviation from the target may represent a loss or vice versa [SE12]. The so-called Economic Model Predictive Control (EMPC), which employs an economic-related cost function for real-time control, is usually preferred.

An EMPC directly and dynamically optimizes the economic operating cost of a process, doing so without reference to any steady-state [RAB12]. This idea of using an economic cost function directly in an MPC scheme was proposed first in [Eng07; RA09]. Since then its popularity amongst researchers and practitioners has significantly increased and has been applied in several domain among which Smart Manufacturing [Dav+12; Chr+07], chemical processes [LEC13; ZL15; SEB16], smart grids and buildings [SE12; Par+15; LG17]. A review of these applications can be found in [TLM14; EDC14]. For the following, when we refer to MPC, we will be indicating to the EMPC.

2.1.3 MPC in Buildings: main variants

From a thermal perspective, buildings can be considered as a single-zone, a multi-zone, or both [Ser+18]. In BEMS, when using MPC, a multi-zone building is often model in its entirety as a whole entity to find an optimal solution for the operation of the entire building. For the single-zone, several controllers in a centralized, *decentralized* or *distributed* approach manage each a separate part of the building.

MPC for a single-zone building

This control focus on the only part of the building related to production/storage energy. It is also referred to as higher level MPC, which returns, for example, the building set-points to utilize. The goal here is to manage the purchased/sold/stored power, given some prediction on the total building consumption. No particular attention is given to the buildings' individual components, as shown by Figure 2.3. Some authors mainly focus on the mathematical description of the Heating Ventilation and Air Conditioning (HVAC) systems for energy-optimal control [Bra90; Gan+19; Gan+20] while some others do not [Tut+13; SB17; Hae+18]. Generally, the models used, in this case, are restricted to an overall description of power flows.

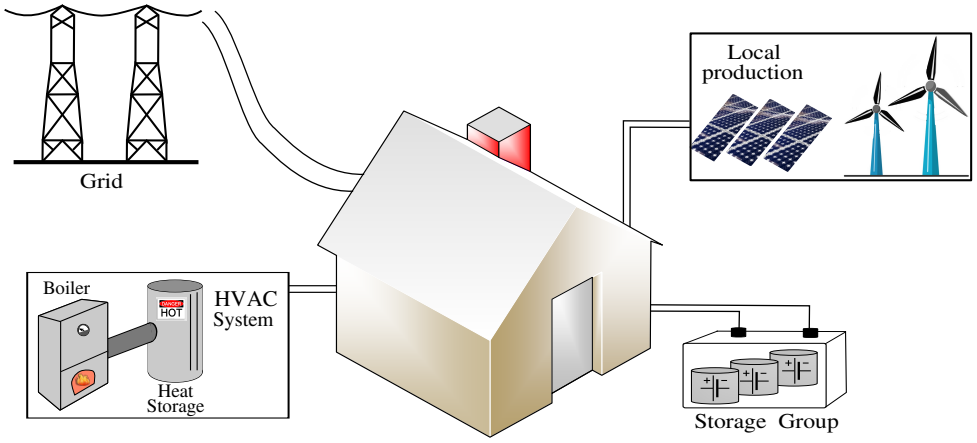

Figure 2.3 – Overview of the main equipment controlled in the single-zone approach

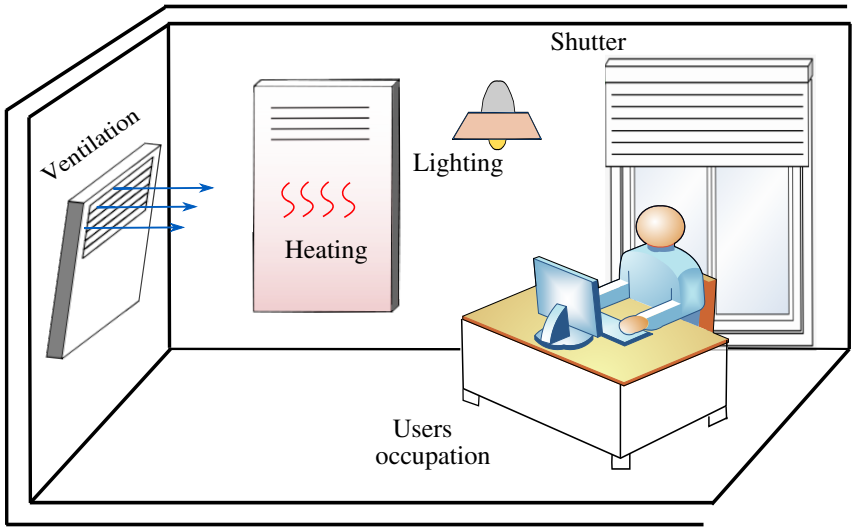

Figure 2.4 – Overview of the main equipment considered in each zone of the multi-zone controlled approach

MPC for a multi-zone building

Also referred to as zone predictive or integrated zone control [Lam12] or Integrated Room Automation (IRA) [GG10], the focus here is in the mathematical description of the equipment and their interaction. The main goal being to address the control of a set of actuators to ensure occupants' comfort. The comfort refers to thermal and/or air quality and/or indoor illuminance and/or humidity. The actuators command components such as HVAC systems, lighting, and shutters, as shown by Figure. 2.4.

For this control, the mixture of binary inputs (for the actuators) together with continuous ones (the temperature of a zone or air volume delivered by the ventilation system for instance) leads to using a hybrid dynamical model and the MPC controller solves a mixed-integer linear program at each step time. Example of recent applications can be found in [Kha+17].

Note that the above-made separation is intended to emphasis that this thesis focuses on one of these two considerations, i.e., MPC for buildings as a single-zone. Indeed, some studies lie beyond this categorization. Recent examples of papers that combine both models are [ABG18; Gan+20]

2.2 Introduction to Reliability theory

In this section, we introduce key concepts of reliability theory that are necessary to model and evaluate faulty behaviours of a system, and that will be of use later on this thesis (see section 5.5 about modelling the electrical grid behaviour). We do not intend doing so, to make a rigorous course on reliability theory; for this, the reader may refer to [Baz61; BPH65; BA92; RH04; Bir04].

The term reliability often covers the broader domain of reliability, availability, maintainability, and safety (RAMS) of components. Although many variations of the definition of reliability exist, the widely accepted form is given in the precursor book [Baz61] as follows: *reliability is the probability of a device performing its purpose adequately for the period of time intended under the operating conditions encountered.*

This definition can be divided into four basic parts:

- Probability
- Adequate performance

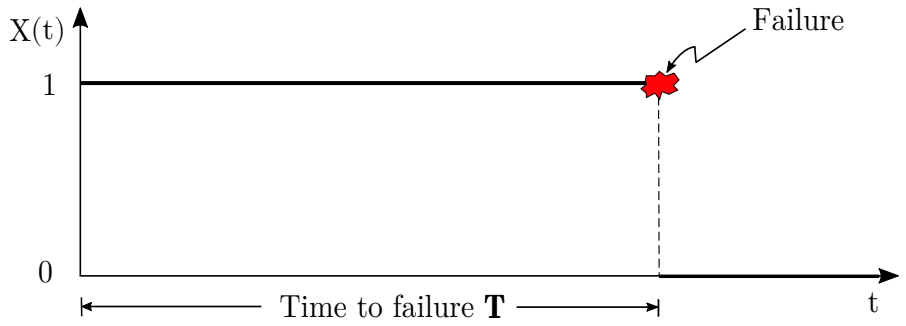

Figure 2.5 – State variable and time to failure of a item

- Time
- Operating Conditions

The operating conditions and adequate performance are all engineering parameters that only the system engineer can provide. The time can either be discrete or continuous, and probability provides the numerical input for assessing reliability and also the first index of system adequacy.

2.2.1 Measures of reliability

Based on the probability, let us introduce some quantitative measures for the reliability of a non-repairable item. The item considered can be anything from a small component to a large system. By supposing that an item is non-repairable, we are interested in the item's behaviour until the first failure occurs. This class of non-repairable item includes those that might be literally non-repairable, i.e. the item is discarded by the first failure but, also those that may be repaired, but we are not interested in what is happening with the item after the first failure.

State variable

The state of the item at time t may be described by a random state variable $\boldsymbol{X}$ [1](t):

$$\boldsymbol{X}(t) = \begin{cases} 1 & \text{if the item is functioning at time } t \\ 0 & \text{if the item is not functioning at time } t \end{cases} \tag{2.9}$$

1. For the rest of the thesis, the following convention is adopted: a random variable is denoted by a bold letter, and its realization is indicated by the same regular letter

Figure 2.5 shows the state variable of a non repairable item.

Time to failure

The elapsed time between the moment when the item is put into operation and fails for the first time is referred to as time of failure. We always consider the starting instant of operation as $t = 0$. The time of failure $\boldsymbol{T}$ is also a random variable. The connection between the state variable $\boldsymbol{X}(t)$ and the time to failure $\boldsymbol{T}$ is illustrated in Figure 2.5.

The time of failure is not always measured in calendar time since it can also be measured by more indirect concepts such as the number of times a switch is operated or the number of kilometres driven by a vehicle. From these examples, we notice that the time to failure can also be a discrete variable.

The cumulative failure distribution

A random variable's Cumulative Distribution Function (CDF) increases (in discontinuous steps for discrete random variable (r.v) and as a continuous curve for continuous r.v) from zero to unity. Let us consider the time to failure $\boldsymbol{T}$. If at $t = 0$, the item is functioning then its probability of failure at that instant is zero. However, as $t \to \infty$ the probability of failure must tend to unity as it is a certainty that the item will eventually fail given that the exposure time is long enough. This is a characteristic of a CDF and is a measure of the probability of failure as a function of time. In reliability terminology, the cumulative distribution is known as the cumulative failure distribution function or simply the cumulative failure distribution and is designated either by $F(t)$ or $Q(t)$.

The reliability function

In many practical examples it is not necessary to evaluate, the probability of failure in a given period of time, but the probability of surviving that period of time. This is the complementary value of the probability of failure and therefore the complementary function of the cumulative failure distribution. In reliability terminology this complement is known as the survivor function or reliability function and is designated as $R(t)$ with

$$R(t) = 1 - F(t) \tag{2.10}$$

The failure density function

The derivative of the CDF of a continuous r.v gives the probability density function. In reliability evaluation, the derivative of the cumulative failure distribution, $F(t)$, therefore gives a function which is equivalent to the probability density function, and is called the failure density function $f(t)$, with

$$f(t) = \frac{d}{dt}F(t) = -\frac{d}{dt}R(t) \tag{2.11}$$

Given the previous definition we can rewrite

$$F(t) = \Pr[\boldsymbol{T} \leq t] = \int_0^t f(u)\mathrm{d}u \quad \text{for t} > 0, \tag{2.12}$$

$$R(t) = \Pr[\boldsymbol{T} > t] = \int_t^\infty f(u)\mathrm{d}u \quad \text{for t} > 0. \tag{2.13}$$

In the presence of discrete random variables, the integrals in Equations (2.12) and (2.13) are replaced by summations.

The relation between the cumulative failure distribution, the reliability function and the failure density function is illustrated by figure 2.6.

Failure rate function

This is one of the most extensively used functions in reliability terminology. It is best described as the transition rate although depending upon the circumstances it is also referred to as hazard rate (function), failure rate (function), repair rate (function), force of mortality, age specific failure rate, etc. In terms of failure, the transition rate is a measure of the rate at which failures occur.

Given that at instant t the item is functioning, the probability that the item will fail in the time interval $(t,\, t + \Delta_t]$ is given by:

$$\begin{aligned} \Pr\left[\, t < \boldsymbol{T} \leq t + \Delta_t \,|\, \boldsymbol{T} > t \,\right] &= \frac{\Pr\left[\, t < \boldsymbol{T} \leq t + \Delta_t \,\right]}{\Pr[\, \boldsymbol{T} > t \,]} \\ &= \frac{F(t + \Delta_t) - F(t)}{R(t)} \end{aligned} \tag{2.14}$$

If we divide the previous equation by the length of the time interval, Δ_t, and compute the limit of the result while letting $\Delta_t \to 0$, we get the *failure rate function* $z(t)$ of the

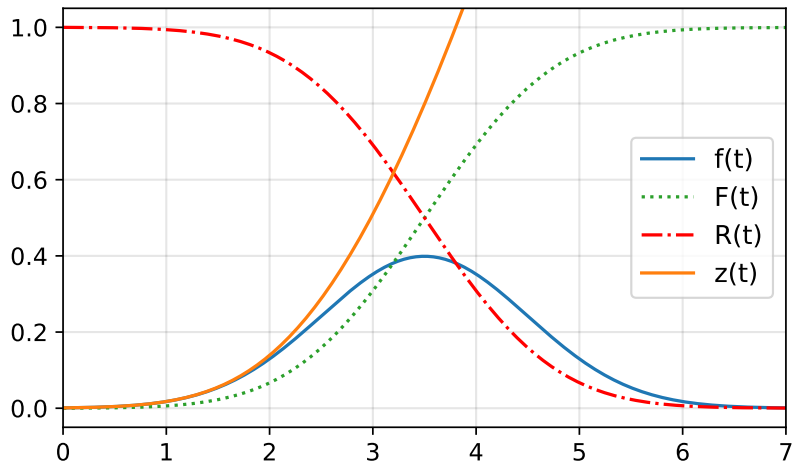

Figure 2.6 – Relation between the cumulative failure distribution $F(t)$, the reliability function $R(t)$ and the failure density function $f(t)$ (Normal distribution with $\mu = 3.5$ and , $\sigma^2 = 1$

)

item as:

$$\begin{aligned} z(t) &= \lim_{\Delta_t \to 0} \frac{\Pr\left[\, t < \boldsymbol{T} \leq t + \Delta_t \,|\, \boldsymbol{T} > t \,\right]}{\Delta_t} \\ &= \lim_{\Delta_t \to 0} \frac{F(t+\Delta_t) - F(t)}{\Delta_t} \frac{1}{R(t)} = \frac{f(t)}{R(t)} \end{aligned} \tag{2.15}$$

The formula relationship between the cumulative failure distribution $F(t)$, the reliability function $R(t)$, the failure density function $f(t)$ and the hazard rate $z(t)$ is illustrated in table 2.3.

2.2.2 Bathtub curve

The failure rate of an item during its life goes through several phases. The much-quoted bathtub (see figure 2.7) divided into three distinct regions seeks to describe it. Region I (also known as initial phase, debugging phase, burn in period or infant mortality) where failure rate is decreasing is linked to manufacturing errors or improper design. When the equipment has survived the debugging phase, it enters region II also known as the Normal operating phase or useful life period. In this region the hazard rate is constant and failures occur purely by chance. This is the region largely used in modeling the lifetime of repairable equipment and this is the only region in which the exponential distribution and its discrete analogue the geometric distribution are valid [Dav52; ES53; Eps58]. Region

Table 2.3 – Relationship between $F(t)$, $f(t)$, $R(t)$ and $z(t)$

	$F(t)$	$f(t)$	$R(t)$	$z(t)$
$F(t) =$	-	$\int_0^t f(u)du$	1- R(t)	1 - $\exp\left(-\int_0^t z(u)du\right)$
$f(t) =$	$\frac{d}{dt}F(t)$	-	$-\frac{d}{dt}R(t)$	$z(t)\ \exp\left(-\int_0^t z(u)du\right)$
$R(t) =$	1 - $F(t)$	$\int_t^\infty f(u)du$	-	$\exp\left(-\int_0^t z(u)du\right)$
$z(t) =$	$\frac{dF(t)/dt}{1-F(t)}$	$\frac{f(t)}{\int_t^\infty f(u)du}$	- $\frac{d}{dt}lnR(t)$	-

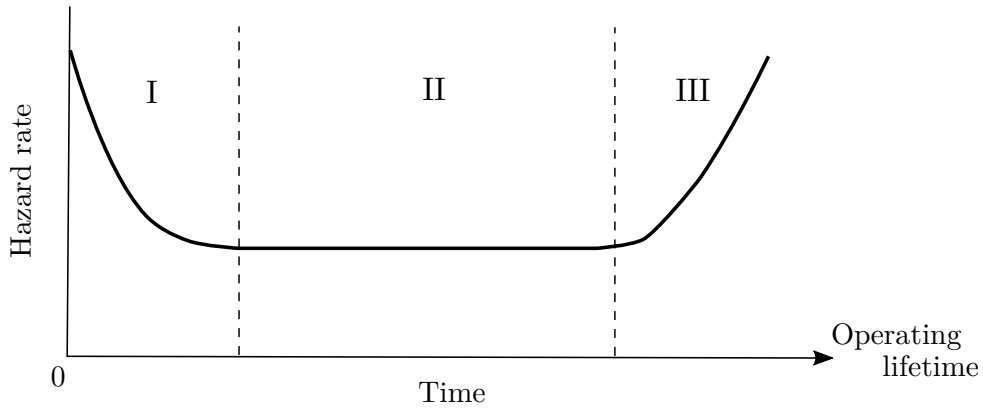

Figure 2.7 – Bath-tub curve showing the Hazard rate evolution function of age

III, the latter part of the curve also known as fatigue phase describes the wearout failures and it is assumed that failure rate increases as the wearout mechanisms accelerate.

2.2.3 The Bernoulli and Geometric distribution

Let us consider a probabilistic experience that can only have two outcomes, A a success and A^* a failure. Let p referred to as the Bernoulli probability, be the probability of success and $1-p$ be the probability of failure in the experience

$$\begin{aligned} \Pr[A] &= p \\ \Pr[A^*] &= 1-p. \end{aligned} \tag{2.16}$$

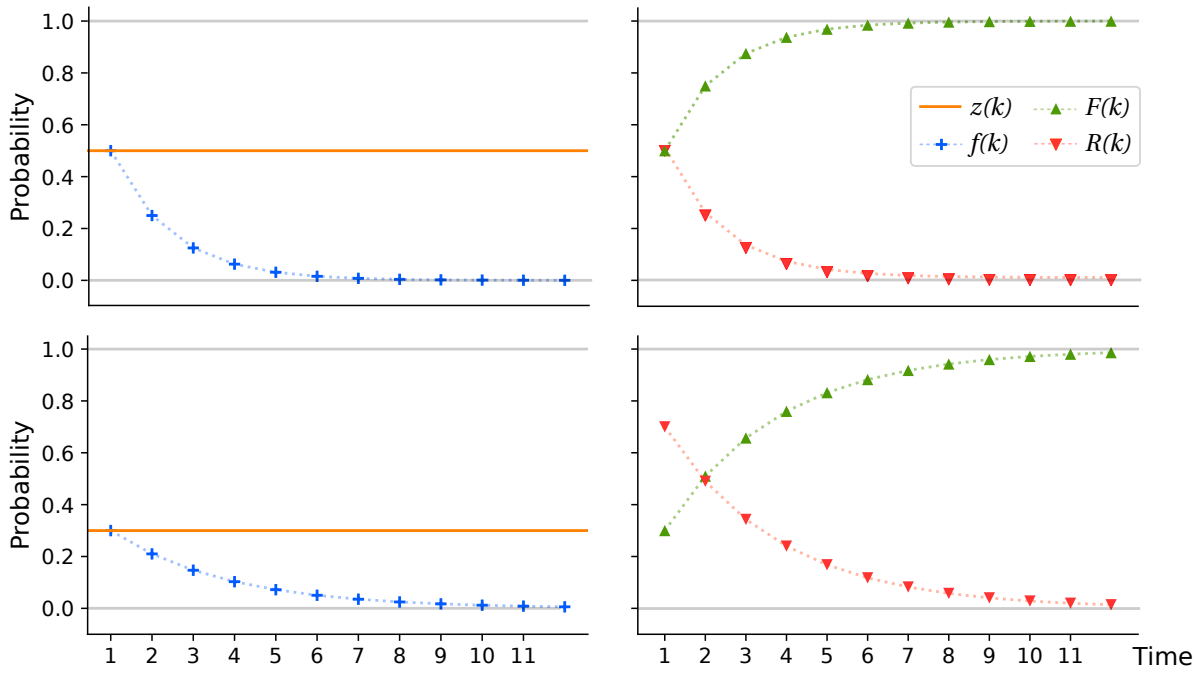

Figure 2.8 – Reliability function of a geometric distribution with a constant failure rate $z(k) = 0.5$ for the first row and $z(k) = 0.3$ for the second row

This probabilistic experience is known as a Bernoulli trial.

Given a sequence of independent Bernoulli trials, where the probability of success p and failure $1 - p$ do not change between the trials, the geometric distribution is given by the number of trials or failures before the first success occurred. Given that the trials happen at specific discrete-time, the geometric distribution can then be considered as the time elapsed before the first success appears.

If we link the geometric distribution to reliability measurements, we would consider a success at instant k in the experience to be failure of an item at instant k. Therefore the probability of success p in each trial is actually the hazard rate,

$$p = z(k) \tag{2.17}$$

and the discrete failure density function is given by

$$f(k) = p(1-p)^k, \quad \forall k \in \mathbb{N}_1^\infty. \tag{2.18}$$

Figure 2.8 shows the evolution of the reliability, failure density and failure rate function

of a geometric distribution with a constant hazard rate $z(k) = 0.5$ for the first row and $z(k) = 0.3$ for the second row.

2.3 Conclusion

In this chapter, we have presented the MPC, that is the framework on which is based the controllers we have developed in this thesis. We had paid particular attention to how such a controller can be designed especially for building energy management applications. We have also presented the essential measures of reliability theory and show what they are in the case of the discrete geometric distribution.

Understanding these basics is very important for the followings chapters i.e., chapter 4 and 5. However, before we continue with these chapters where the proposed new controller's actual design is explained, the next chapter will present a description of the building that is considered.

Chapter 3

Description of the solar home

One man cannot do right in one department of his life whilst he is occupied in doing wrong in any other department. Life is one invisible whole[a]

a. Mahatma Ghandi

Contents

3.1 Introduction 47

3.2 Model of the solar home 48

3.2.1 Solar home's components 48

3.2.2 Dataset of the solar home 51

3.2.3 Sizing of components 52

3.3 Rule based controller for HEMS in absence of outage 58

3.4 Conclusion 59

3.1 Introduction

To test all the various algorithms that we design in the following chapters, we provide in this section a succinct description of the case study.

The chapter is divided as follows. Section 3.2 describes the solar home model thoroughly with an emphasis on the different components and their sizing. In the same section, we also present the dataset that will be used through all the thesis. The next section presents a ruled-based algorithm to manage the solar home's energy flow in the absence of a grid power outage.

3.2 Model of the solar home

The considered energy system model is a solar home, i.e. a photovoltaic system with storage for the self-consumption of a residential consumer connected to the electrical grid. Its power flow model is given by Figure 3.1. The system equation is usually written in continuous time t, but since the controller takes and applies decisions at discrete time, here we are going to use discrete-time equations written in k. Note that for the rest of the thesis, we are going to use the words decision/control variable interchangeably.

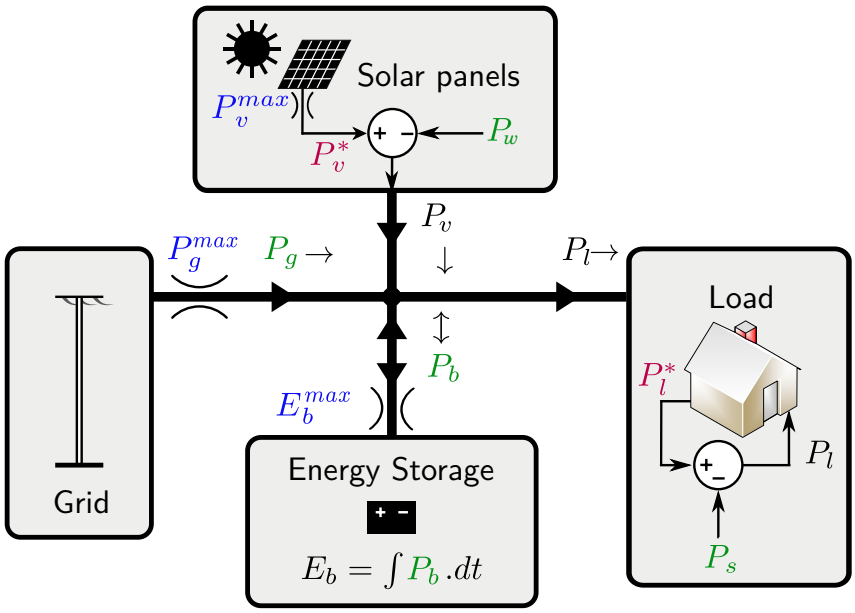

Figure 3.1 – Power flow model of a solar home. The decision/controlled variables are colored in green, external data are colored in red (Solar potential and desired consumption), internal variables are colored in black, fixed variables are colored in blue.

3.2.1 Solar home's components

The system comprises four main parts which consist of several variables on which the controller impinges.

The electrical network

This is the electricity provider with which the user subscribed to get access to energy. The maximum power allowed with the subscription is given by P_g^{max}[kW]. The electrical

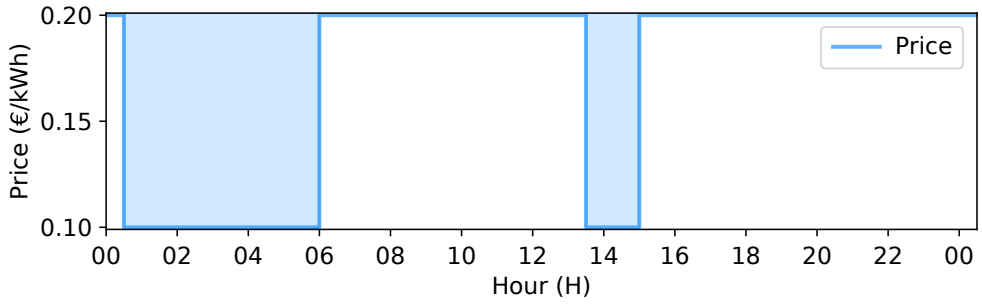

Figure 3.2 – Evolution of the electricity's price for a day. The off-peak periods (12h30 to 05h59 and 13h30 to 14h59) where the electricity price is the lowest are colored in light blue.

network can either be available or unavailable, let P_{g0}^{max}[kW] and P_{g1}^{max}[kW] be respectively the corresponding values depending on the grid's state such that:

$$P_g^{max} = \begin{cases} P_{g1}^{max} & \text{if electrical network is available} \\ P_{g0}^{max} & \text{if electrical network is unavailable.} \end{cases} \tag{3.1}$$

The power needed to be drawn at each discrete time k is the control variable $P_g(k)$[kW]. Since selling energy back to the electricity grid is not authorized, $P_g(k)$ is non-negative; therefore we have the following physical constraint

$$0 \leq P_g(k) \leq P_g^{max}. \tag{3.2}$$

The electricity drawn from the grid is bought at different prices depending on the period of the day following the off-peak or peak hours principle.

The price that is applicable for a certain period is sent to the users at least 24 hours before the said period starts throughout a vector $c_g(k)$[€/kWh] and for simplicity sake, covers at least the length of the prediction horizon. An example of the evolution of the price for 24 hours is given by Figure 3.2.

The solar panels

They are the second source of energy of the building with a nominal power given by P_v^{max} and a production in Maximum Power Point Tracking (MPPT) [BI12; BI17] at instant k given by $P_v^*(k)$[kW]. When the energy production of the solar panels is higher than what can be used within the system at an instant k, it needs to be reduced. The control variable $P_w(k)$[kW] (Power wasted) is used to do so; therefore, it acts as a degree

of freedom to set the energy provided by the solar panels to the system. At each instant k, the actual power provided by the solar panels $P_v(k)$[kW] to the system is given by:

$$P_v(k) = P_v^*(k) - P_w(k) \tag{3.3}$$

with

$$0 \leq P_w(k) \leq P_v^*(k) \tag{3.4}$$

The storage unit

The Energy storage unit is used to deal with the variations of the renewable electricity sources, i.e., it allows for shifting, at least partially the solar production. The power stored or provided by the storage at each instant is given by the decision variable $P_b(k)$[kW] (Power battery). The accumulation of the latter over time gives the energy within the storage E_b[kWh](Energy battery) or the state of charge as:

$$E_b(k+1) = E_b(k) + P_b(k)\Delta_t. \tag{3.5}$$

Storage losses are neglected because they are out of the scope of this thesis, but the interested reader might refer to [KLS17] and the reference within. The maximum capacity of accumulation of the storage is a fixed data that is E_b^{max} and since no energy can be provided when the battery is empty, the physical constraints on the state of charge at each instant k is given by

$$0 \leq E_b(k) \leq E_b^{max}. \tag{3.6}$$

which is rewritten as

$$-\frac{E_b(k)}{\Delta_t} \leq P_b(k) \leq \frac{E_b^{max} - E_b(k)}{\Delta_t}. \tag{3.7}$$

when equation (3.5) is introduced.

The load/building/user

The energy of the three previously described components are used by the building that we modeled as a single zone (see section 2.1.3 for more on this). The energy demand of the building at each instant is given by the external data $P_l^*(k)$[kW]. One can imagine that at some moment, the building demand would be above what the main (the electrical network) and the auxiliaries (the solar panel and the storage unit) sources can provide;

a part of the demand must be reduced (shedded). The power to be shedded is a control decision and is given by P_s[kW]. Since the energy demand of the building at an instant cannot be reduced past its own value, the following constraint is expected to be respected:

$$0 \leq P_s(k) \leq P_l^*(k). \tag{3.8}$$

The actual energy provided to the building is given by P_l and can be computed as follows:

$$P_l(k) = P_l^*(k) - P_s(k) \tag{3.9}$$

Remark 3.1. Accumulation of the shedded power over a certain period of time would be considered as a metric to measure the energetic dissatisfaction of the building.

Remark 3.2. We define the "net load" as the difference between the building demand $P_l^*(k)$ and the solar production $P_v^*(k)$:

$$P_{nl}^*(k) = P_l^*(k) - P_v^*(k). \tag{3.10}$$

Remark 3.3. We define the "controlled net load " as the difference between the actual energy provided to the building and the solar production:

$$P_{nl}(k) = \underbrace{P_l^*(k) - P_s(k)}_{P_l(k)} - P_v^*(k). \tag{3.11}$$

These fours component exchange energy among themselves, which allows us to write the following load balance equation :

$$P_g(k) - P_b(k) + \underbrace{P_v^*(k) - P_w(k)}_{P_v(k)} = \underbrace{P_l^*(k) - P_s(k)}_{P_l(k)} \tag{3.12}$$

3.2.2 Dataset of the solar home

Data are needed to test the different algorithms we describe and discuss in this thesis. The one that we use is extracted from the "Solar home electricity data"[Com; Rat+17], a freely accessible and real dataset made available by Australia's largest distributor of electricity Ausgrid. The dataset contains the load demand $P_l^*(k)$ and the solar production $P_v^*(k)$ generated every 30 minutes ($\Delta_t = 0.5h$) of 300 randomly selected solar customers

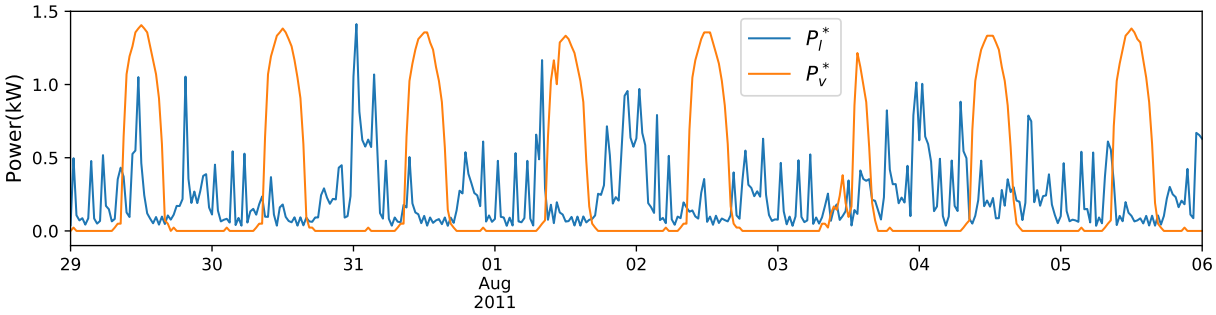

Figure 3.3 – Load demand and solar production (after scaling) for 8 days of the training test.

in Ausgrid's electricity network area and covers the period from 1 July 2010 to 30 June 2013.

The load demand of each user is used directly but, a scaling of the solar production $P_v^*(k)$ is done as follows:

$$\begin{aligned} P_v^*(k) =& P_v^{max} \times P_v^{1k} \\ =& P_v^{max} \times \frac{GP(k)_n}{PN_n} \end{aligned} \tag{3.13}$$

where P_v^{1k} is the production of a solar panel of $1kWp$, $GP(k)_n$ and PN_n are respectively the actual production and the nominal capacity (in kWp) of the solar panels of the client number n chosen from the data set. We choose to divide the given data in two sets i.e. the training set (from 1 July 2011 to 30 June 2012) that is used to train the different algorithms that need training and the test set (1 July 2010 to 30 June 2011 and 1 July 2012 to 30 June 2013) that is used to evaluate the algorithms performances.

Figure 3.3 shows an example of load demand and solar production of a one user. Figure 3.5 and Figure 3.6 also show the monthly solar production of the same user for the test set.

3.2.3 Sizing of components

Although the performance of a Photovoltaic (PV) system depends greatly on the type of control algorithm used, it is also impacted by the sizing of its main components, i.e., the storage unit maximum capacity E_b^{max}, the maximum power delivered by the electrical grid P_g^{max} and the nominal power of the solar panels P_v^{max}[kWp].

Of course, the optimal sizing of these components is an interesting question but is out

of the scope of the thesis; nevertheless, we think it is essential to find a way to obtain a " realistic" size of the components to be used for the different simulations.

Methodology

First of all, let us emphasize that the sizing that we propose depends on the building energy needs, the location considered, and the installed solar panels production. To help with the process, we have at our disposal a dataset described in section 3.2.2 .

A sensibility analysis is done considering the nominal power of the solar panel and the storage maximum capacity varying their values as:

- $E_b^{max}(k) \in \{0 : 0.5 : 20\}$[kWh]
- $P_v^{max} \in \{0 : 0.2 : 6\}$ [kWp].

For each pair of values, the problem of controlling the house is simulated over the first 100 days of the training set using the simple rule-based algorithm (described in section 3.3) that minimizes at each instant the energy drawn from the grid.

Figure. 3.4 shows the result obtained for the daily average energy drawn from the grid $\langle P_g \rangle$ for each sizing. The controller draws the highest energy ,i.e., $\langle P_g \rangle$ = 17,7kWh/day when there is no storage or solar panels (both variables equal zero) and its value decreases as E_b^{max} and P_v^{max} increases. To be more precise, increasing the value of the storage with

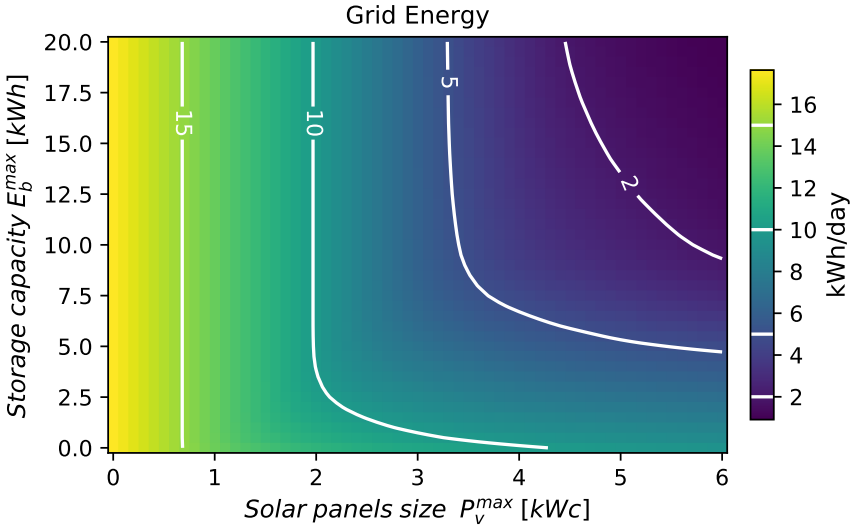

Figure 3.4 – Effect of the solar home's components sizing on its energy consumption from the electrical grid.

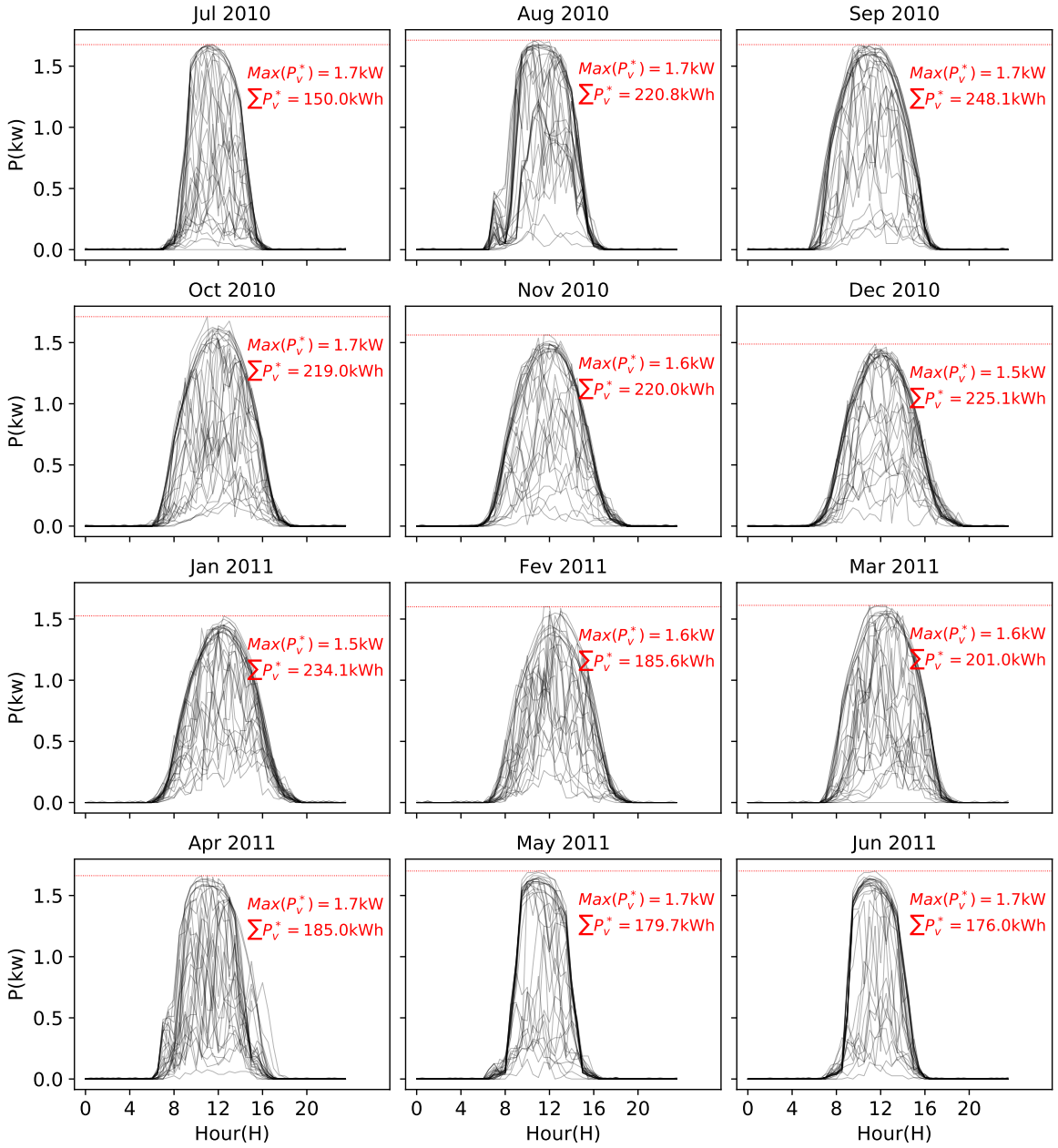

Figure 3.5 – Solar production (after scaling) of client number 60 for the test set, year 2010-2011.

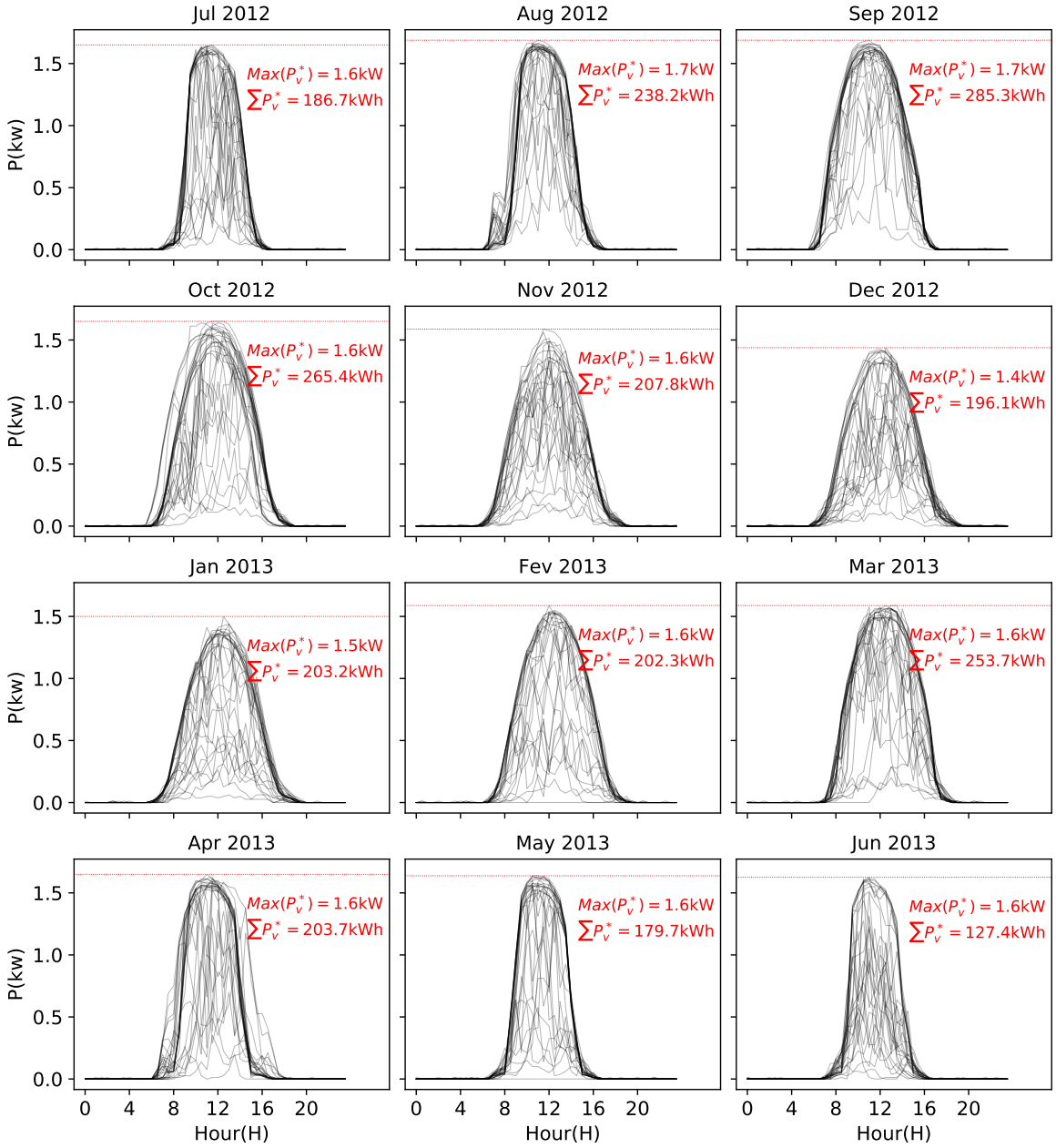

Figure 3.6 – Solar production (after scaling) of client number 60 for the test set, year 2012-2013.

no solar panels does not make sense (charging the storage with energy drawn from the grid is not allowed); hence it does not impact $\langle P_g \rangle$ while on the contrary increasing the size of the solar panels with the storage fixed at zero decreases $\langle P_g \rangle$ to 9.4kWh/day. Daily consumption isolines (in white) are curved and show that the optimal sizing must be located at one of them.

Let us consider that the optimal sizing is the one that minimises the global cost of the components (solar panels and storage unit) over their lifetime. This global cost C_{glob} is given by the initial investment C_{inv} to acquire the components added to the operational cost C_{ope}

$$C_{glob} = C_{inv} + C_{ope}. \tag{3.14}$$

We suppose the initial investment to be proportional to the nominal power of the solar panels P_v^{max} and the storage unit maximum capacity E_b^{max} as follows

$$C_{inv} = c_E E_b^{max} + c_P P_v^{max}, \tag{3.15}$$

where $c_E = 0.5$k€/kWh given that a Tesla Powerwall of 14 kWh costs about 7k€[Car17] and $c_P = 2$k€/kWp [inf15]. Figure 3.7 shows the investment cost for each pair of values P_v^{max} and E_b^{max}.

As for the operational cost C_{ope}, we suppose it to be equal to the daily average electricity bill multiply by the lifetime of the installation

$$C_{ope} = T_{life} \times \langle c_g P_g \rangle \tag{3.16}$$

where $T_{life} = 20$ years (converted in days). Since the rule-based algorithm cannot take advantage of different tariffs, we choose the energy price to be constant, i.e. $c_g = 0.2€/kWh$. It follows that the operational cost (3.16) is proportional to the daily average energy drawn from the grid.

Figure 3.8 shows the global cost of the installation over 20 years with an energy cost of $0.2€/kWh$ in function of each pair of values P_v^{max} and E_b^{max}. We superposed on the same figure, the daily consumption and initial investment cost isolines. Given the global cost, the optimal sizing can be choose in two different manners:

1. We set an initial investment cost and we find the sizing corresponding to the minimum global cost located on the initial investment isoline considered.

Table 3.1 – Sizing parameters of the solar home and mean of input variables over the test period

Sizing chosen		**Input data statistics**	
E_b^{max}	8kWh	$\langle P_l^* \rangle$	17.65 ± 0.33 kWh/day
P_v^{max}	4kWp	$\langle P_v^* \rangle$	15.50 ± 0.93 kWh/day
P_g^{max}	3kW	$\langle P_{nl} \rangle$	2.13 ± 0.93 kWh/day

2. We find the sizing corresponding to the minimum total global cost;

We have chosen the first strategy such that the initial investment is 12 k€ (red dotted investment isoline) and the sizing that we have chosen is given by the red pentagon (4kWp, 8kWh). Following the second strategy yields the sizing given by the green petagon. Around this pentagon, is the optimum region (in yellow) that is around about 1.5% of the minimum. It is interesting to notice that the sizing that we have chosen is located within that region. Table 3.1 gives some statistics about the input data that lead to the optimal sizing. The reader interested in more details about the sizing can refer to the paper [Hae+18].

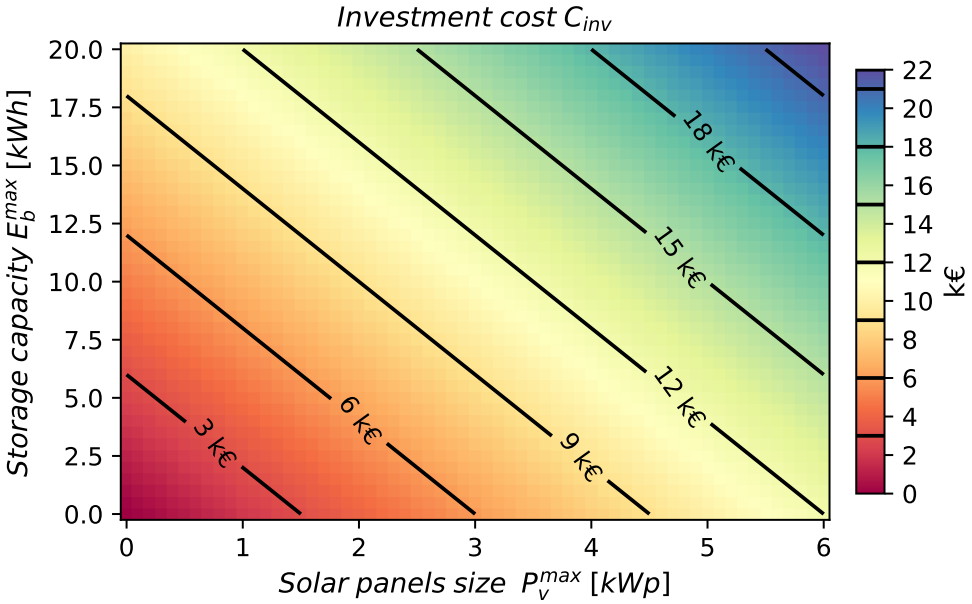

Figure 3.7 – Investment cost depending on the sizing of the solar home components

3.3 Rule based controller for HEMS in absence of outage

Building control has a long story of using simple heuristic base on " *if condition* then *actions*" patterns. Those are the rule-based control algorithms. Although easy to implement and fast enough to run, they are limited when the number of control variables is high (the designer cannot consider all the possible different combinations); hence, it depends greatly on the designer's inspiration and capacity to find good heuristics.

Considering the model described in section 3.2, if the aim is to minimize the energy drawn from the grid, a simple heuristic is to charge the storage units when there is a surplus of solar energy (i.e., solar production P_v^* > to building demand P_l^*) and to use the saved energy to provide the building with its demand once the opposite case occurs. (i.e, $P_v^* < P_l^*$).

In the first case ($P_{nl}(k) < 0$), there is never a need to draw energy from the grid, and no energy is wasted as long as the storage is not full. In the second case, no energy is wasted, but the grid is tapped into as soon as the storage units' energy is not enough to sustain the building demand. In both cases, the shedding variable P_s can either be ignored (to simplify the numbers of variables considered) or set to zero since we suppose

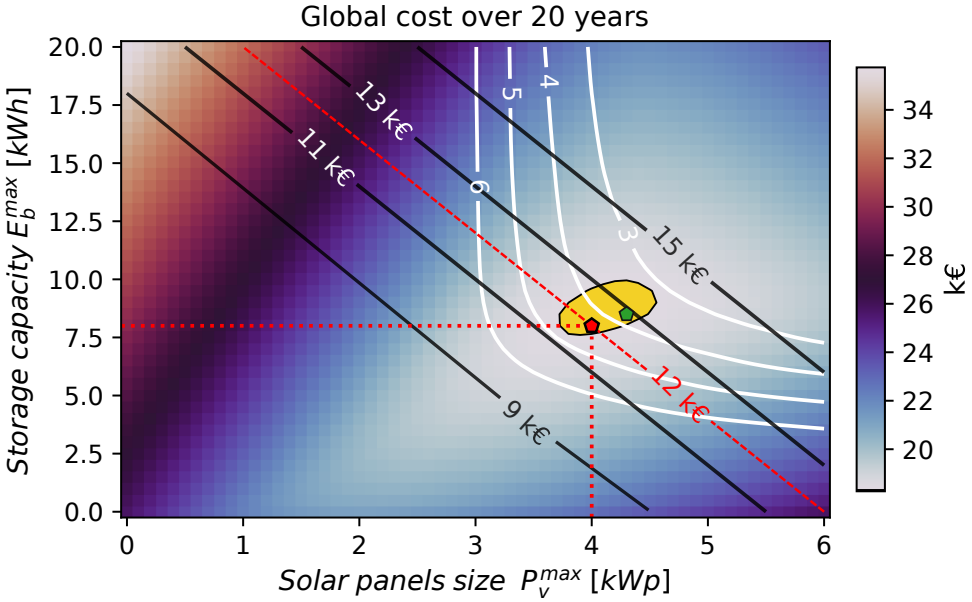

Figure 3.8 – Global cost depending on the sizing of the solar home components with an energy cost of 0.2€/kWh

that at instant k, the nominal grid power P_g^{max} is always sufficient to sustain the higher demand of the building.

Note that it will also be interesting to minimize the electricity bill $c_g(k)P_g(k)$, but since the basic rule-based algorithm cannot take into consideration the variation of the electricity tariffs, both minimization results in the same outcome. The algorithm as described is resumed by its flowchart model given by Figure 3.9.

3.4 Conclusion

This chapter has presented the subject of the application of the algorithms we are going to describe in the following chapters. It is a solar home divided in four parts which can easily be scale to any type of buildings. For our purpose, we have explained the components sizing process, mainly the storage and the solar panels based on the load demand and the minimisation of the global cost. This concludes the first part of our dissertation. In the second part we shall investigate the design of two type of controllers.

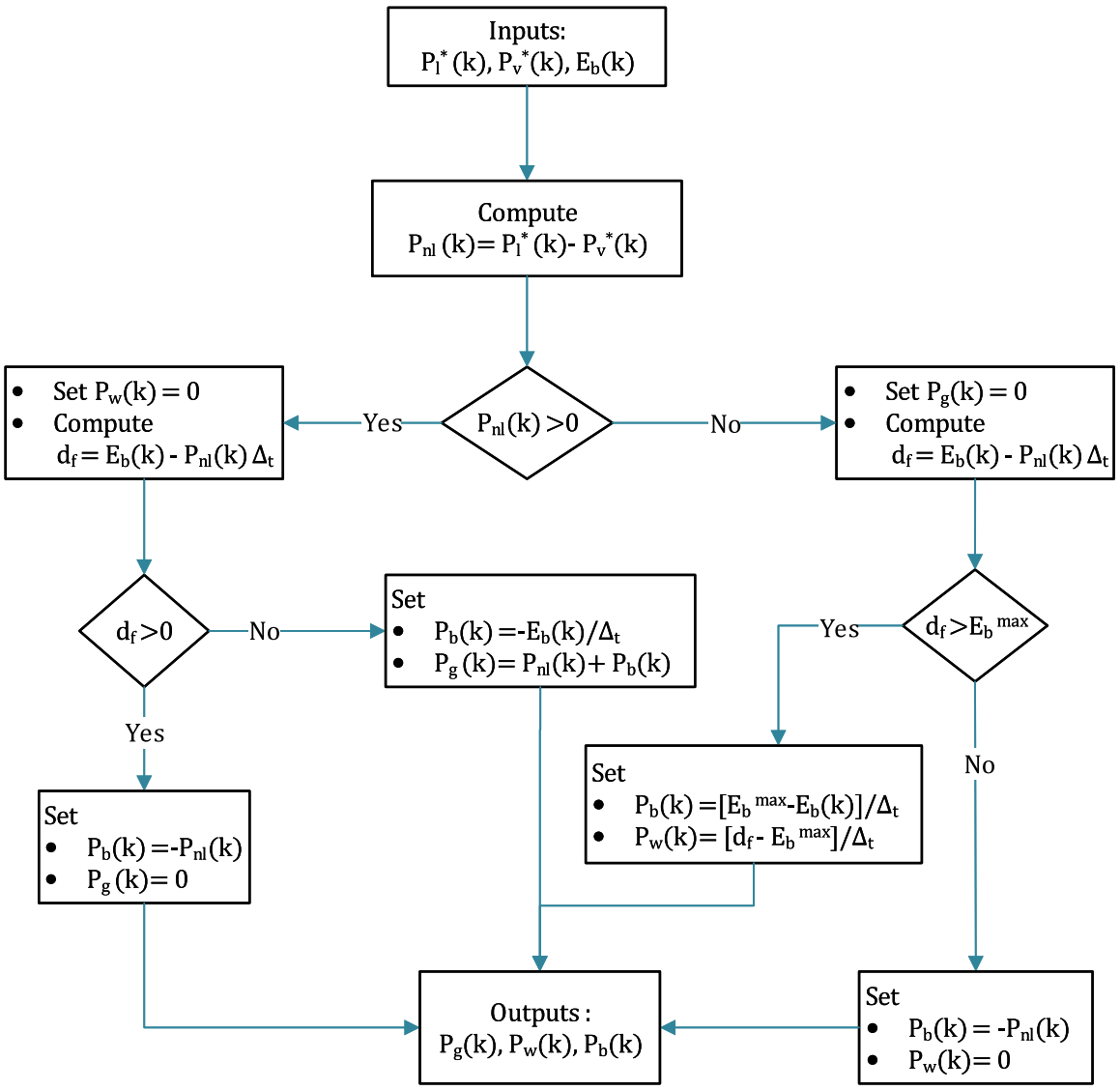

Figure 3.9 – Flowchart algorithm of a Rule-based controller for HEMS.

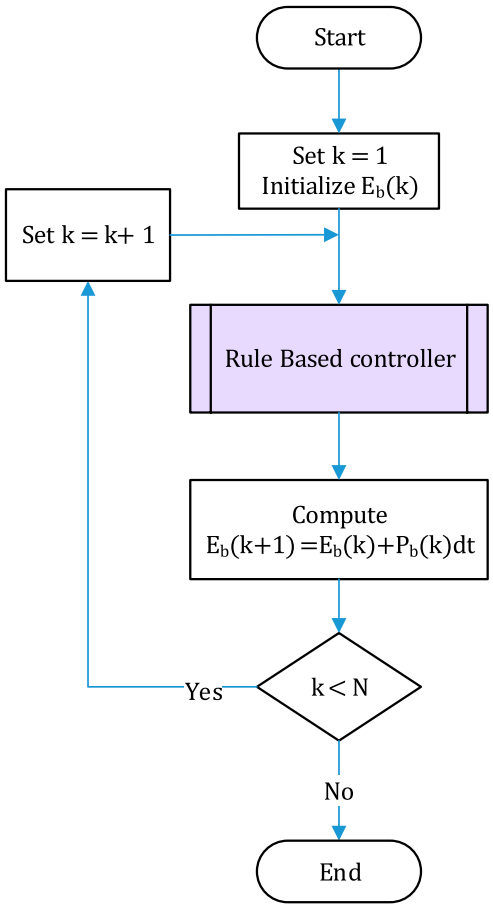

Figure 3.10 – Flowchart algorithm of the Rule-based controller simulation for HEMS.

Part II

Resilient HEMS

Chapter 4

Deterministic discrete Rare event

For me, I am driven by two main philosophies: know more today about the world than I knew yesterday and lessen the suffering of others. You'd be surprised how far that gets you[a]

a. Neil deGrasse Tyson

Contents

4.1 Introduction . . . 65
4.2 Existing methods strategies . . . 66
4.3 Control goals . . . 70
4.4 Classic MPC . . . 70
4.4.1 Main objectives . . . 70
4.4.2 Auxiliary objective . . . 71
4.4.3 Global Objective . . . 71
4.5 The Resilient MPC . . . 74
4.5.1 Global objective . . . 75
4.6 Comparison metrics . . . 76
4.7 Simulation and results . . . 77
4.7.1 Simulation settings . . . 77
4.7.2 Simulation results . . . 79
4.8 Conclusion . . . 88

4.1 Introduction

Most extreme weather events are word-widely becoming more common [Jul+20] and have a significant impact on societies and the environment. One of the many consequences can be the loss of electricity supply for long periods on the buildings' level. During these

periods, the need for electricity supply resilience is prominent. This implies that users should be supplied with electric power even when the grid is undergoing an outage. In this cases, when a nominal level of service cannot be provided, a degraded mode should be used, in which a limited amount of energy, lower than their usual consumption, is provided to customers.

In this chapter, therefore, we are concerned with introducing the concept of resilience in existing controllers. We investigate this integration with controllers based on Model Predictive control described in Chapter 2 when the Rare and Extreme Event (REE) is deterministic. Here, by deterministic REE, we refer to the fact that we have either a complete or no information about the occurrence of the event. This motivates us to focus on the cases of planned (see definition (4.1)) and unplanned (see definition (4.2)) Grid Power Outage (GPO). The resulting controller called ReMPC aims at improving energy resilience during power outages by maintaining at least a minimum level of energy set by the user.

The chapter is organized as follows: in section 4.2, we provide a thorough state of the art of different papers introducing resilience to GPO in their control strategy from the user viewpoint. Section 4.3 explains what are the main goals of a HEMS. Based on these goals, the following section 4.4 introduces the well known *Classic* Model Predictive controller. We present our proposal, a new controller which is an improved version of the classical one well suited to handle GPO in section 4.5. The following section shows and explains simulations' results between our proposed controller, the classical and two states of the art controllers. Conclusion are drawn in the last section 4.8.

4.2 Existing methods strategies

Grid power outages are generally categorized into two classes:

Definition 4.1 (**Unplanned GPO**(UGPO))**.** It refers to an unexpected outage event and is often caused by a sudden grid fault with unknown duration.

It follows that if the controller uses a prevision of the electrical grid state to manage the energy flow within the building, the GPO is not considered until it happens. Once it occurs, the controller considers that it will last forever unless there is a change in the grid's state. Figure 4.1 shows on the third subplot the grid's state over the prevision horizon for an unplanned GPO.

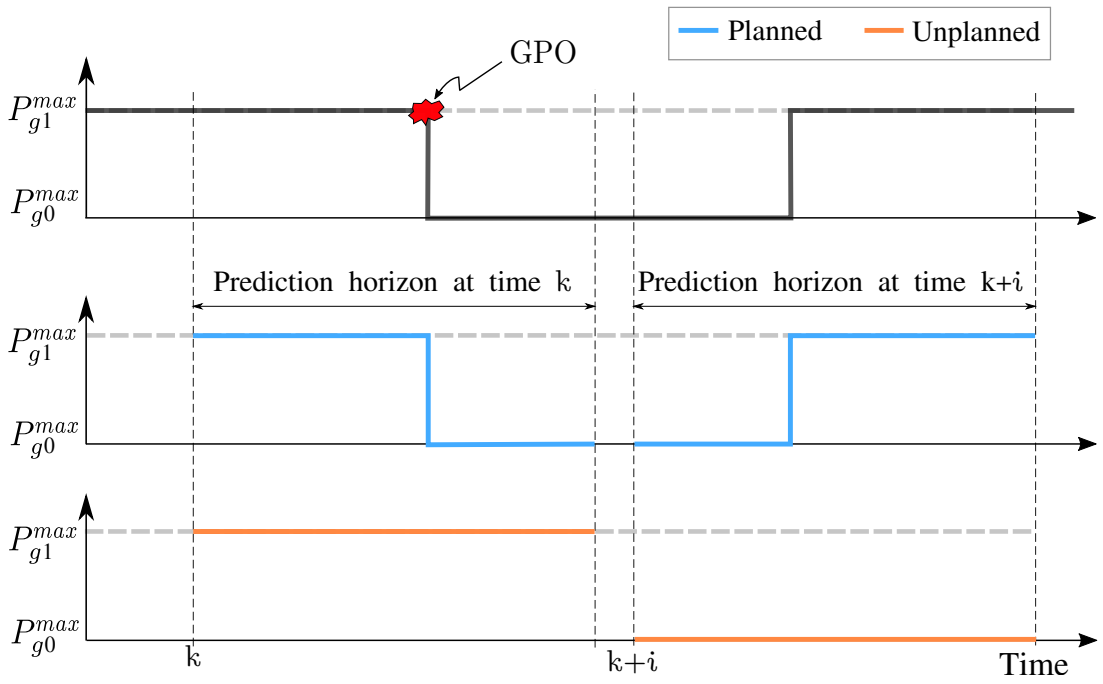

Figure 4.1 – Prevision on the grid state for planned and unplanned GPO

Definition 4.2 (**Planned GPO**(PGPO))**.** It refers to the outage event for which customers are informed in advance and provided with complete information including the date, begin time and duration of the outage.

It follows that if the controller uses a prevision of the electrical grid state to manage the building's energy flow, the GPO is already considered before it occurs. Once it happens, the controller knows exactly how long it will last and can therefore incorporate this information within its prevision. Figure 4.1 shows on the second subplot the grid's state over the prevision horizon for a planned GPO.

Although there are many works on BEMS [BHJ15; Ahm+16; ABG17; Mar+17] to cite only those, a few of them focus on the behavior of the controller before and during outages.

The authors of [Gha+15] proposed three strategies (*greedy, smart, Conservative*) in order to introduce resilience to outages in a house modeled by a Petri-nets (PN). Their *smart strategy* always reserves a fixed part of the storage to be used during outages and offers the best compromise between resilience and flexibility. Their analysis showed a direct relationship between resilience and flexibility since increased resilience, i.e., reserving a higher battery capacity for backup, decreases the storage unit's flexibility. In their

following works, firstly [Jon+16a], the notion of *survivability* (i.e., the probability of surviving a grid outage) is evaluated with a matching yearly production and demand using the *smart strategy*. Secondly, in [Jon+16b], they have proposed a new battery management strategy, the so-called *power-save*, which directly reduces the demand in the case of a power outage.

Using the battery of Plug-in Electric Vehicles (PEVs) as backup generators instead of PV panels+Storage units (often refers to as the "Vehicle-to-Home, V2H" technology), the same demand's reduction, i.e., switching directly to a degraded mode in case of occurrence of outages, is also proposed by the authors of [Roc+14]. However, here two types of degraded modes, high comfort and soft comfort, are proposed and are chosen according to the user settings and the expected outage duration (supposed to be given by the utility). The strategy of using V2H combined with PV panels+Storage units as a backup generator during a GPO is firstly investigated by [Tut+13]. An extension is proposed in [SB17], where they focus on optimizing the energy provided by the PHEV through its onboard engine generator since the latter has a higher efficiency compared to a conventional backup generator. Due to the optimization problem's complexity, they end up proposing a heuristic algorithm based on the optimization result. An extension of V2H to Vehicles to Homes (Vs2Hs) is also proposed where multiple homes, Plug-in Hybrid Electric Vehicles (PHEVs), and PV panels are managed as a small microgrid. This microgrid enables all residences in the system to be provided with backup power regardless of their energy resources possession by sharing energy generation from PHEVs and PVs panels.

From all the previous papers, it is interesting to see that efforts are being made to tackle buildings and houses' energy dispatching during GPOs. However, as engaging as these papers are, they are each limited in one or several manners, as resumed in Table 4.1. Mainly they do not fully exploit flexibility and forecasts in demand as well as in the supply. This chapter comes to close this existing gap.

Table 4.1 – Main features of works on HEMS resilience before and after our proposal.

	Before GPO						**During GPO**	
Paper	Control	Objective	Reserve bat	Active	PGPO	UGPO	Degraded mode	Switching
[Tut+13]	RB V2H	–	×	×			×	–
[Roc+14]				✓			✓: Multiples	✓: Stg dpt
[SB17]			×	×			×	–
[Gha+15]	RB PN	min P_g	✓ Stg dpt	✓			×	–
[Jon+16a]			✓				✓(2modes)	✓: Stg dpt
[Jon+16b]							✓	✓
Our proposal	Opt	min CgP_g	✓ Smart	✓	✓	✓	✓ Smart	✓ Opt dpt
[Zha+19]	Heur Opt	–	×	×			✓: Ld shift	✓: Opt dpt
[Zha+20]	Opt, Heur Opt			✓	✓	×		
[Abe+20]	Opt			×			✓: User dpt	
[GRB20]	Opt				–	✓		

"×": No;

"✓": Yes;

"–": Not considered or not mentioned;

"RB": Rule Based;

"Stg dpt": Setting dependent;

"Heur Opt": Heuristic Optimization, i.e, Natural Aggregation Algorithm (NAA);

"Ld shift": Load shifting;

4.3 Control goals

Considering the house described in Chapter 3, in nominal mode, when there is no outage, our HEMS aims at satisfying two principal goals:

Obj 1: Minimizing the electricity bill;

Obj 2: Maximizing the user comfort.

Maximizing the user comfort means ensuring that at every instant k the whole demand P_l^* is satisfied, i.e., $P_l^* = P_l$. During the consumption peak period, the house demand P_l^* might be higher than the production (by production, we mean the power provided by the grid, the storage units, and the solar panels all together), so the demand ought to be reduced or shedded with P_s.

This implies that satisfying Obj 2. is the same as minimizing the shedding.

During outages, the user would like its house to be provided with a critical power P^c, that is, at least the minimum energy needed to run essentials equipment. The critical power P^c is computed as

$$P^c(k+h) = \alpha(k+h)P_l^*(k+h) \tag{4.1}$$

where

$$\alpha(k+h) \in [0,1] \tag{4.2}$$

is the "comfort coefficient/Critical load fraction".

Note that as described by the equations (4.1) and (4.2) the critical load can either be a fixed quantity or variable quantity. In the former case α must vary depending on the demand P_l^* whereas in the latter case it a constant.

In the following, we are first of all going to describe the classic MPC controller and from that description we would introduce the resilient MPC.

4.4 Classic MPC

4.4.1 Main objectives

Mathematically expressed, the controller objective (1) is to minimize the electricity bill at each instant k over the MPC prediction horizon H :

$$C_G(k) = \sum_{h=0}^{H-1} c_g(k+h) P_g(k+h|k), \quad \forall\, k \in \mathbb{N}_1^N. \tag{4.3}$$

We recall that $c_g(k+h)$ is the electricity tariff at the instant $k+h$ of the prediction horizon. Note also that if $c_g(k+h)$ is constant on the time horizon, minimizing the electricity bill is the same as minimizing the energy consumed from the grid.

The control objective (2) is to minimize the total load shedding cost given by

$$C_S(k) = \sum_{h=0}^{H-1} c_s(k+h) P_s(k+h|k), \quad \forall\, k \in \mathbb{N}_1^N. \tag{4.4}$$

where $c_s(k+h)$ is the the shedding usage penalty, i.e., a virtual tariff associated with shedding energy at instant $k+h$.

4.4.2 Auxiliary objective

Besides its main objectives, the controller should also satisfy an additional constraint that is to avoid wasting the PV energy as long as possible. This is insured by minimizing the following cost

$$C_W(k) = \sum_{h=0}^{H-1} c_w(k+h) P_w(k+h|k) \tag{4.5}$$

where $c_w(k+h)$ is the the energy wasting usage penalty, i.e., a virtual tariff associated with curtailing energy at instant $k+h$.

4.4.3 Global Objective

The global objective of the controllers is to minimize simultaneously three sub-objectives functions given by (4.3), (4.4) and (4.5) among which two are conflicting, namely (4.3) and (4.4). It is so since the easiest way to minimize the electricity bill is to draw no energy from the grid, which can be achieved by maximizing the load shedding (not providing the house with its demand). This gives rise to a high discomfort that must be avoided; hence, the need to minimize the load shedding.

A multiple objectives optimization problem ought to be solved. Many methods to solve a multi-objective optimization convert it into one or a set of single-objective problems. The most common approaches are:

- Linear scalarization [Nog15]: Also known as the *weighted-sum method*; the sub-objectives are aggregated with user-supplied positive weights which serve to normalize the main cost functions as well as organize the sub-objectives function priority;

- ε-Constraint method [YLD71; Deb14]: Only one of the sub-objectives is kept in the reformulated optimization problem objective while the rest are restricted within user-specified values, i.e., they are converted to constraints;

- Lexicographic optimization [Ise82; CPS18]: The sub-objectives are ordered by a user-defined priority called the *lexicographic order*. Then a sequential optimization where the low sub-objectives are optimized as far as they do no interfere with the higher priority sub-objectives is solved.

Linear scalarization is the most common method that is used to solve applied multi-criterion optimization problems. Because of its simplicity, it is also the one we use in this thesis. Although simple, the weights associated with each sub-objective function ought to be chosen such that it transcribes the wanted priority. We especially want to associate both the auxiliary (4.5) and (4.4) with higher proportional priority while a lower priority is given to (4.3). At each instant $k+h$ of the prediction horizon,

$$c_w(k+h) = c_s(k+h) \tag{4.6a}$$
$$c_w(k+h) \gg c_g(k+h). \tag{4.6b}$$

The cost J_{CLAS} optimized by the classic MPC is therefore given by:

$$\begin{aligned} J_{CLAS}(k) &= C_G(k) + C_C(k) + C_S(k) \\ &= \sum_{h=0}^{H-1} c_g(k+h)P_g(k+h|k) + c_s(k+h)P_s(k+h|k) \\ &\qquad + c_w(k+h)P_w(k+h|k) \end{aligned} \tag{4.7}$$

and the classic controller optimization is set as follow:

Problem 4.1 (Classic MPC).

$$\min_{\{P_g,P_b,P_s,P_w\}(k+h|k)} \quad J_{CLAS}(k) \tag{4.8a}$$

s.t. $\forall h \in \mathbb{N}_0^{H-1}$

$$0 \leq P_g(k+h|k) \leq P_g^{max} \tag{4.8b}$$

$$0 \leq P_w(k+h|k) \leq P_v^*(k+h) \tag{4.8c}$$

$$0 \leq P_s(k+h|k) \leq P_l^*(k+h) \tag{4.8d}$$

$$0 \leq E_b(k+h|k) \leq E_b^{max} \tag{4.8e}$$

$$P_v(k+h|k) = P_v^*(k+h) - P_w(k+h|k) \tag{4.8f}$$

$$P_l(k+h|k) = P_l^*(k+h) - P_s(k+h|k) \tag{4.8g}$$

$$E_b(k+h+1|k) = E_b(k+h|k) + P_b(k+h|k)\Delta_t \tag{4.8h}$$

$$P_g(k+h|k) - P_b(k+h|k) + P_v(k+h|k) = P_l(k+h|k) \tag{4.8i}$$

Let us consider in the prediction horizon two separates instants indexed by $(k+i|k)$ and $(k+j|k)$ with $i < j < H$. At these two instants, the building demand is the same, i.e., $P_l^*(k+i) = P_l^*(k+j)$, the PV panels are not producing any energy, i.e., $P_v^*(k+i) = P_v^*(k+j) = 0$, a GPO is occurring and the energy within the storage is enough to sustain the load for only one of the considered instants. Given that the shedding tariff at both instants is the same $c_s(k+i) = c_s(k+j)$, optimally, the controller can either shed the demand at either of these instants since they are costly equivalent. However, from the user perspective, from a comfort viewpoint, it is best to shed the energy at the last instant because it does not make sense that the storage unit has some energy but does not provide the building with its demand.

In order to avoid this situation we use a simple trick that is to set different tariffs at both instants; respectively a higher and lower tariff at $k+i$ and $k+j$, i.e., $c_s(k+i) > c_s(k+j)$. This compels the controller to delay the shedding until the instant $k+j$ since its cost is lower than that of $(k+i)$. Considering the whole MPC horizon, we have:

$$c_s(k) > c_s(k+1) > \ldots > c_s(k+H-1). \tag{4.9}$$

The same logic is also valid for the wasted energy when the battery is full, the energy

provided to the load meets the demand, and the grid is not used. In this case, we have:

$$c_w(k) > c_w(k+1) > \ldots > c_w(k+H-1). \tag{4.10}$$

Considering (4.9), (4.10) and that different tariffs are applied at different instants of the prediction horizon, the relation between all the tariffs (4.6a) stays the same but (4.6b) is rewritten as follows:

$$c_s(k+H-1) \gg max\Big[c_g(k+h), \quad \forall\, h \in \mathbb{N}_0^{H-1}\Big]. \tag{4.11}$$

4.5 The Resilient MPC

The classsic controller is by no doubts the best controller to be used in nominal mode. However its main drawback appears in degraded mode, i.e., during a GPO: it does not consider the user specified demand which is to provide the house with a critical power P^c, the minimum energy needed to run essentials equipment. The ReMPC finds a solution to this problem by improving the classsic controller as follows.

The user specified demand that must be satisfied during GPO is expressed as the constraint:

$$P_l^*(k+h) - P_s(k+h|k) \geq P^c(k+h). \tag{4.12}$$

which means that the minimum energy that must be provided to the building is $P^c(k+h)$, but if there is a possibility to provide more, the controller can do so as long as it does not imply going bellow the critical energy on the overall prediction horizon.

It is important to notice that (4.12) cannot hold at all time since if there is no energy within the storage units, even the critical power cannot be satisfied. In this situation, to ensure that the problem is always feasible, we introduce the critical shedding P_s^c that is a relaxation decision variable of (4.12) as

$$P_l^*(k+h) - P_s(k+h|h) \geq P^c(k+h) - P_s^c(k+h|h). \tag{4.13}$$

with

$$P_s^c(k+h|h) \geq 0 \tag{4.14}$$

Remark 4.1. Note that there is a high similarity between both the shedding P_s and the critical shedding P_s^c. The former relaxes the nominal demand (see equation (3.9))

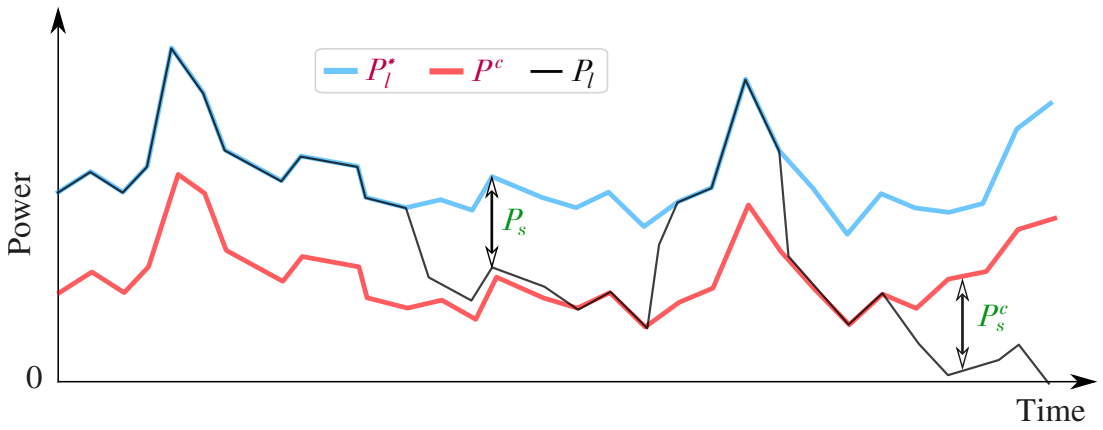

Figure 4.2 – Relation between P_l^*, P_s P^c, P_s^c

while the latter relaxes the critical energy demand. Figure 4.2 shows the relation between P_l^*, P_s P^c, P_s^c

In order to use the added critical shedding P_s^c only when needed, i.e., only when the controller can no longer provide the critical power P^c to the house, the following critical shedding cost must be minimized :

$$C_S^C(k) = \sum_{h=0}^{H-1} c_s^c(k+h) P_s^c(k+h|k), \quad \forall\, k \in \mathbb{N}_1^N. \tag{4.15}$$

where $c_s^c(k+h)$ is the the critical energy shedding usage penalty, i.e., a virtual tariff associated with shedding the critical energy at instant $k+h$.

4.5.1 Global objective

The global objective of the ReMPC is given by:

$$\begin{aligned} J_{ReMPC} &= C_G(k) + C_C(k) + C_S(k) + C_S^C(k) \\ &= J_{CLAS}(k) + C_S^C(k) \end{aligned} \tag{4.16}$$

Giving that we are using linear scalarization as a mean of solving the multi objective optimization, the new added sub-objective given by (4.15) must be associated with a priority in the global objective. It gets the higher priority since we only want to use the

critical shedding as last resort. We therefore set the cost associated $c_s^c(k+h)$ as follows:

$$c_s^c(k+h) > c_s(k). \tag{4.17}$$

The problem resolve by the ReMPC controller is given by:

Problem 4.2 (**Resilient MPC**).

$$\min_{\{P_g,P_b,P_s,P_w,P_s^c\}(k+h|k)} \quad J_{ReMPC}(k) \tag{4.18a}$$
$$\text{subject to } \forall h \in \mathbb{N}_0^{H-1},\ (4.8b), (4.8c), \ldots, (4.8i), (4.13), (4.14)$$

4.6 Comparison metrics

In order to compare both the Classical and Resilient model predictive controllers (CMPC and ReMPC, we have defined the following metrics:

- The load satisfaction ratio L_{sr}
$$L_{sr} = \frac{P_l}{P_l^*} \tag{4.19}$$
computed for each instant k of the problem horizon. During a GPO, the controller must provide the house with at least its critical power, i.e., $P_l = P^c$ such that the minimum or critical satisfaction ratio is given by:
$$L_{sr}^c = \frac{P^c}{P_l^*}. \tag{4.20}$$

- The load satisfaction level L_{sl} which is divided in three parts:
  - ◇ Bad (L_{sl}^-)
  $$L_{sl}^- := 0 \leq P_l < P^c \text{ or } 0 \leq L_{sr} < L_{sr}^c;$$
  - ◇ Good (L_{sl}^+)
  $$L_{sl}^+ := P_c \leq P_l < P_l^* \text{ or } L_{sr}^c \leq L_{sr} < 1;$$
  - ◇ Perfect (L_{sl}^*)
  $$L_{sl}^* := P_l = P_l^* \text{ or } L_{sr} = 1.$$

- The fraction of time spent at each of the three previous defined levels during the total period of GPO,

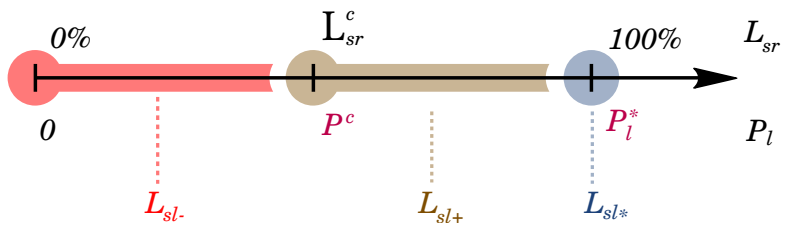

Figure 4.3 – Load satisfaction levels and their corresponding load satisfaction ratios.

- ◇ τ^-: Fraction of Time spent at L^-_{sl}
- ◇ τ^+: Fraction of Time spent at L^+_{sl}
- ◇ τ^*: Fraction of Time spent at L^*_{sl}.

- The energy cost [€]

$$En_{cost} = \sum_{k=1}^{N} c_g(k) P_g(k) \Delta_t. \tag{4.21}$$

Figure 4.3 shows the relationship between the load satisfaction ratio L_{sr}, the power provided to the house P_l and the different load satisfaction levels.

Besides the previous metrics, we also use the control variables, mainly the power drawn from the grid P_g, the power not provided to the house P_s and the power wasted P_w.

4.7 Simulation and results

4.7.1 Simulation settings

For the rest of this chapter, we compare our ReMPC firstly with the CMPC, then with two other rule-based controllers, of which the first is the *smart strategy controller* described by [Gha+15; Jon+16b] and the second is *the power save controller* also described in [Jon+16b]. We emphasize that, in these papers, the controllers are implemented using Petri Nets. However, since we are not familiar with this framework but understand the algorithms' logic, we have re-coded them. Both controllers are mainly based on the Rule-based algorithm described in section 3.3 but with some improvements to make them resilient.

The *smart strategy controller* that we have renamed the Rule Based Controller with Reserve (RBC-R) always keeps the storage at a certain minimum capacity E_b^{min} as a backup when the grid is available. This restriction is removed once a GPO occurs. The

the power save controller that we have renamed the Rule Based Power Save Controller with Reserve (RBPSC-R) behaves exactly the as *smart strategy controller* when the grid is available, thus reserving a part of the storage capacity as backup. However, during a GPO, a predetermined part of the demand is reduced, i.e., the controller provides only the critical load demand. The simulations are carried with a battery backup capacity of 20% and 30% of the maximum storage capacity E_b^{max}, as stipulated by the authors.

We simulate over a low, normal and high load demand and solar production period in order to observe the controllers behaviour in different situations. Given the data of the test set shown in Figures 3.5 and 3.6, the lowest PV production period is June 2013 (127kWh) while the highest is September 2012 (285kWh). We compute the monthly average PV production (i.e. $\simeq$ 208 kWh), and we choose the month with the closest value, that is November 2012 to be the normal PV production period. For the given months, the load demand are 234kWh, 239kWh and 242kWh for respectively June 2013, November 2012, September 2012 and the period where the GPOs occur are highlighted in light red in figure 4.5. For each month, we have chosen the total duration of the GPO to be ten days spread heuristically over the month, in four different periods. Whether scheduled or unscheduled, we suppose that a GPO always starts at 00h the first day and finishes at 23h59 the last day. The electricity's tariff during a day for the selected customer consists of two energy prices for two periods:

- c_{night}: Off peak hours from 00h to 05h59
- c_{day} Peak hours, from 06h to 23h59

and are resumed by Figure 4.4.

In the event of a GPO, the user specifies that the building's energy needs must be met

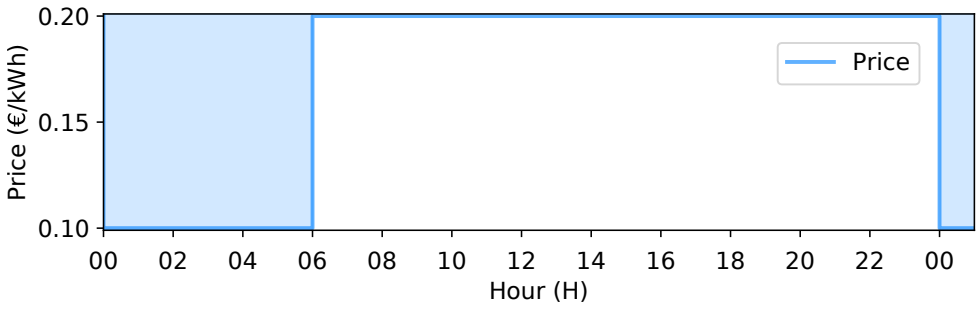

Figure 4.4 – Evolution of the electricity's price for a simulation day. The off-peak period (00h to 05h59) where the electricity price is the lowest are colored in light blue.

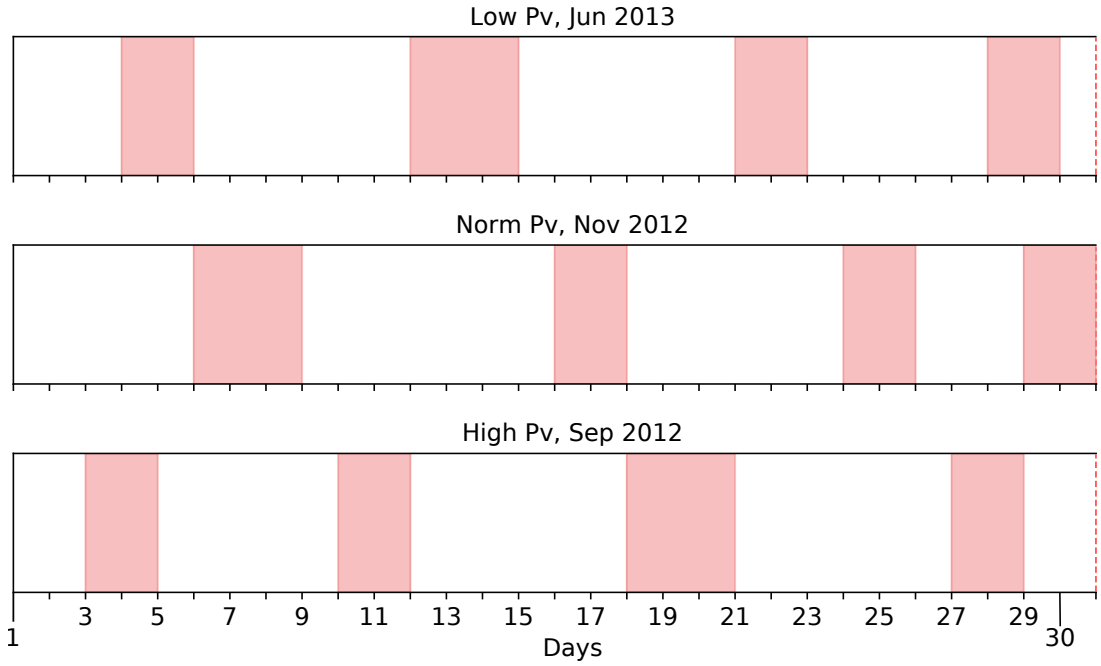

Figure 4.5 – GPO period within the test set.

by at least 50% of its nominal demand, that is:

$$P^c(k+h) = 0.5P_l^*(k+h) \tag{4.22}$$

We consider a whole day (H=48, i.e., 24h) as prediction horizon based on the work presented in [Hae+18]. We also add a virtual day with zero load demand and solar production at the end of each simulated month to make up for the last day MPC horizon and have an empty storage at the end of each simulation, which facilitates the comparisons.

4.7.2 Simulation results

The analysis in this section is divided into two parts. First, we compare the ReMPC and the CMPC that does not consider resilience; then, the following is a comparison with two existing controllers that integrate resilience, i.e., the RBC-R and RBPSC-R. We emphasize that since the latter, given their nature, cannot incorporate predictions, it makes more sense that the comparison is performed considering unscheduled GPOs.

Tables 4.2 (associated with the ReMPC and the CMPC) and 4.3 (associated with the RBC-R and the RBPSC-R) show the global result mainly the cumulated energy (in kWh) of the most important decision variables , the energy cost En_{cost} and the comparison

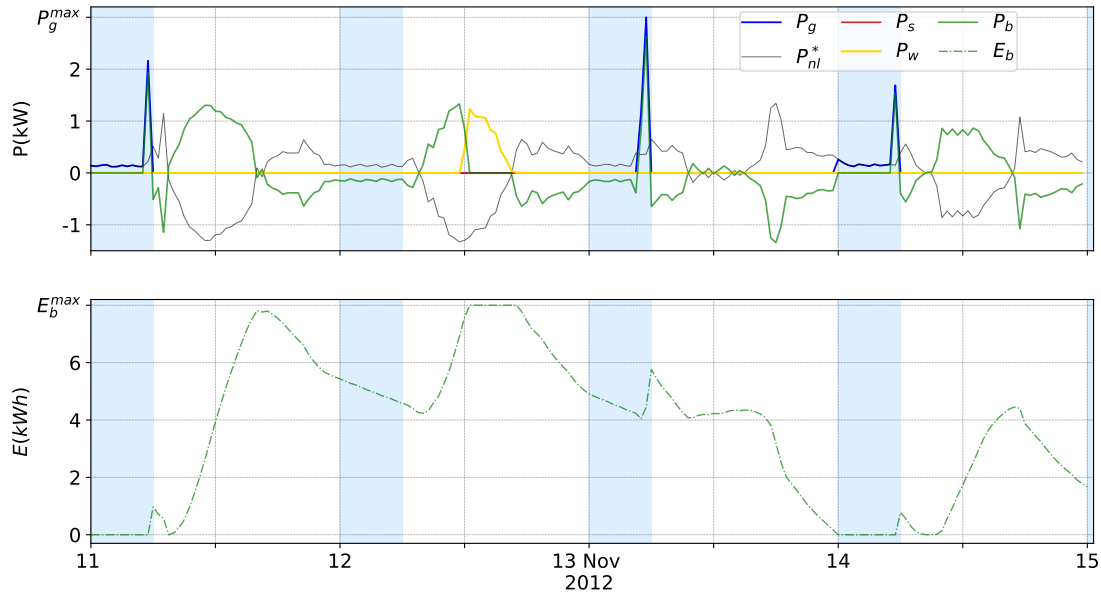

Figure 4.6 – Evolution of the net load P_{nl}^*, the decision variables P_g, P_s, P_w, P_b (First sub-figure) and the energy within the storage E_b (Second sub-figure) for 4 days without outage for the CMPC (Identical to the ReMPC).

metric L_{sl}. About the latter, the tables mentions the time spent at each load satisfaction level τ in percentage of the total GPO duration.

ReMPC vs CMPC

Figure 4.6 shows on its first and second subplots respectively the evolution of the decision variables P_g, P_s, P_w, P_b and energy in the storage E_b for a period (11 to 14 November 2012) with no outages. Figures 4.8 and 4.7 depict the behavior of both controllers respectively during an Unplanned Grid Power Outage (UGPO) and Planned Grid Power Outage (PGPO) for the same normal PV production and load demand period. The considered period covers from 14 to 17 November 2012 and the outage starts at the beginning of 16 November, as indicated by Figure 4.5.

Both controllers have the same behaviour as long as there is no GPO. They do not draw energy from the grid during peak times. However, during off-peak hours, they draw more than needed by the load (since the energy tariff is lower than usual), but just enough so that during the daylight time, the surplus of energy provided by the PVs panels fills the storage without going to waste. The excess of energy is indicated by a negative netload, while a positive one reflects a load demand higher than the PV production. The first subplot of Figures 4.8 and 4.7 show that the integration of the starting instant of the GPO results in the controllers changing their behaviour: to anticipate the GPO, they draw more energy from the grid. This implies for each month simulated that the energy drawn from the grid in the case of a PGPO is always higher than that of an unscheduled GPO. For example, as indicated by Table 4.2, 30kWh compared to 23.7kWh for a normal PV period. More energy drawn from the grid, in its turn, results in reducing the total energy not provided to the house P_s during the whole simulation.

During the outage, a critical load satisfaction ratio L^c_{sr} of 50% is wanted given the user specifications. A horizontal red line indicates this on the second subplot of Figures 4.8 and 4.7. Referring to the same figures, as soon as the UGPO occurs, both controllers go under the L^c_{sr} since there is no energy within the storage. During the daylight time, when the PVss generate enough energy, both controllers provide the whole demand. However, at the beginning of 17 November, the ReMPC switches to provide only the minimum energy needed to the house while the CMPC provides the whole demand. Due to the energy reserve resulting from the switching, the former outperforms the latter, providing the minimum energy needed longer. It is also the case in all the different PV production

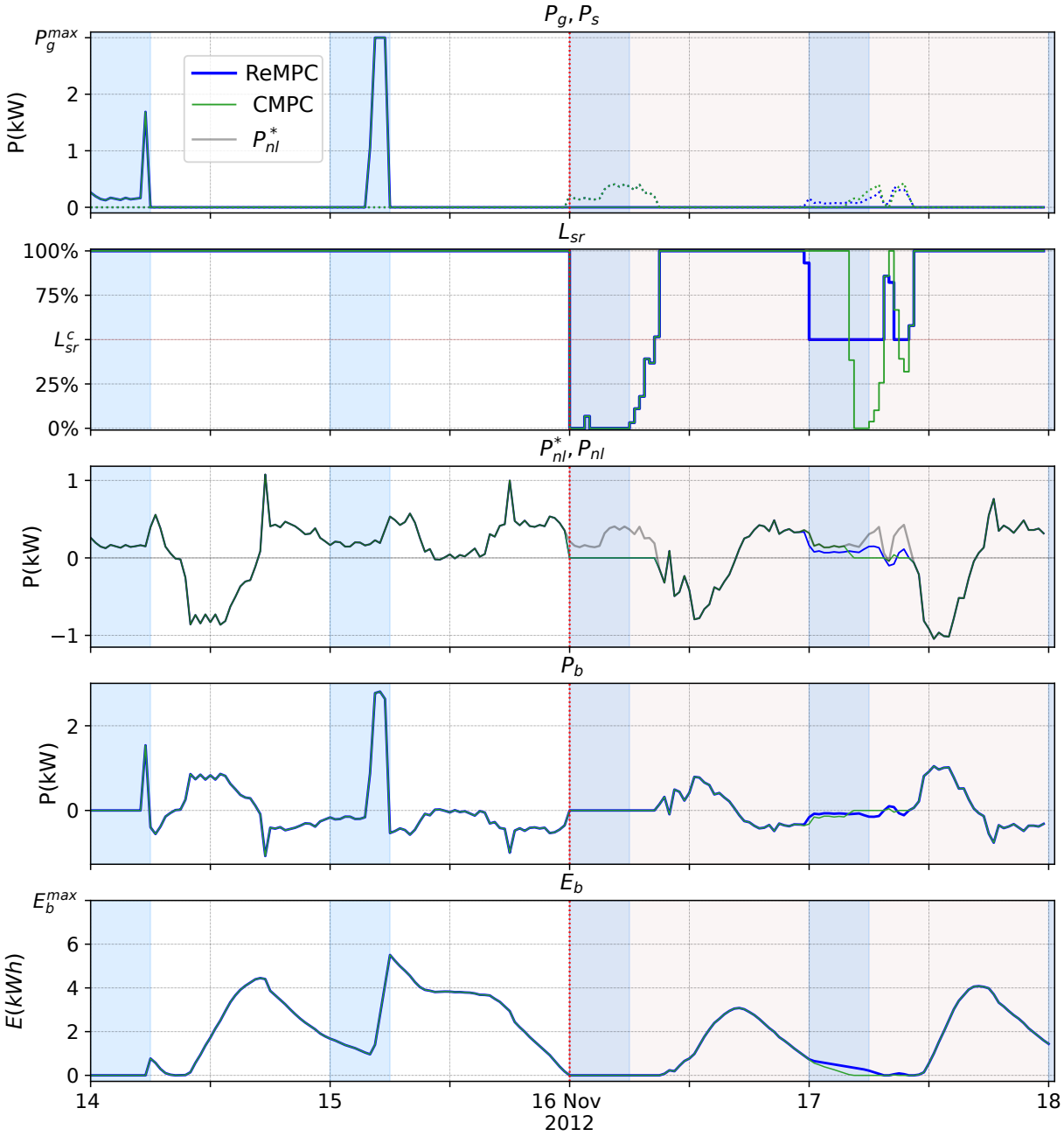

Figure 4.7 – Behaviour of CMPC and ReMPC in case of an unplanned GPO. The figure shows the evolution of the energy drawn from the grid P_g (solid line) the energy not provided to the load P_s (dotted lines) (first sub-figure), the load satisfaction ratio L_{sr} (second sub-figure), the net load P_{nl}^* (grey) and the net load controller P_{nl} (third sub-figure), the energy out of/into the storage P_b (fourth sub-figure) and the energy within the storage E_b (fifth sub-figure) for a simulation of 4 days where the GPO appears at the beginning of 16 November 2012). All the lines colored in blue are related to the ReMPC while the one colored in green are related to the CMPC.

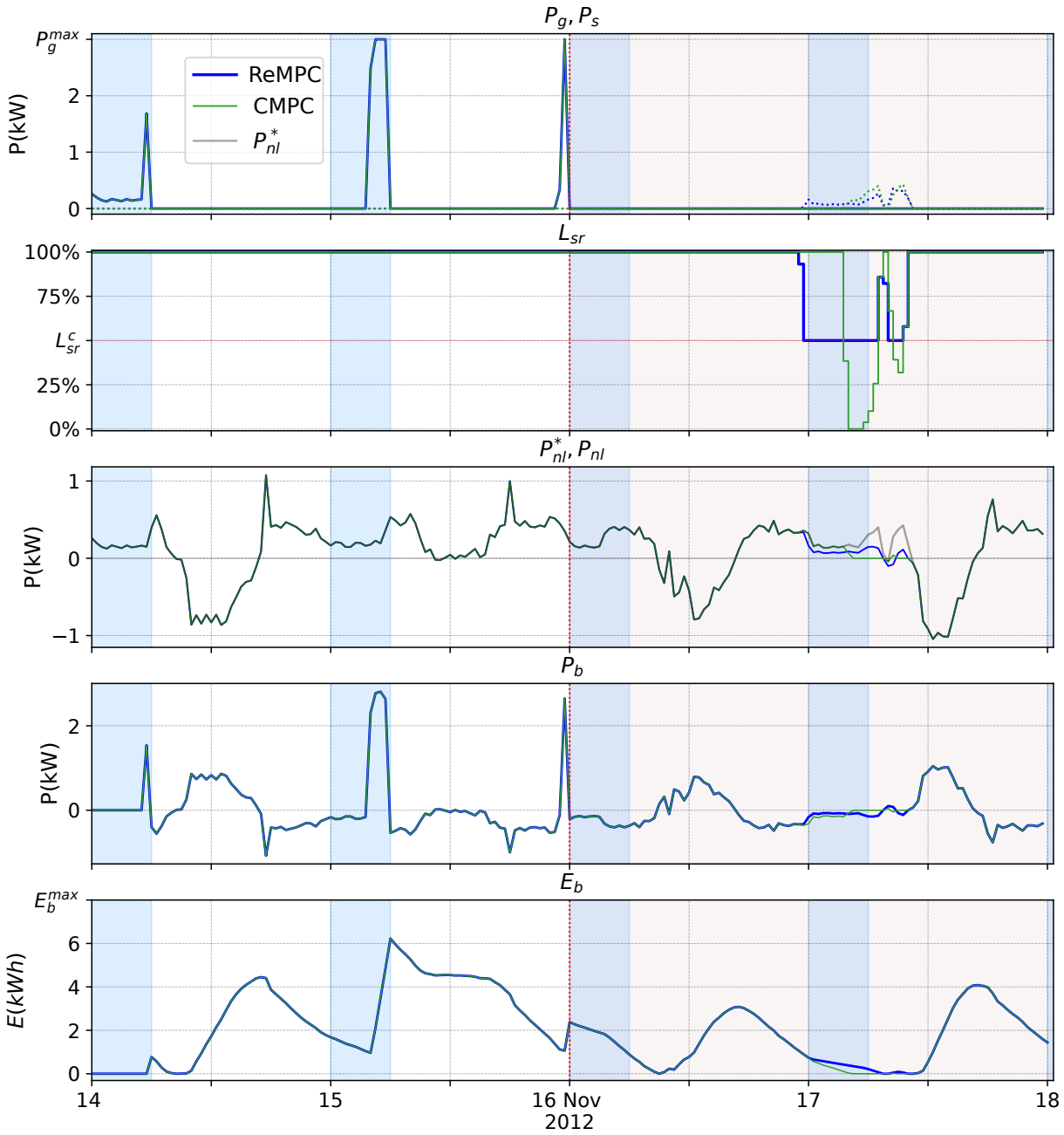

Figure 4.8 – Behaviour of CMPC and ReMPC in case of an planned GPO. The figure shows the evolution of the energy drawn from the grid P_g (solid line) the energy not provided to the load P_s (dotted lines) (first sub-figure), the load satisfaction ratio L_{sr} (second sub-figure), the net load P_{nl}^* (grey) and the net load controller P_{nl} (third sub-figure), the energy out of/into the storage P_b (fourth sub-figure) and the energy within the storage E_b (fifth sub-figure) for a simulation of 4 days where the GPO appears at the beginning of 16 November 2012). All the lines colored in blue are related to the ReMPC while the one colored in green are related to the CMPC.

scenarios apart from the planned GPO high PV. Let us consider column τ^- of Table 4.2 for both GPO. For all cases, on average, the classic stays $\simeq 8.5\%$ longer under the bad load satisfaction level.

During the whole simulation, as for wasted energy, integrating the GPO starting time does not affect it since we notice the same quantity in both cases of outages. Besides the higher the PVs production, the higher the wasting since the load demand does not follow the production's evolution. Mainly the monthly energy difference between the high and low PV production is $\simeq 81$kWh while it is only $\simeq 8$kWh for the load demand.

ReMPC vs RBC-R and RBPSC-R

We recall that the comparison is made between the controllers in the case of an UGPO and that we refer to Table 4.2 and 4.3.

Let us first consider the energy drawn from the grid before the outage. The ReMPC is below both contenders in all cases apart from the Low PV production scenario with the RBPSC-R. If we focus on the total energy not provided to the house during the simulation, the ReMPC falls short behind the RBC-R but outperforms the RBPSC-R in all cases. For the wasted energy, the resilient controller outperforms both contenders by wasting less energy in all scenarios. As for the energy cost, the ReMPC's is lower than its contenders' since it can anticipate the electricity tariffs.

Let us now consider the fraction of time spent at each satisfaction level, especially the time spent not satisfying the minimum energy needed P^c; we refer to the column τ^-. Although the RBC-R has drawn more energy from the grid in all scenarios due to its storage backup, it falls slightly behind the ReMPC in the Low and normal PV with 20% storage but has approximately the same performance for the other cases. As for the RBPSC-R, it outperforms the resilient controller in all cases but in the High PV scenario. This is certainly due to the fact that at the starting instants of the outages, the remaining energy inside the battery with the resilient strategy is always lower than the contenders' with 20% and 30% backup.

To prove this point, we have simulated the ReMPC for the UGPO with the same storage backup capacities as the contenders by modifying equation (4.8e) as follows:

$$S_b E_b^{max} \leq E_b(k+h|k) \leq E_b^{max}, \tag{4.23}$$

Table 4.2 – Performances of the CMPC and the ReMPC for planned and unplanned GPOs

		Planned GPO						**Unplanned GPO**					
		$P_g \mid En_{cost}$	P_s	P_w	Time spent at L_{sl} during GPO (in %)			$P_g \mid En_{cost}$	P_s	P_w	Time spent at L_{sl} during GPO (in %)		
Scenario	Controller				τ^-	τ^+	τ^*				τ^-	τ^+	τ^*
Low PV	CMPC	90.6 | 10	16	0	22.5	1.6	75.9	76.5 | 7.6	30.1	0	37.7	2.3	60
	ReMPC				4.4	34.3	61.3				24.3	39.1	36.6
Norm PV	CMPC	30.1 | 3.55	11.8	11	9.5	1.0	89.5	23.7 | 3.37	18.1	11	17.8	13.7	68.5
	ReMPC				0	19.4	80.6				10	132.4	57.6
High PV	CMPC	6.9 | 0.75	0	45.7	0	0	0	6.0 | 0.6	0.92	45.7	1.9	0	98.1
	ReMPC										0.2	3	96.8

Table 4.3 – Performances of the RBC-R and RBCPS-R controllers for Unplanneds GPOs

		RBC-R						**RBCPS-R**					
		$P_g \mid En_{cost}$	P_s	P_w	Time spent at L_{sl} during GPO (in %)			$P_g \mid En_{cost}$	P_s	P_w	Time spent at L_{sl} during GPO (in %)		
Scenario	Bat Backup				τ^-	τ^+	τ^*				τ^-	τ^+	τ^*
Low Pv	20%	85.5 | 14.8	21.1	0	27.1	2.3	70.6	73.6 | 12.8	37.7	4.9	10.9	89.1	0
	30%	89.3 | 15.5	18.7	1.28	24.1		73.6	76.1 | 13.3	37.0	6.4	9.0	90.9	
Norm PV	20%	31.9 | 5.21	14.8	15.9	12.0	1.4	86.6	24.8 | 4.1	37.7	28.4	2.1	97.9	
	30%	36.7 | 6.0	13.2	19.1	10	1	89.	29.5 |4.9	37.1	32.4	0	100	
High PV	20%	13.1 |1.78	0	51.9	0	0	100	11.2 | 1.5	35.9	85.4	0	100	
	30%	18.4 | 2.69		57.2				16.1 |2.3		90.4			

Table 4.4 – ReMPC with storage reserve performances: Unplanned GPO

Scenario	Bat Backup	Unplanned GPO					
		$P_g \mid En_{cost}$	P_s	P_w	Time spent at L_{sl} during GPO (in %)		
					τ^-	τ^+	τ^*
Low PV	20%	83.6 | 9.04	24.62	0	10.9	47.4	41.7
	30%	88.4 | 10.3	21.8	1.2	9.0	43.3	47.7
Norm PV	20%	31.7 | 3.35	14.9	15.8	3	24.1	72.9
	30%	35.5 | 4.00	13.3	17.9	1.4	22.4	76.2
High PV	20%	11.1 | 1.18	0	49.9	0	0	100
	30%	15.6 | 1.71		54.4			

where S_b is the storage backup defined as

$$S_b \begin{cases} \in \{20\%, 30\%\} & \text{if } P_g^{max}(k) = P_{g1}^{max} \\ = 0 & \text{if } P_g^{max}(k) = P_{g0}^{max}. \end{cases} \tag{4.24}$$

Table 4.4 summarises the results associated.

Including a storage reserve in the resilience, strategy leads to drawing more energy from the grid. In average, for $20\%E_b^{max}$ and $30\%E_b^{max}$ we observe, respectively $\simeq$ 7kWh and $\simeq$ 11kWh (when compared to the ReMPC with no reserve), and $\simeq$ 6kWh (when compared to the RBPSC-R). However the total energy, cost is still lower in contrast to the RBC-R and RBPSC-R.

Concerning the time spent not providing the building with its critical load demand, the performances have improved, mainly they are equal (in the low and high PV scenarios) and closer (Norm PV) to the RBPSC-R's. On this metric, if we focus on the norm PV scenario, although the gap between the controller's performances is tight, one could argue that the RBCPS-R is better and yet it is essential to notice that it spends no time satisfying the total demand while the ReMPC does. This is due to the prevision horizon H of the MPC strategy. Exhaustively, during a GPO, as long as the energy dispatching over the prediction horizon allows satisfying the total demand for a certain period (within the prediction horizon) without, later on, going bellow the critical threshold, L_{sr}^c the controller

does so. Therefore, setting the ReMPC with a longer prevision horizon during an outage becomes essential if we care about reducing, even more, τ^-. For instance, setting the prevision horizon to 32 Hours during a GPO moves τ^- to 2.1 and 0 for respectively, the 20% and 30% storage backup. We emphasize that the added value of increasing the prevision horizon is not very important since, even with the default prevision horizon of 24 Hours, when the RBPSC-R is better at the τ^- the ReMPC makes up for it by spending more time at L^*_{sl}.

4.8 Conclusion

We have presented in this chapter a new type of controller for HEMS called the Resilient Model Predictive Controller (ReMPC). It is a multi-objective model predictive controller for resilience, i.e., it adapts its behaviour during GPOs in order to provide buildings with their minimum energy demand or more if possible, all this minimizing the time spent under a critical user-defined load. We have compared its performances to state of the art controllers designed for the same purpose. The results have shown that during outages, the RMPC outperforms its contenders since sometimes, it satisfies more than the building's demand without getting under the critical demand later on.

We emphasize that since our paper [Pri+19] (on which this chapter is based) has been published, to the best of our knowledge four others have proposed resilient controllers similar to ours. In the first [GRB20], a model predictive-based controller sends signals directly to actuators controlling three critical loads according to a certain priority defined by the user but does not include a strategy for before and after the outage. The authors of [Zha+19] propose a controller for residential communities, aiming to maximize the energy provided to loads during a planned GPO by the process of load shifting (see [CRC14]). The paper focuses on the control at the Community Energy Management System (CEMS) level leaving the individuals HEMS for their following paper [Zha+20]. In [Abe+20], PHEVs are used in a Vehicle to Grid (V2G) scheme during short duration planned GPO.

It goes without saying that all these works are interesting each in their way. However they all integrated the GPO considering that a deterministic information is known about its occurrence: the GPO is planned or unplanned following definitions (4.2),(4.1). Given that in real life, it is more likely that the outage occurrence might be known with some probability, the next chapter is interested in how to integrate the probabilistic information into the design of our controller.

Chapter 5

Stochastic discrete Rare event

I was gratified to be able to answer promptly, and I did. I said I didn't know[a].

a. Mark Twain

Contents

5.1 Introduction 90

5.2 Problem statement 91

5.2.1 System description 91

5.2.2 Problem formulation 92

5.2.3 Decision structure 93

5.3 State of the art of resolution methods 95

5.3.1 Robust Optimization 95

5.3.2 Stochastic programming 96

5.4 Stochastic Discrete Constraint Model Predictive Controller (SDCMPC) 102

5.4.1 Relaxed constrained 102

5.4.2 Deterministic equivalent problem 103

5.4.3 Important remarks 105

5.5 Model of the grid behavior 105

5.5.1 Markov Chain 105

5.6 Application 107

5.6.1 Optimization variables 107

5.6.2 Simulation settings 108

5.6.3 Extreme failure rate 108

5.6.4 Varying the failure and repair rate 114

5.6.5 Varying the failure, repair rate and c_1 117

5.6.6 SDCMPC vs. MSP wait and see 117

5.7 Conclusion 121

5.1 Introduction

As presented in the previous chapters, in Optimization-based controllers family, MPC provides a practical solution that easily handles the physical and operational constraints which have to be considered. However, in most real-time applications, constraints are subject to uncertainties and disturbances. These can be continuous or discrete and, depending on their amplitudes, can severely deteriorate the system's performance. We are interested in the discrete disturbance that denotes discrete events, which are mathematically modelled by discrete constraints. These represent radical changes in a system, as, for example, when a wind turbine enters a safe mode by stopping its energy production or when a GPO occurs. The latter is the one that interests us in this chapter.

Two families of MPC are often used to address uncertainty: Robust MPC (RMPC) and Stochastic MPC (SMPC). When no other information is available, but the uncertainty is known to lie in a given set, explicitly assessing the worst-case uncertainty lead to robust optimization [ALA09; BYH15] in general and RMPC [BM99; Rak15] in particular. Less conservative approaches that exploit the knowledge of uncertain variables' probability distribution leads to SMPC. The latter consists of two approaches.

The first one is Chance Constraints (CC) optimization [CCS58; Pré70; Hen07; NCW19]. CC optimization provides explicit probabilistic guarantees on the feasibility of optimal solutions. However, Although very attractive, CC problems can be challenging to solve in the presence of discrete r.vs [Ada+18; GX19].

The second used approach is the Multistage Stochastic Programming (MSP) based on a scenario tree (that we shall se in section 5.3.2). When the length of the prediction horizon and the number of elements in the random variables' sample space lead to an exponential growth of the scenario tree, a simple strategy to reduce this growth is to consider that the uncertainty becomes constant after the so-called "robust horizon". This simplification is applicable due to the sliding horizon nature of the strategy; Modeling the far future very accurately is not critical because all the control inputs will be recomputed at the next sampling time [Luc+14]. Another method that helps to avoid dealing with the exponential growth of the scenario tree is the *Stochastic Dual Dynamic Programming* (SDDP) [PP91] that reformulates the initial problem in dynamic programming and solve it through bender's cut method as applied in energy management in [Pac+18].

In the previous chapter, we have considered the electrical grid as a deterministic

variable that either equals zero (i.e. P_{g0}^{max}) during an outage or P_{g1}^{max} in a nominal functioning state. In both cases, the GPO occurs with the control strategy, either knowing or not when it will happen and how long it will last. When the outage occurs, in the former case, the strategy is ready for the incidence, and in the latter, it must cope with the current energy within the system to meet the user's needs. The information fed to the system in both cases is complete. Here, however, we take a more realistic approach by considering incomplete information about the grid's state prior to the occurrence or during a GPO respectively, whether the grid is currently available or not. This incomplete information is given as the electrical grid's failure and repair rates and, therefore, can be modelled as a Markov chain (see section 5.5). The rates can be modelled from historical data. As a consequence of the incomplete information, the electrical grid is now a discrete random variable associated with some probability. Instead of considering a *robust horizon* or using SDDP to tackle the resulting problem, we present in this chapter a new method to prevent the exponential growth of a scenario tree.

The chapter is structured as follows. A rigorous formalisation of the problem of right-hand side stochastic discrete constraints is given in section 5.2. We then present a state of the art of the existing methods to tackle the problem with their inconvenient in our specific case in section 5.3. The following section 5.4 presents rigorously the newly proposed method within a model predictive controller. To consider the incomplete information about the electrical grid, the model used to integrate the later in our application is given in section 5.5. The previously presented model is used in section 5.6 for the application where we compare the controller resulting from the new method to an existing one, i.e., the Multistage Stochastic Programming Wait and See (see 5.3.2).

5.2 Problem statement

5.2.1 System description

Let us consider the generic MPC problem (2.1). Let us recall the control constraints (2.7b) given by:

$$u(k+h|k) \in \mathbb{U}$$

Let us assume we can separate (2.7b) into two groups of control constraints,

- n_d deterministic inequality constraints given by:

$$D_d u(k+h|k) \leq d, \tag{5.1}$$

  where $D_d \in \mathbb{R}^{n_d \times n_u}$, and $d \in \mathbb{R}^{n_d}$ a column vector.

- n_s stochastic inequality constraints given by:

$$e_i^T u(k+h|k) \leq \boldsymbol{\xi}_i(k+h|k), \ \ \forall i \in \mathbb{N}_1^{n_s} \tag{5.2}$$

For the rest of the thesis, the following convention is adopted: a r.v is denoted by a bold letter, and its realization is indicated by a regular letter.
Note that the index " i " indicates that we can have different sources of uncertainty at the same moment

Assumption 5.1. $\forall i \in \mathbb{N}_1^{n_s}$, the r.v $\boldsymbol{\xi_i}(k+h|k)$ belongs to a discrete set defined as follows:

$$\Xi_i = \{\xi_{1,i}, \xi_{2,i}, ... \xi_{N_i,i}\} \tag{5.3}$$

with $N_i = \text{card}\{\Xi_i\}$ and its elements sorted as follows

$$\xi_{1,i} < \xi_{2,i} < \ldots < \xi_{N_i,i}; \ \ \forall i \in \mathbb{N}_1^{n_s} \tag{5.4}$$

Assumption 5.2. At the instant indexed by $(k+h|k)$, for all $i \in \mathbb{N}_1^{n_s}$, for all realizations of the r.v $\boldsymbol{\xi_i}(k+h|k)$ and for all $x(k+h|k) \in \mathbb{X}$, there exists a $u(k+h|k)$ that satisfies (5.1) and (5.2) such that $x(k+h+1|k) \in \mathbb{X}$

Assumption 5.3. At the instant indexed by $(k+h|k)$ the sources of uncertainty are independent of one another.

5.2.2 Problem formulation

From the previous section, through introduction of the stochastic constraints, we can write the stochastic MPC problem as follows:

Problem 5.1 (**Stochastic MPC problem**).

$$J_s^*\Big(x(k)\Big) = \min_{u(k|k),\dots,u(k+H-1|k)} \quad V_f\Big(x(k+H|k)\Big) + \sum_{h=0}^{H-1} l_h\Big(x(k+h|k), u(k+h|k)\Big) \tag{5.5}$$

$$\text{s.t. } \forall h \in \mathbb{N}_0^{H-1}$$

$$D_d u(k+h|k) \leq d \tag{5.6}$$

$$e_i^T u(k+h|k) \leq \boldsymbol{\xi}_i(k+h|k) \ , \forall i \in \mathbb{N}_1^{n_s} \tag{5.7}$$

$$x(k+h|k) \in \mathbb{X} \tag{5.8}$$

$$x(k+H|k) \in \mathbb{X}_f \tag{5.9}$$

$$x(k|k) = x(k) \tag{5.10}$$

$$x(k+h+1|k) = f\Big(k, x(k+h|k), u(k+h|k)\Big) \tag{5.11}$$

We make the following assumptions:

Assumption 5.4. $l_h(\cdot)$ and $V_f(\cdot)$ are convex function with respect to x and u.

Assumption 5.5. At the first instant of the prediction horizon indexed by $(k|k)$, for all $i \in \mathbb{N}_1^{n_s}$ the r.v $\boldsymbol{\xi}_i(k|k)$ is known and for the rest of the prediction horizon $\Big\{(h = 1, \dots, H-1)|k\Big\}$, the marginal probability

$$\Pr\Big[\boldsymbol{\xi}_i(k+h) = \xi_{n_i,i} \,|\, \boldsymbol{\xi}_i(k|k)\Big] = \pi_{n_i,i}(k+h|k) \tag{5.12}$$

where $n_i \in \mathbb{N}_1^{N_i}$, is also known.

Note that it is important to mention here that the **Problem 5.1** is ill defined since we have yet to specify the meaning of the stochastic inequality (5.7). In the literature, two main optimizations domain based on some hypothesis give a clear meaning to such an inequality constraints. These are Robust Optimization (RO) [ALA09] and Probabilistic programming [Pré95].

Before diving into the different possibilities offered by the resolution methods, let us clarify a point which is often neglected because judged obvious, but which we find helpful to discuss. It is the stochastic optimization decision structure.

5.2.3 Decision structure

In our context, decision structure refers to how the decisions and randomness intertwine with one another. **Problem 5.1** is defined on the whole prediction horizon H. This

means that at each instant, the solution should also be defined on the whole prediction horizon, i.e., one decision for each instant considered in the future: the decision is time-dependent. This results in the optimization problem's solution being either a decision vector or a decision tree according to a chosen resolution method. The literature offers two types of decision structures which are named *here-and-now* and *wait-and-see* [Wet02]. We emphasize that the decisions at any one time are based on data available (i.e., history of past observations) at the time the decisions are made and do not depend on future observations. This feature reflects the $non-anticipative$ nature of the dynamic decision problem and ensures its causality [GKW18].

Here-and-now Over the whole optimization horizon, all the decisions from the current instant indexed by $(k|k)$ to the last one indexed by $(k+H|k)$, are computed at once at the current instant before the sequence of r.v is unveiled. By sequence of r.v, we refer to a particular vector that consists of each realization of the r.v $\boldsymbol{\xi}$ at the sub-sequential instant $(k+h|k)$, $\forall h \neq H$. For every sub-sequential instant considered a unique associated decision is computed such that it must be feasible for all possible observations, but cannot depend on the unrevealed value assumed by the random variable. The resulting decision vector is too restrictive since, in reality, there may be situations in which the decisions must adjust themselves to the actual data.

To model adjustability of the decision variables, the problem can be transformed by adding news variables (i.e., *recourse/adjustable* variables). The additional variables are extra decisions, which depend on the actual value assumed by the random variable's realization.

Wait-and-see As in the *Here-and-now* decision structure, all the decisions from the current instant to the last one, are computed at once at the current instant. Here however, at every sub-sequential instant $(k+h|k)$, $\forall h \neq H$ the associated decision is not unique. There are as many decisions as there are elements in the probabilistic space of the random variable such that every computed decision is optimal for a corresponding possible observation.

we highlight that more explanatory examples of the decision structures are given in 5.3.2

5.3 State of the art of resolution methods

In this section we are going to give an insight of the main existing different methods to solve problem (5.1) which are RO and stochastic programming. They are considered to be two alternative techniques to deal with uncertain data both in a single period and in a multi-period decision making process.

5.3.1 Robust Optimization

RO also called the worst-case oriented approach, addresses the uncertain nature of a problem without making specific assumptions on probability distributions: the uncertain parameters are assumed to belong to a deterministic uncertainty set. [Soy73; GOL98; GGN04] and many others give ideas on the different hypothesis that must be imposed on the structure of the uncertain set in order to have a computationally tractable problem. These hypotheses also determine what the meaningful, feasible solutions to an uncertain problem are. The feasible solution should be robust feasible; that is, it should guarantee feasibility and optimality of the solution against all instances of the parameters within the uncertainty set [BBC11]. This is done through a min-max approach that results in adopting a pessimist approach and solving the problem considering the value of the r.v that produces the worst objective cost value.

In its basic form, RO deals with static problems where all the decision variables must be determined before any of the uncertain parameters are realized: that is *here-and-now* solutions to the problem. However, this is not often the case in most applications which are multi-period in nature, and where a decision at any given instant can and should account for uncertainty realizations in previous instants. The authors in [GGN04; ALA09; BG10] and many others have extended the RO methodology to the dynamic framework by introducing the adjustable and affinely adjustable robust counterpart which make RO less conservative. In these cases, decisions can be split, i.e., a part of the decision variables, the so-called adjustable variables, have to be determined after a portion of the uncertain data is realized.

Considering the definition of the robust feasible solution and the ordered relationship given by equation (5.4) among the different values $\xi_{\cdot,\cdot}$ that the random parameter can assume, one can easily see that the only feasible solution that satisfies all the constraints of Problem 5.1, whatever the realization of the data from the uncertainty set $\Xi_i,\ \forall i \in \mathbb{N}_1^{n_s}$,

is the one computed when $\boldsymbol{\xi}_i(k+h)$ takes the value $\xi_{1,i}$. Therefore the RO version of problem (5.1) is the same problem where constraint (5.7) is replaced by the deterministic constraint given by:

$$\forall h \in \mathbb{N}_0^{H-1};\ \forall i \in \mathbb{N}_1^{n_s};\ \ e_i^T u(k+h) \leq \xi_{1,i}. \tag{5.13}$$

The new problem considering constraint (5.13) is undoubtedly a valid, robust optimal solution. However, it is not attractive to be applied in our framework mainly because it would mean that for the prediction horizon of the problem, we only consider that the r.v takes one value, i.e., the smallest value in the set Ξ_i. What is utterly wrong due to the rarity of occurrence of the considered $\xi_{1,i}$.

5.3.2 Stochastic programming

In contrast to RO, stochastic programming, also known as probabilistic programming starts by assuming the uncertainty has a probabilistic description. The problems considered here can be formulated using two different approaches, the *probabilistic constraint* or *Chance Constraint* CC and the multistage stochastic programming (MSP).

Chance constraints

Chance Constraints (CC) is a very attractive framework which allows the user to ensure that the probability of meeting a certain constraint is above a certain level. CC has been first introduced by [CCS58] and further developed in [CC59; CC62; CC63]. The field received later on several contribution among which [Pré70; Szé88; PVB98; Hen02; Hen07].

Chance constraint programming deals with constraints of the form

$$\Pr\Big[g(u, \boldsymbol{\xi}) \geq 0\Big] \geq p, \tag{5.14}$$

where $u \in \mathbb{R}^{n_u}$ is the decision vector, $\boldsymbol{\xi} \in \mathbb{R}^{n_s}$ a r.v and $g : \mathbb{R}^{n_u} \times \mathbb{R}^{n_s} \to \mathbb{R}^m$ a constraint mapping. The level $p \in (0, 1)$ is user defined and represent the safety for the decision u.

Chance constraint programming applied to problem 5.1 will mainly act on constraint (5.8) which therefore can be rewritten in two forms:

Individual constraints In the first form of CC the probabilistic constraints are imposed individually on the inequalities (i.e., on each instant of the prediction horizon) as following:

$$\forall i \in \mathbb{N}_1^{n_s};\ \forall h \in \mathbb{N}_0^{H-1};\quad \Pr\Big[e_i^T u(k+h|k) \leq \boldsymbol{\xi}_i(k+h|k)\Big] \geq p_i(k+h). \quad (5.15)$$

Joint constraints In the second form of CC the probabilistic constraint is imposed jointly on the whole problem as following:

$$\forall h \in \mathbb{N}_0^{H-1};\ \Pr\Big[e_i^T u(k+h|k) \leq \boldsymbol{\xi}_i(k+h|k),\ \forall i \in \mathbb{N}_1^{n_s}\Big] \geq p(k+h); \quad (5.16a)$$

$$\forall i \in \mathbb{N}_1^{n_s};\ \Pr\Big[e_i^T u(k+h|k) \leq \boldsymbol{\xi}_i(k+h|k),\ \forall h \in \mathbb{N}_0^{H-1}\Big] \geq p_i; \quad (5.16b)$$

$$\Pr\Big[e_i^T u(k+h|k) \leq \boldsymbol{\xi}_i(k+h|k),\ \forall i \in \mathbb{N}_1^{n_s};\ \forall h \in \mathbb{N}_0^{H-1}\Big] \geq p. \quad (5.16c)$$

Since we consider several r.vs. and the whole prediction horizon H, the joint constraints has three different meanings.

The joint constraints are imposed:

- in (5.16a), individually on each instant of H but, together for all the r.vs.;
- in (5.16b), individually on each r.v but together on the prediction horizon;
- in (5.16c), the combination of both previously described, i.e., on the whole horizon and the r.vs. altogether.

The constraints (5.15, 5.16a, 5.16b, 5.16c) expresses that we wish to take a decision u that satisfies the random inequalities system either individually or jointly with a probability p often chosen to be high.

An important case of chance constraint is where u and $\boldsymbol{\xi}$ are not coupled through the mapping but appear separate as in (5.16) and (5.15). In these cases, in the classic literature, under some assumptions and mainly by using the *cumulative distribution function* of $\boldsymbol{\xi}$ when the latter is continuous, the problem can be transformed, therefore becomes easily solvable. In the context of problem (5.1), we are in the presence of discrete r.v for which a chance constraint is difficult to solve. For this simple reason, we are not to develop further about CC.

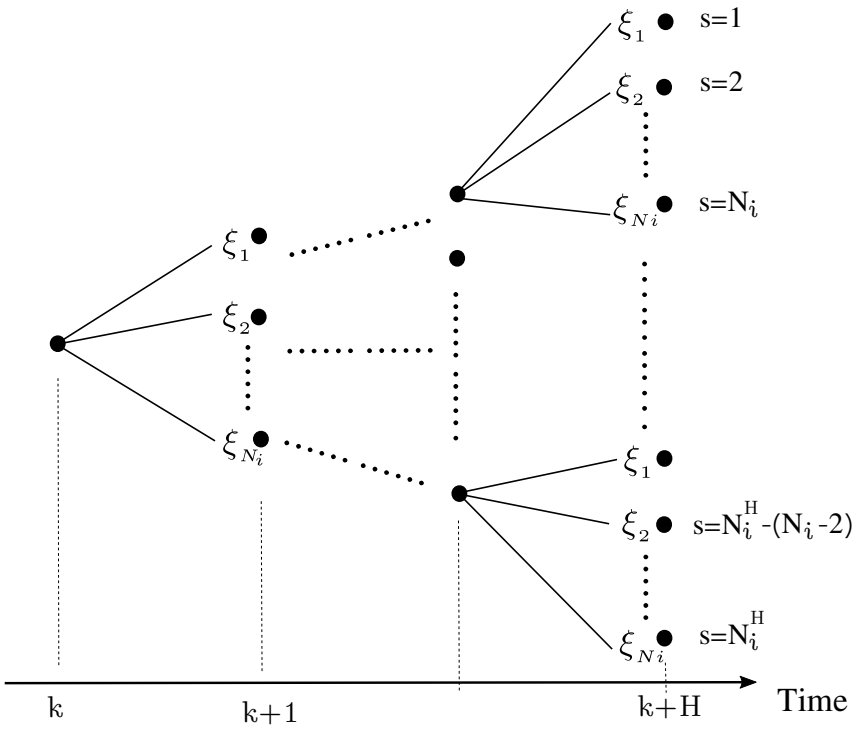

Figure 5.1 – A simple example of a scenario tree

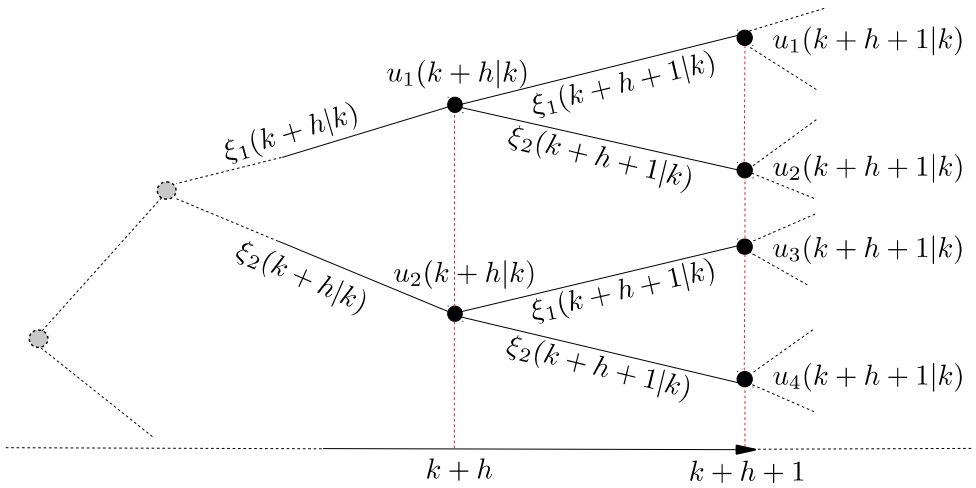

Figure 5.2 – Multistage Stochastic Programming Wait and See

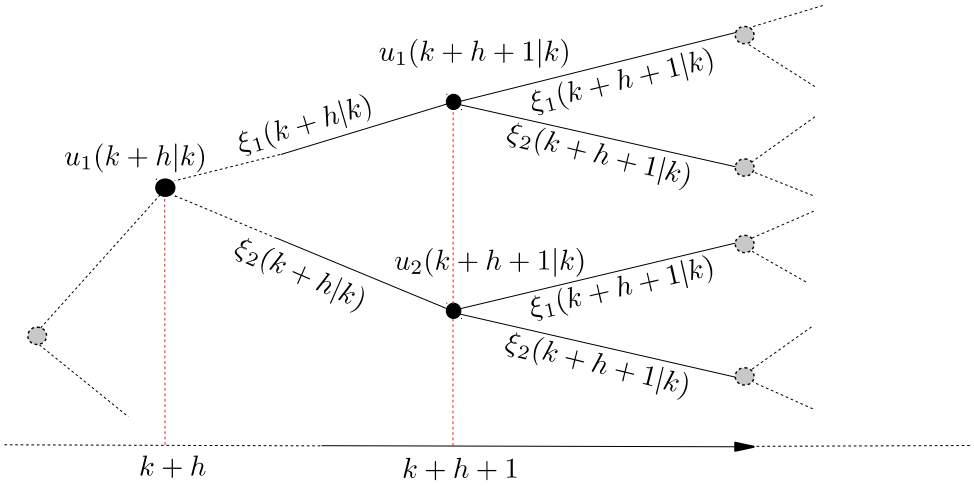

Figure 5.3 – Multistage Stochastic Programming Here and Now

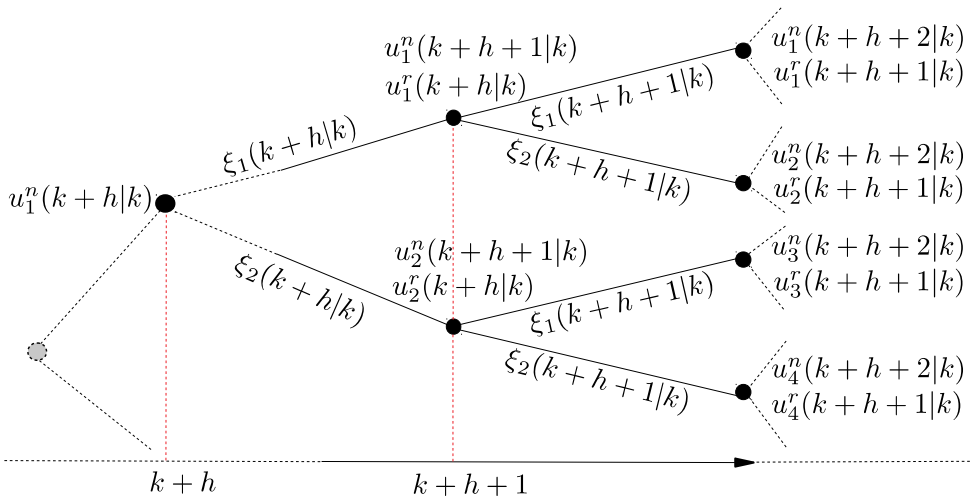

Figure 5.4 – Multistage Stochastic Programming Here and Now with recourse

Multistage Stochastic Programming(MSP)

The multistage stochastic optimization or programming considers all the possible realizations of a r.v at each stage to solve a unique optimization problem accordingly. The resulting problem is a scenario tree that grows exponentially in consonance with the distribution of the r.vs. and the number of periods (stages). A scenario represents a path described by a succession of nodes in a particular order such that it starts at a node located at the root (beginning) of the tree and finishes at a node positioned at the last instant of the problem. Each node of the tree at a particular stage corresponds to a realization of the r.v at that stage and is associated with one or several decisions. Figure 5.1 shows the scenario tree associated with a r.v $\boldsymbol{\xi}$ which takes values in the set $\{\xi_1, \xi_2, \ldots, \xi_{Ni}\}$ such that the total numbers of scenario is given by $S = N_i^H$

Borrowing from game theory, let us suppose that the decision-maker (the decision computed) and the realization of the randomness are two players in a sequential game (problem). In each stage of the problem, both players must make a move one after the other. The order in which they play allows to distinguish between two types of MSP:

- "Multistage Stochastic Programming Wait and See" (MSPWS);
- "Multistage Stochastic Programming Here and Now" (MSPHN).

For simplicity sake, let us consider a simple case of problem (5.1) where $n_s = 1$, and $N_1 = 2$.

MSP wait and see In this framework, the randomness is considered to be the first player, then follows the decision computed. This implies that at each stage, there is one decision associated with each and every value that the r.v assumes. The decision is computed given that the random variable's value is known. Figure 5.2 shows the scenario tree associated.

MSP Here and Now In this case, the decision-maker is considered to be the first player. Accordingly, the decision is taken knowing only the distribution of the random variable. The decision is computed such that it is feasible no matter the realization of the randomness, which is considered as the second player. For instance, a decision is made at the beginning of each instant $k + h$. Between $k + h$ and $k + h + 1$, the randomness associated with the previous decision is revealed. At the following instant, $k + h + 1$ the same process is repeated. The process, as described, begets the scenario tree given by Figure 5.3.

As explained in section 5.2.3 the MSPHN is too strict and in reality there may be situations in which the decisions must adjust themselves to the actual data. In order to achieve this, the decision at each node is split into two sets ($u = [u^n \ u^r]^T$) i.e. the decision maker in each stage can play twice:

i- The set of decision taken before the r.v is unveiled: the first move of the decision maker that we name u^n;

ii- The set of decision that are taken after the r.v is unveiled: the second move of the decision maker that we name u^r.

This is the MSPHN with recourse. Here, the decision-maker decides before the randomness reveals, once it does the decision-maker makes another decision to correct the first one according to the revealed random variable. Figure 5.4 shows the scenario tree associated with the MSPHN with recourse. The deterministic equivalent form of problem (5.1) in its MSPHN with recourse form is given by problem 5.2.

We emphasize that, although on the different scenario tree, we only show the decision variables at each node, they are in no case the sole variables considered. Each node is associated with its own dynamic. The variables in the deterministic equivalent problem are therefore not only indexed by the instant $(k+h|k)$ but also by the corresponding scenario s with $s \in \mathbb{N}_1^S$, (S the total number of scenarios) and $\cdot$ which associates the suitable variables and scenario to the problem to be solved.

Problem 5.2 (**Generic deterministic equivalent form of problem 5.1**).

$$J^*_{Deq}\Big(x(k)\Big) = \min_{u_{\cdot,s}(k|k),\dots,u_{\cdot,s}(k+H-1|k)} \quad \Bigg\{ l_0\Big(x(k), u(k|k)\Big) + \sum_{s=1}^{S} \Pr[s] \Bigg\{ V_f\Big(x_{\cdot,s}(k+H|k)\Big) + \sum_{h=1}^{H-1} l_h\Big(x_{\cdot,s}(k+h|k), u_{\cdot,s}(k+h|k)\Big) \Bigg\} \Bigg\} \tag{5.17}$$

subject to $\forall s \in \mathbb{N}_1^S$

$$D_d u_{\cdot,s}(k+h|k) \leq d \tag{5.18}$$

$$e_i^T u_{\cdot,s}(k+h|k) \leq \xi_{\cdot,s}(k+h|k) \tag{5.19}$$

$$x_{\cdot,s}(k+h|k) \in \mathbb{X} \tag{5.20}$$

$$x_{\cdot,s}(k+H|k) \in \mathbb{X}_f \tag{5.21}$$

$$x(k|k) = x(k) \tag{5.22}$$

$$x_{\cdot,s}(k+h+1|k) = f\Big(k, x_{\cdot,s}(k+h|k), u_{\cdot,s}(k+h|k)\Big) \tag{5.23}$$

Problem 5.1 converted into its deterministic equivalent form in the three precedent described cases (MSPWS, MSPHN, MSPHN with recourse) is given by the generic problem 5.2. In the latter, the cost to minimized is an expectation over all the possible scenarios. It follows that, even though the general form of the written problem is the same in these three cases, depending on how the associated tree is built, the considered variables indexed by $._s(k+h|k)$ and therefore the solved problems are entirely different.

5.4 Stochastic Discrete Constraint Model Predictive Controller (SDCMPC)

We want to develop a controller that does not suffer from the combinatorial explosion of variables experienced by the MSP. That is, the decision u over the prediction horizon should not depend on the realization of the random variable. In this case, as explained in section 5.3.1 the resulting decision sequence is too conservative. In order to remove the conservation, we propose the following.

5.4.1 Relaxed constrained

We propose to relax the constraints (5.7) using relaxation variables which, unlike u, can depend on the r.v $\boldsymbol{\xi}_i(k+h|k)$. Our goal in doing so is to make the decision u deterministic by transferring the randomness associated, to the relaxation variables. Therefore the relaxation variables become random variables.

The relaxed constraint is given by:

$$\begin{aligned} \forall h \in \mathbb{N}_1^{H-1};\quad \forall i \in \mathbb{N}_1^{n_s}\ \ ; e_i^T u(k+h|k) - \boldsymbol{y}_i(k+h|k) &\leq \boldsymbol{\xi}_i(k+h|k) \\ \boldsymbol{y}_i(k+h|k) &\geq 0 \end{aligned} \tag{5.24}$$

Each relaxation variable $\boldsymbol{y}_i$ often call *recourse* variable in the Stochastic Programming literature is random, because its optimal value is a function of its corresponding uncertain bound $\boldsymbol{\xi}_i$.

The constraint violations that occur due to the relaxation variables' usage must be penalized in the new problem's cost. The new cost is therefore given by the cost function

of problem (5.1) with an additional term related to the penalized variables as follows:

$$J_{SDCMPC}\Big(x(k), y\Big) = J_s\Big(x(k)\Big) + J_y(k), \tag{5.25}$$

with

$$J_y(k) = E\left[\sum_{h=1}^{H-1}\sum_{i=1}^{n_s} c_i \boldsymbol{y}_i(k+h)\right] \tag{5.26}$$

the expected penalization cost of all the r.v $\boldsymbol{y}_i(k+h)$ over all of the prediction horizon's instants excepted the first one, since, given assumption 5.5, the r.v has revealed itself already and c_i is the penalization associated to utilizing $\boldsymbol{y}_i$.

It is worth mentioning that c_i is a user-setting parameter which exact range value is still an important open question. The control variables obtained by solving the optimization problem will be different depending on the chosen value, as we will show in the application section 5.6.5.

The control problem becomes a minimization on the decision variables u and the recourse variables $\boldsymbol{y}$ function of $\boldsymbol{\xi}$. It can be solved by formulating its "deterministic equivalent".

5.4.2 Deterministic equivalent problem

We formulate the deterministic equivalent problem by introducing the variables

$$y_{1,i}(k+h|k),\ \ldots\ , y_{N_i-1,i}(k+h|k) \tag{5.27}$$

all non negative which are the different values taken by $\boldsymbol{y}_i(k+h|k)$ for all elements except the last one in the sample space of the r.v $\boldsymbol{\xi_i}$ at the instant $(k+h|k)$.

Therefore the stochastic constraints become a list of deterministic constraints as:

$$\forall i \in \mathbb{N}_1^{n_s};\ \forall h \in \mathbb{N}_1^{H-1} \quad \begin{cases} e_i^T u(k+h|k) - y_{1,i}(k+h|k) \leq \xi_{1,i}; \\ \vdots \\ e_i^T u(k+h|k) - y_{N_i-1,i}(k+h|k) \leq \xi_{N_i-1,i}; \\ e_i^T u(k+h|k) \leq \xi_{N_i,i}. \end{cases} \tag{5.28}$$

We highlight that we did not relax the last constraints, since in our application it makes

sense to forbid their relaxation. This means setting all the

$$y_{N_i,i}(k+h|k) = 0 \tag{5.29}$$

so that the N_i-th constraints are hard constraints.

With this notation in mind,

$$\begin{aligned} J_{\boldsymbol{y}}(k) &= \sum_{h=1}^{H-1}\sum_{i=1}^{n_s} c_i \mathrm{E}\Big[\boldsymbol{y}_i(k+h|k)\Big] \\ &= \sum_{h=1}^{H-1}\sum_{i=1}^{n_s}\sum_{n_i=1}^{N_i-1} c_i \pi_{n_i,i}(k+h|k) y_{n_i,i}(k+h|k). \end{aligned} \tag{5.30}$$

The final problem to be solved is given by:

Problem 5.3 (**Stochastic Discrete Constraint MPC problem**)**.**

$$\begin{aligned} J^*_{SDCMPC}\Big(x(k), y\Big) = \min_{\substack{u(k|k),\,\dots\,,u(k+H-1|k)\\ y(k+1|k),\,\dots\,,y(k+H-1|k)}} \quad & \Bigg\{ J_{\boldsymbol{y}}(k) + V_f\Big(x(k+H|k)\Big) \\ & + \sum_{h=0}^{H-1} l_h\Big(x(k+h|k), u(k+h|k)\Big) \Bigg\} \end{aligned} \tag{5.31}$$

subject to:

$\forall h \in \mathbb{N}_0^{H-1}$

$$x(k+h+1|k) = f\Big(k, x(k+h|k), u(k+h|k)\Big) \tag{5.32}$$

$$D_d u(k+h|k) \leq d \tag{5.33}$$

$$x(k+h|k) \in \mathbb{X} \tag{5.34}$$

$$x(k+H|k) \in \mathbb{X}_f \tag{5.35}$$

$$x(k|k) = x(k) \tag{5.36}$$

$\forall h \in \mathbb{N}_1^{H-1},\ \ \forall i \in \mathbb{N}_1^{n_s}$

$$e_i^T u(k+h|k) \leq \xi_{N_i,i} \tag{5.37}$$

$$\forall n_i \in \mathbb{N}_1^{N_i-1},\ \xi_{n_i,i} \geq e_i^T u(k+h|k) - y_{n_i,i}(k+h|k) \tag{5.38}$$

$$\forall n_i \in \mathbb{N}_1^{N_i-1},\ y_{n_i,i} \leq 0 \tag{5.39}$$

Now that the formulation of the problem is finished let us highlight some important points.

5.4.3 Important remarks

Let us consider problem (5.1). The total number of variables computed to solve this problem for the MSPWS is given by

$$(n_x + n_u)\Big[1 + \sum_{h=1}^{H-1} \Big(\prod_{i=1}^{n_s} N_i\Big)^h\Big] \tag{5.40}$$

while it is

$$n_x + n_u + (H-1)\Big(n_x + n_u + \sum_{i=1}^{n_s} N_i - n_s\Big) \tag{5.41}$$

for the SDCMPC. A comparison between both numbers shows a great reduction from an exponential growth to a linear one with the new controller depending on the prediction horizon H. The difference in the number of variables is of great importance in time and memory usage performances, as we will show in section 5.6.6. Another advantage of the new formulation is that it is applicable for any type of r.vs. as long as the marginal probability of occurrence of the considered r.vs. $\pi_{n_i,i}(\cdot|k)$ can be computed.

5.5 Model of the grid behavior

5.5.1 Markov Chain

Let us consider that the maximum power allowed to be drawn from the electrical grid during each period time takes the values P_{g1}^{max} or P_{g0}^{max} respectively when the grid is available and unavailable. The maximum power allowed to be drawn from the electrical grid at time period k becomes a random variable that we denote $\boldsymbol{P_g^{max}}(k)$.

We model the evolution of the process associated in the time by a two states Markov Chain (MC) [BA92] given by figure 5.5. λ $(0 \leq \lambda \leq 1)$ and μ $(0 \leq \mu \leq 1)$ are respectively said to be the *failure rate* and the *repair rate* of the electrical grid. Whenever the process is in some state, there is a fixed probability that it will be next in the other state or remain in the same. That is:

$$\Pr\Big[\boldsymbol{P_g^{max}}(k+1|k) = P_{g0}^{max} | P_g^{max}(k) = P_{g1}^{max}\Big] = \lambda, \tag{5.42a}$$
$$\Pr\Big[\boldsymbol{P_g^{max}}(k+1|k) = P_{g1}^{max} | P_g^{max}(k) = P_{g1}^{max}\Big] = 1-\lambda, \tag{5.42b}$$
$$\Pr\Big[\boldsymbol{P_g^{max}}(k+1|k) = P_{g1}^{max} | P_g^{max}(k) = P_{g0}^{max}\Big] = \mu, \tag{5.42c}$$
$$\Pr\Big[\boldsymbol{P_g^{max}}(k+1|k) = P_{g0}^{max} | P_g^{max}(k) = P_{g0}^{max}\Big] = 1-\mu, \tag{5.42d}$$

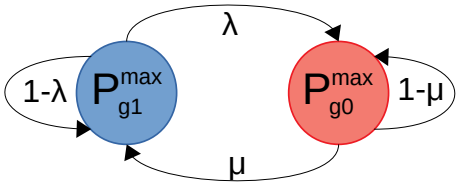

Figure 5.5 – Markov chain model of the electricity grid

where $P_g^{max}(k)$ and $\boldsymbol{P_g^{max}}(k+1|k)$ represent respectively the present and the future states. Equation (5.42) states that, for the MC represented in Figure 5.5, the conditional distribution of any future state $P_g^{max}(k+1|k)$ given the present state $P_g^{max}(k)$ is independent of the past states and depends only on the present state. This is summarized in the one step transition probability matrix representing the MC given by:

$$T = \begin{bmatrix} 1-\lambda & \lambda \\ \mu & 1-\mu \end{bmatrix}. \tag{5.43}$$

Let's denote the h-step transition probability vector of the process from the initial instant k by $\Pi^{k+h|k}$ with

$$\Pi^{k+h|k} = \begin{bmatrix} \pi_1(k+h|k) & \pi_0(k+h|k) \end{bmatrix}. \tag{5.44}$$

The *Chapman–Kolmogorov equations* provide a method for computing the h-step transition probability vector such that:

$$\Pi^{k+h|k} = \Pi^k T^h \quad \forall h \geq 1 \tag{5.45}$$

with

$$\Pi^{k|k} = \Pi^k. \tag{5.46}$$

Since the electricity grid state is supposed to be known at the initial instant (assumption 5.5), the initial probability state vector Π^k takes either the value [1 0] when the grid is available and [0 1] on the contrary.

Finally, we emphasize that this Markov chain is just a simple example, but more advanced reliability models could be used as well. In particular, our control method does not require the uncertain signals to be Markov processes.

5.6 Application

5.6.1 Optimization variables

For our problem, we only have one stochastic inequality, therefore $n_s = 1$, which implies $i = 1$ and $c_i = c$. Since the sole random variable can only assume two values, it follows that $N_i = N_1 = 2$.

From all the previous sections, and given the solar home defined in chapter 3 let us, for the optimization problem define:

- The system's dynamic

$$f\Big(k, x(k+h|k), u(k+h|k)\Big) = Ax(k+h|k) + Bu(k+h|k); \tag{5.47}$$

- The decision variable

$$u(k) = \Big[P_g(k), P_w(k), P_b(k), P_s(k)\Big]^T; \tag{5.48}$$

- The state variable

$$x(k) = E_b(k); \tag{5.49}$$

- The state matrix and input vector

$$A = I_1, \tag{5.50a}$$
$$B = \Big[0, 0, \Delta_t, 0\Big]; \tag{5.50b}$$

- The stochastic constraint variable

$$e^T = \Big[1, 0, 0, 0\Big], \tag{5.51a}$$
$$\boldsymbol{\xi}(k) = \boldsymbol{P_g^{max}}(k); \tag{5.51b}$$

- The deterministic constraints variables

$$D_d = \begin{bmatrix} -1 & 0 & 0 & 0 \\ 1 & 0 & 0 & 0 \\ 0 & 1 & 0 & 0 \\ 0 & -1 & 0 & 0 \\ 0 & 0 & \Delta_t & 0 \\ 0 & 0 & -\Delta_t & 0 \\ 0 & 0 & 0 & 1 \\ 0 & 0 & 0 & -1 \\ 1 & -1 & -1 & 1 \\ -1 & 1 & 1 & -1 \end{bmatrix} \quad (5.52a) \qquad d(k) = \begin{bmatrix} 0 \\ max\left\{P_{g0}^{max}, P_{g1}^{max}\right\} \\ P_v^{max}(k) \\ 0 \\ E_b^{max} - E_b(k) \\ E_b(k) \\ P_l^*(k) \\ 0 \\ P_l^*(k) - P_v^{max}(k) \\ P_v^{max}(k) - P_l^*(k) \end{bmatrix} \quad (5.53a)$$

- The optimization cost

$$J_{SDCMPC}\Big(x(k), y\Big) = J_{\boldsymbol{y}}(k) + J_{CLAS}(k) \quad (5.54)$$

5.6.2 Simulation settings

We consider the same settings as described in section 4.7.1 of chapter 4. Here however, we do not consider the critical load.

5.6.3 Extreme failure rate

First we are interested in the behavior of the controller at the extreme points, respectively for an extremely low ($\lambda = 10^{-15}$) and high failure ($\lambda = 0.99$) rate for constant values of the repair rate ($\mu = 10^{-2}$) and the user-setting parameter ($c = 10^2$) . We consider the low Pv production period (June 2013), and we run two simulations.

In the first simulations (low and high λ no outage) , the GPO does not occur at the intended moment while it does in the second (low and high λ with outage). For the period of June 19 to 24, GPO occurring from June 21 to 22, the controller behavior is shown by figures 5.6, 5.7, 5.8, 5.9. The first two and last two are respectively associated with the very low and high default rate. Table 5.1 shows the controller performances for the low and high failure rate during the considered month of Low PV production.

It can be seen that for the low failure rate, the controller only draws energy from the grid during the night at low electricity tariff since the outage might not occur. For the

Table 5.1 – Controller Performances for both Low and High failure rate

	No outage			**With outage**		
λ	$P_g \mid En_{cost}$	P_s	P_w	$P_g \mid En_{cost}$	P_s	P_w
Low	106.6 | 10.66	0	0	79.1 | 07.91	27.6	0
High	106.6 | 17.67			91.1 | 13.56	15.6	

high failure rate, however, the controller draws energy at any hour of its convenience. When we observe the energy reserve E_b in the storage at the starting instant of the GPO, with the high failure rate (figure 5.8) is about 2kWh while it is null (figure 5.7) for the low failure rate. Due to the reserve that incurred when considering the high λ, the controller can provide the building with its energy demand during the whole first day of the outage. In general, this leads to reducing the energy not provided to the building during all the outage (27.6 kWH vs 15.6kWh). The shedded energy difference between both cases (12kWh) is the surplus drawn from the grid (91.1kwh - 79.1kwh = 12kWh) during peak periods.

In the case of the outage occurrence, we emphasize that the energy drawn from the grid for a low and high failure rate are respectively close to the energy drawn from the grid for the ReMPC (described in chapter 4, see table 4.2) in the unplanned and planned GPO scenario. We can conclude that the SDCMPC with a low default rate behaves like the ReMPC with no information about a GPO occurrence. With a high failure rate, the SDCMPC behaves like the ReMPC with perfect information about a GPO occurrence. This is a salient point because the only information provided to the SDCMPC is the electrical grid's failure and repair rate.

Figure 5.9 shows that even with a higher probability of failure, from the beginning of 22 June the SDCMPC can no longer provide the house with its energy demand since there is no energy left inside the battery. However, going back on 20 June, one could ponder why the controller, given the GPO's high occurrence does not draw energy from the grid, especially during the 2^{nd} half-day although the storage is not full.

An answer is given by the grey curve on the second sub-figure of figure 5.9. The curve depicts the cumulative net load over the predictive horizon computed as follows:

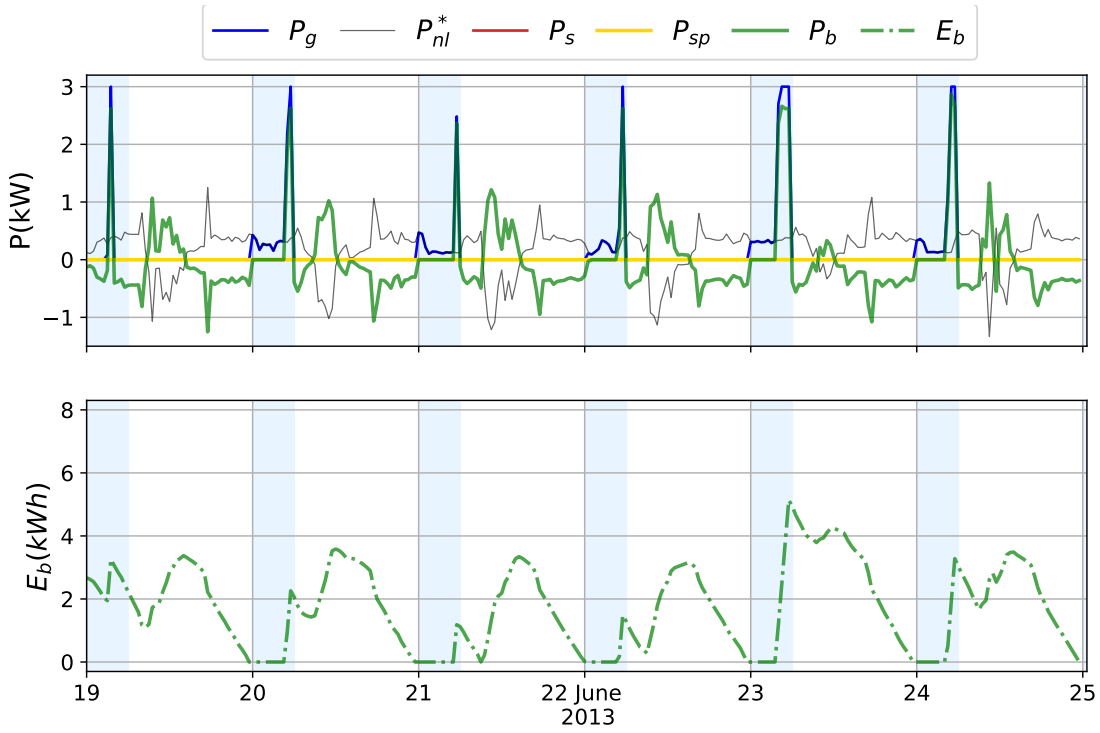

Figure 5.6 – Low prob of failure, no outage

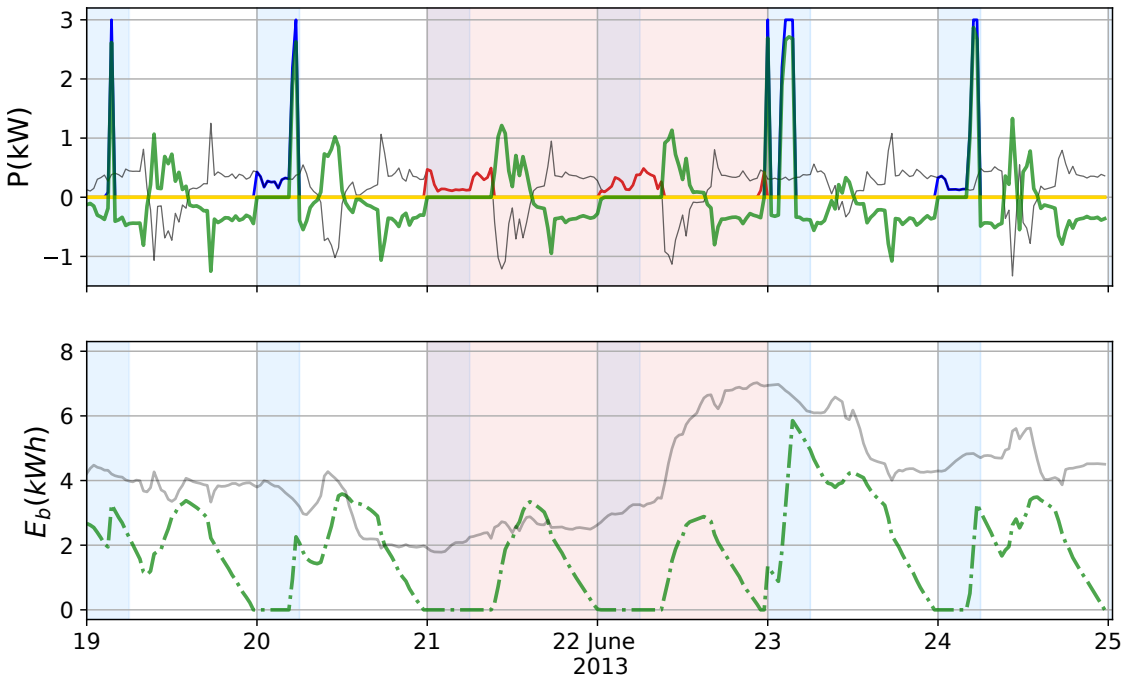

Figure 5.7 – Low prob of failure, with outage

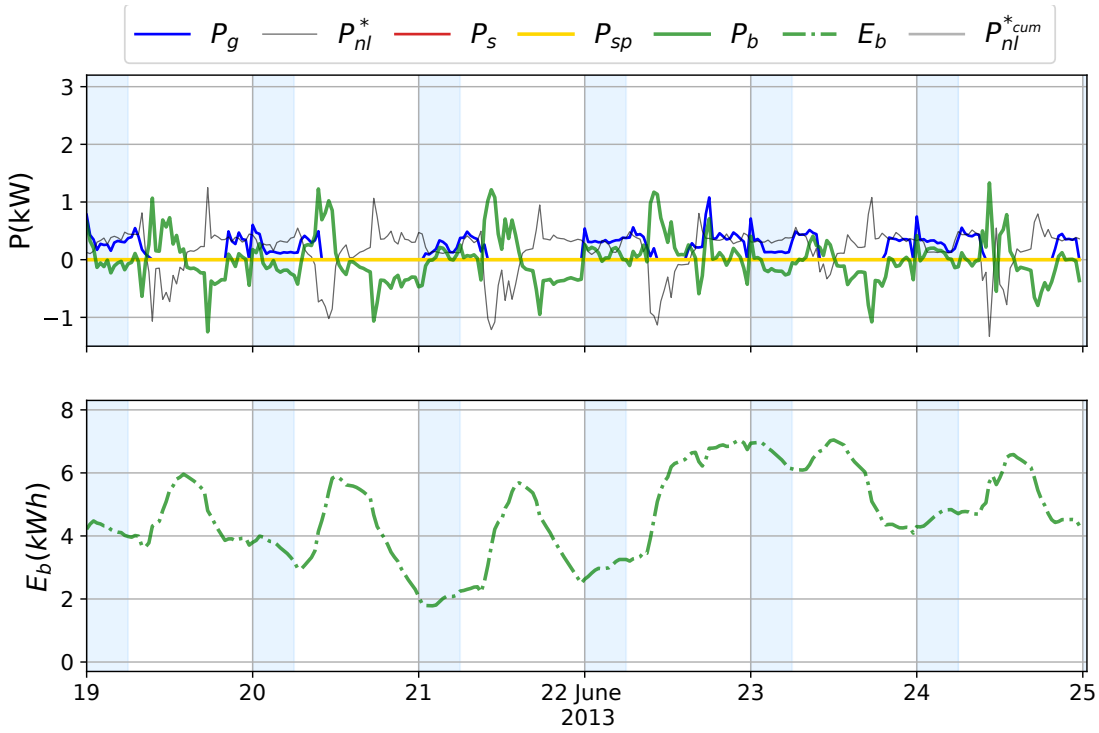

Figure 5.8 – High prob of failure, no outage

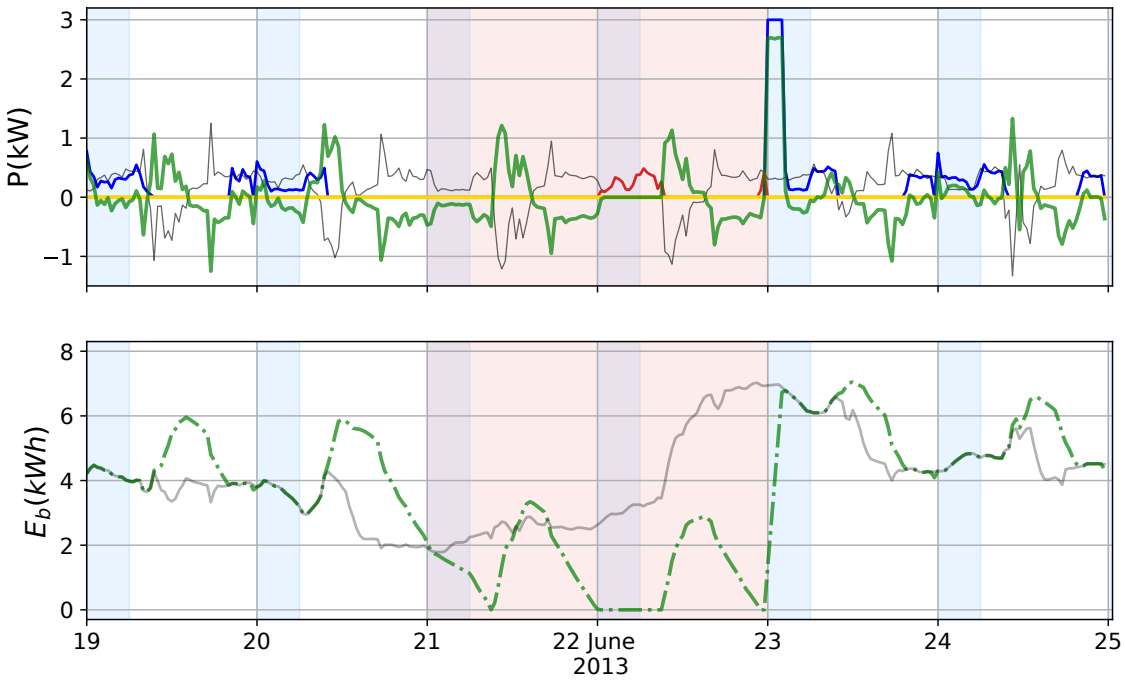

Figure 5.9 – High prob of failure, with outage

$$P_{nl}^{*cum}(k) = \sum_{i=k+1}^{k+H-1} P_{nl}^{*}(i). \tag{5.55}$$

We recall that P_{nl}^{*} (given by equation (3.10)) is defined as the difference between the building demand $P_{l}^{*}(k)$ and the solar production $P_{v}^{*}(k)$. State differently, $P_{nl}^{*}(k)$ is the energy needed to be drawn from the grid ($P_{nl}^{*}(k) \geq 0$) or to be store ($P_{nl}^{*}(k) < 0$) at period k. Then, $P_{nl}^{*cum}(k)$ is the total energy needed at instant k to satisfy the building demand over the whole prediction horizon (from the next instant $k+1$ to the instant $k+H-1$) without drawing from the grid. With this information we can better understand the behavior of the SDCMPC.

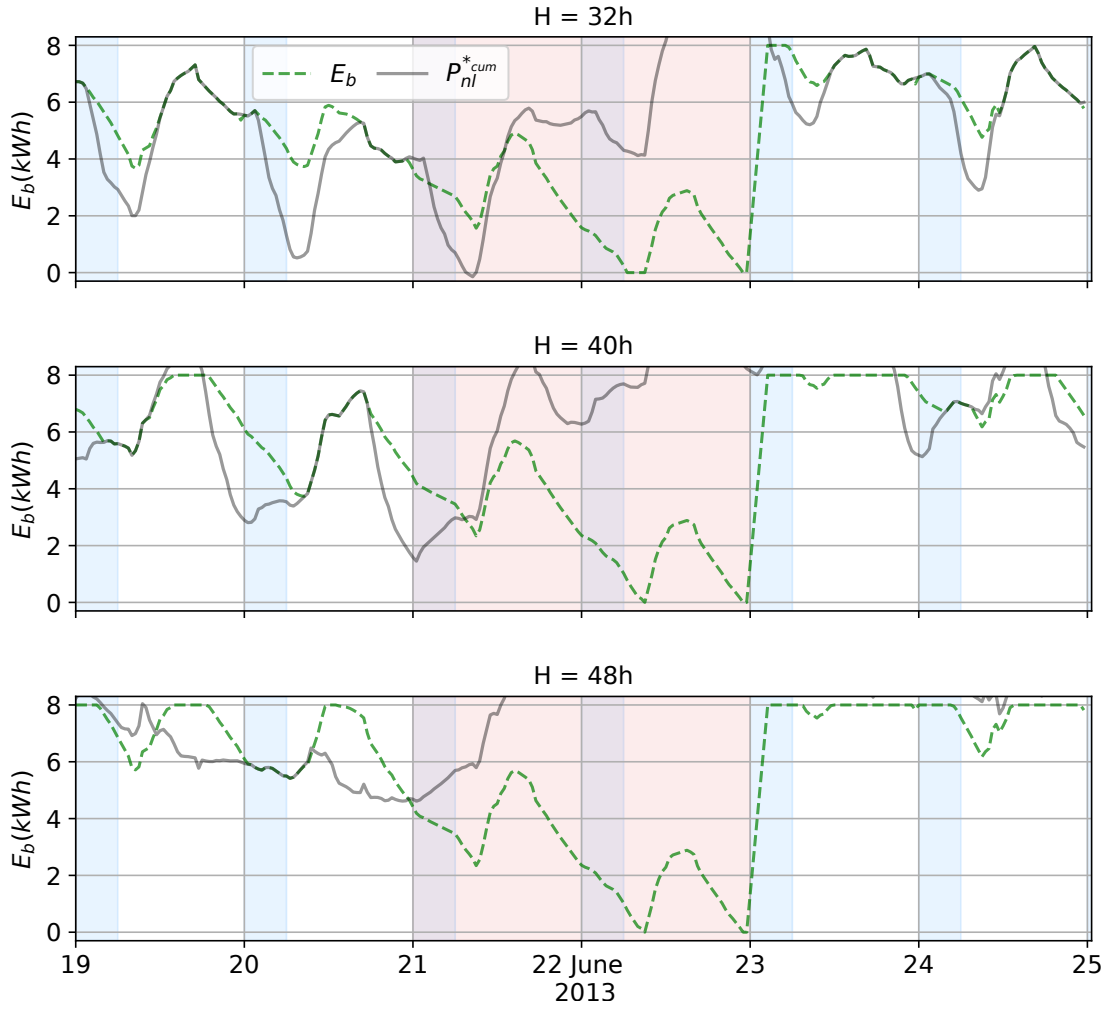

Figure 5.10 – Variation of the energy in the storage function of the MPC horizon with a high failure rate

Considering the high failure rate, the controller does not draw energy from the grid during the second half part of 20 June because the energy inside the storage is above what is needed to sustain the house over the prediction horizon. Moreover, we can see that every time the grid is used, it is such that the energy within the storage at that instant equals the energy needed to sustain the building over the prediction horizon without drawing from the grid.

This point is further proven by figure 5.10 which shows the evolution of $P_{nl}^{*cum}(k)$ and E_b for different values of the prediction horizon H. For $H = 32$ and $H = 48$ the storage at the starting instant of the GPO equals $P_{nl}^{*cum}(k)$ as expected. For $h = 40$ however, they are not equal because the battery discharges depending on the load demand while $P_{nl}^{*cum}(k)$ reduces depending on both the load demand and solar production.

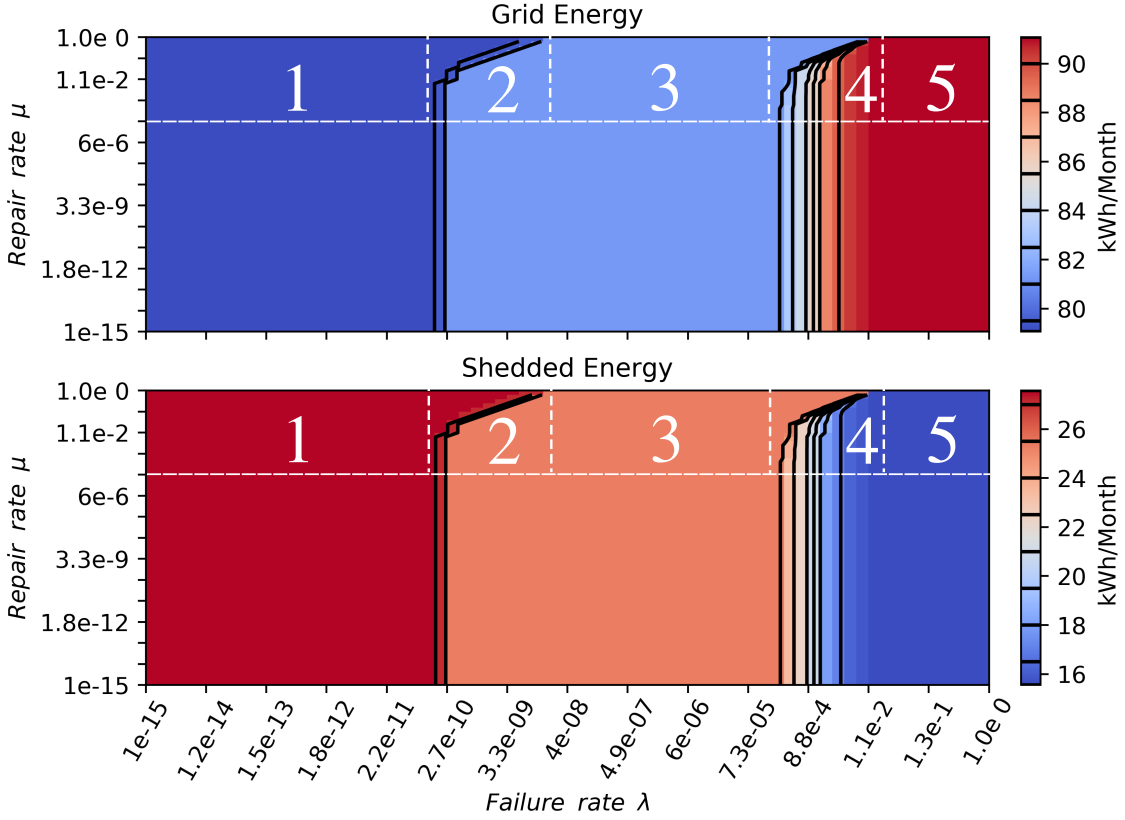

Figure 5.11 – Variation of the grid and shedded energy function of the repair and failure rate

5.6.4 Varying the failure and repair rate

Previously we have shown the effect of the extreme failure rates at a constant repair rate. Next, we vary both the failure and repair rate as

- $\lambda \in 1e\{-15 : 0.215 : -0.01\}$
- $\mu \in 1e\{-15 : 0.215 : -0.01\}$

to see how they interact with each other in the global controller behaviour.

Figure 5.11 shows the result of the variation for the energy drawn from the grid (first subplot) and not provided to the building (second subplot) over the low PV production month. As expected, the more energy is drawn from the grid; the less is the energy not provided to the building during outages. We notice that the repair rate, for its values bellow the white horizontal doted line, i.e., 7.3 10^{-5}, does not affect the failure rate. Considering, therefore, the values of the repair rate above the horizontal white line and the failure rate, we can divide the subplots into five different zones. Within the zones 1, 3 and 5, λ has locally no effect on the SDCMPC behaviour. Therefore, we are going to focus our efforts on the zones 2 and 4 where changes occur.

We recall that for a constant λ, the lower the repair rate the longer the grid's repair might last in case of a GPO while for a constant μ, the lower the failure rate the longer the grid might operate without failing.

For the energy drawn from the grid, a zoom on the zones 2 and 4 with a more finely

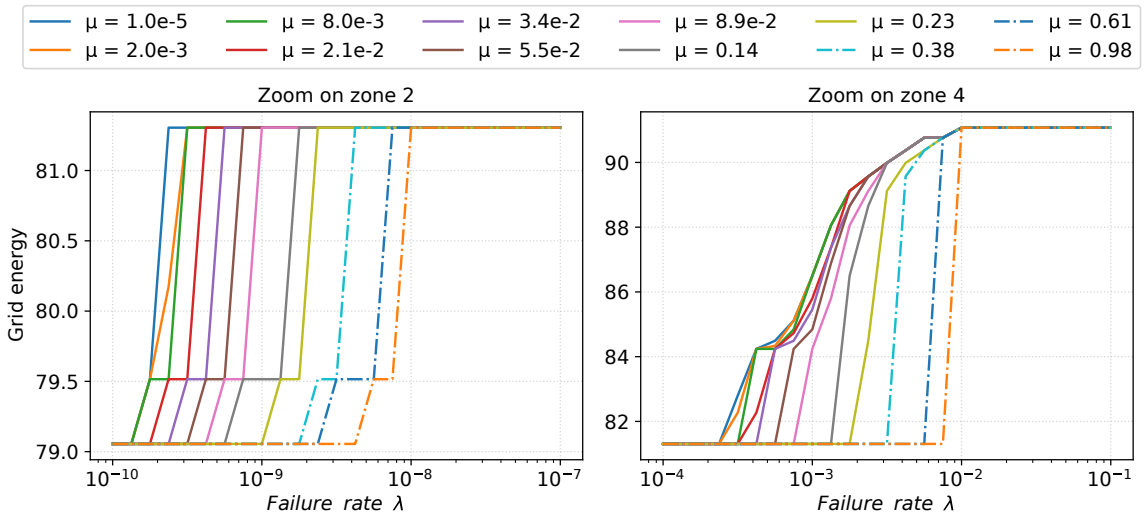

Figure 5.12 – Zoom on Zone 2 and 4 of figures 5.11

discretised λ and μ is given by figure 5.12. We can conclude that for a constant failure rate, the lower the repair rate and the higher is the energy drawn from the grid while for a constant repair rate, the lower the failure rate, the lower the energy drawn from the grid. This goes with the logical intuition: the longer the system is likely to undergo a faulty period, the higher should be the energy drawn from the grid to reduce the energy not provided to the system.

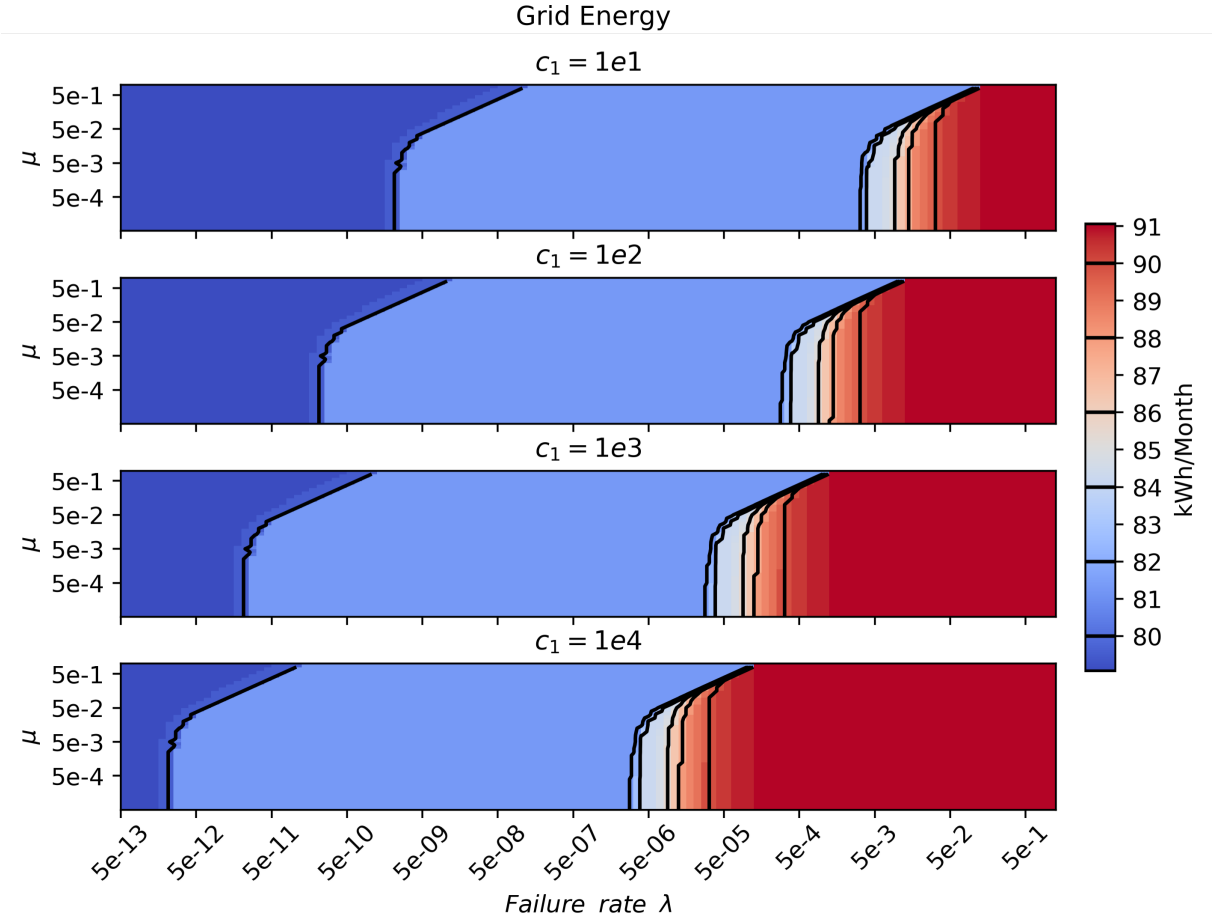

Figure 5.13 – Monthly energy drawn from the grid function of λ, μ and c_1

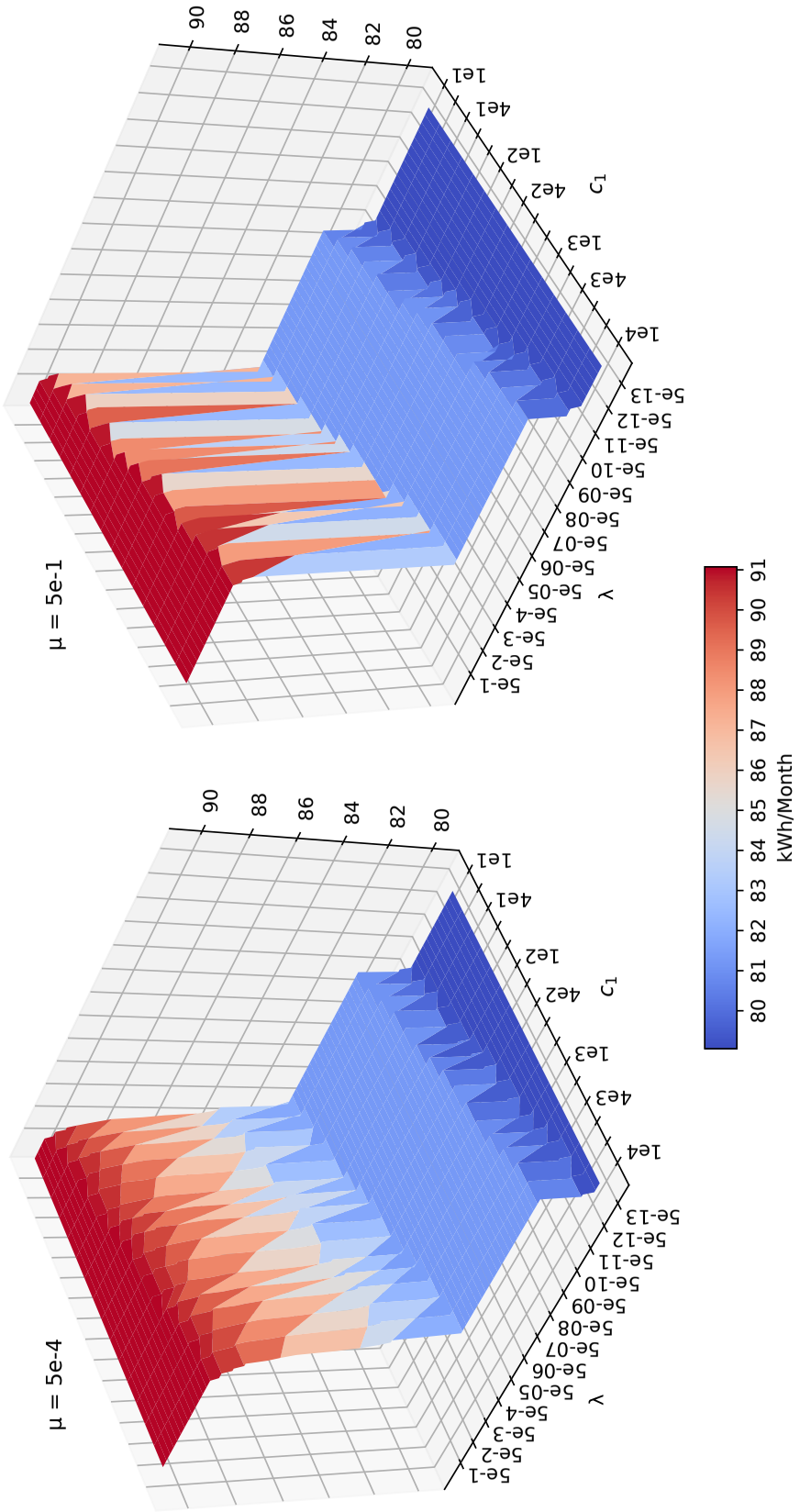

Figure 5.14 – Cut in the energy drawn from the grid at $\mu = 5.10^{-4}$ and $\mu = 5.10^{-1}$

5.6.5 Varying the failure, repair rate and the stochastic relaxation variable cost

In order to observe the stochastic relaxation variable cost c_1 effect on the system we perform a global sensitivity analysis by varying it alongside λ, and μ as follows:

- $\lambda \in 5e\ \{-13 : 0.1 : -0.7\}$
- $\mu \in 5e\ \{-4.7 : 0.1 : -0.7\}$
- $c_1 \in \{1e1\,, 2e2\,, 4e1\,, 6e1\,, 8e1\,, 1e2\,, 2e2\,, 4e2\,, 6e2\,, 8e2\,, 1e3\,, 2e3\,, 4e3\,, 6e3\,, 8e3\,, 1e4\}$.

Figure 5.13 shows the energy drawn from the grid function of the failure and repair rate for four values (1e1, 1e2, 1e3, 1e4) of the stochastic relaxation variable cost c_1. Figure 5.14 shows a 3D cut at $\mu = 5.10^{-4}$ and $\mu = 5.10^{-1}$ for the energy drawn from the grid.

In all the cases, the global behavior is the same, we still clearly distinguish fives zones, however, their frontier move along in power of 10 depending on the c_1. The latter can therefore serves as a setting parameter helping the user to chose an expected given controller behavior according to the grid's failure and repair rate.

5.6.6 SDCMPC vs. MSP wait and see

In this subsection, we compare the performance of the state of the art controller MSP wait and see described in section 5.3.2 to our proposed controller the SDCMPC.

Computational cost comparison

We are interested in comparing the memory estimate usage and the computing time of both controllers.The related simulations are done in open loop (we solve the associated problem for only the first instant) since we can extrapolate the results obtained for closed loop simulations. We provide more technical details about the strategy and the package used in appendix B.

The simulation results are given by figure 5.15. We can see that the memory usage and the computing time both grow exponentially according to the prediction horizon for the MSPWS, while the growth is much much slower for the SDCMPC. Let us emphasize that our laptop ran out of memory for a prediction horizon higher than 7.5 hours with the MSPWS.

The conclusion is pretty straightforward; for the same prediction horizon, the SDCMPC has better computing time and memory usage than the MSPWS. The low computing time and memory usage of the SDCMPC allows extending its prediction horizon from the maximum admissible by the MSPWS (given the simulation computer characteristics) to a much longer one. Figure 5.15 shows that even with an extended prediction horizon of 24 hours for the SDCMPC, there still a massive gap in the computing time and memory usage compared to the MSPWS.

Monte Carlo simulations

Based on a constant failure and repair rate $\mu = \lambda = 10^{-2}$ for the Markov chain describing the grid state and the stochastic relaxation variable cost $c_1 = 10^2$ we have created 40 independent scenarios of grid availability, each over a period of ten days. For each scenario, the starting day is chosen randomly between one and eighty such that:

- Day 1 to 30 correspond to the Low Pv period i.e., 1 - 30 June 2013
- Day 31 to 60 correspond to the Normal Pv period i.e., 1 - 30 November 2012
- Day 61 to 80 correspond to the High Pv period i.e, 1 - 20 September 2012.

We have simulated the SDCMPC and MSPWS with a prediction horizon of 7.5 hours and the SDCMPC considering the extended horizon 24 hours (SDCMPC2). Figure 5.16 shows the evolution of the main variables we are interested in for one of these scenarios. The second subplot represents at each instant, the cumulative energy not provided to the building from the beginning of the simulation up to the considered instant.

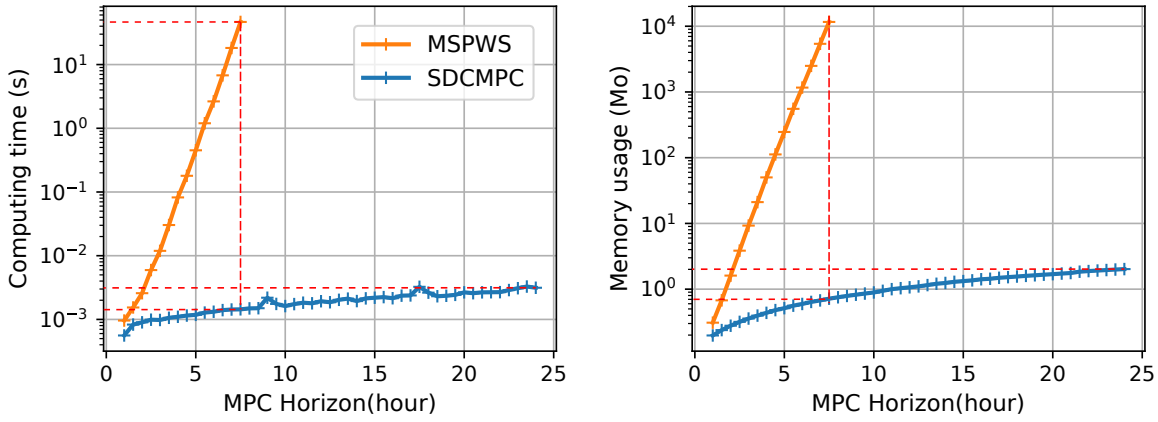

Figure 5.15 – Evolution of the computing time and memory estimate usage function of the prediction horizon from 1 to 7.5 hour for the MSP wait and see and from 1 hour to 24 hour for the SDCMPC

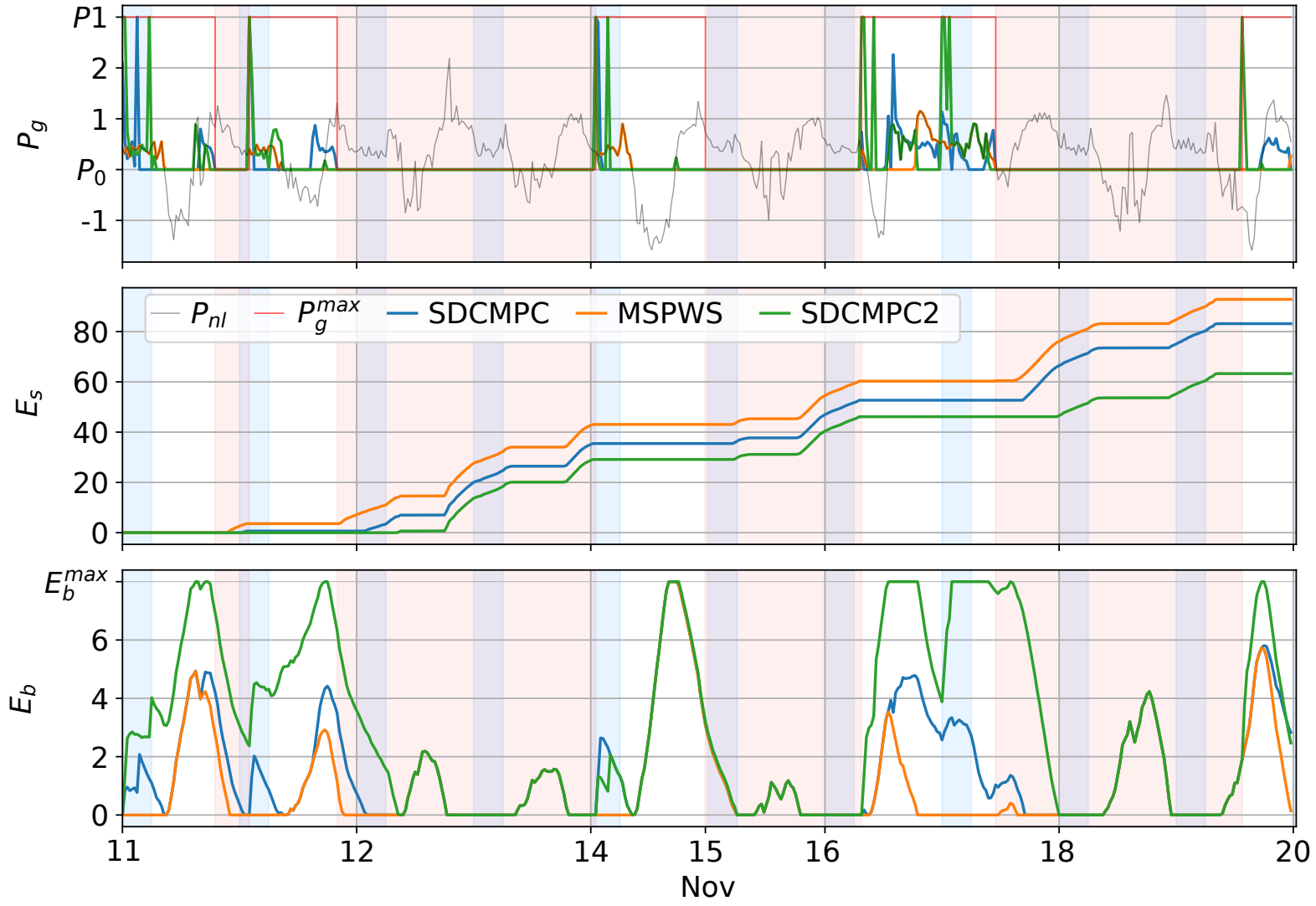

Figure 5.16 – Example of one simulation scenario

For each scenario and each controller, we have considered the following performance indices:

- The energy cost given by equation 4.21;
- The cumulative energy not provided to the building E_s[kWh]

$$E_s = \sum_{k=1}^{N} P_s(k)\Delta_t; \tag{5.56}$$

- The reconstructed optimization cost,

$$J_{re} = \sum_{k=1}^{N} \begin{bmatrix} c_g(k) & c_w(k) & 0 & c_s(k) \end{bmatrix} u(k) \tag{5.57}$$

There is a large variability across the 100 scenarios. The grid availability is 53 % on average for all scenarios, but it is only 3 % in the worst case and 98 % in the best. Therefore, comparing the average performance across all scenarios for each controller yields statistically meaningless differences. Instead, for each scenario, we compute differences in performance indices for pairs of controllers.

In table 5.2, we show the mean and the standard deviation of these differences across all scenarios. The SDCMPC2 does better on average compared to other controllers. This is due to its higher prediction horizon, which allows better anticipation, in particular, to take most of grid energy at a lower price.

In figure 5.17, we show the unaggregated performance indices for each scenario and each controller. We did not plot the cumulative energy not provided to the building E_s,

Table 5.2 – Stochastic Controller Performances for a Monte Carlo simulation of 10 days in Closed loop with a prediction horizon of 7.5 hours for SDCMPC and MSPWS and 24 hours for SDCMPC2

	J_{re}		En_{cost}		E_s	
	Mean	Std	Mean	Std	Mean	Std
MSPWS - SDCMPC	36.75	22.54	-1.03	0.47	3.78	2.29
SDCMPC - SDCMPC2	58.15	40.24	0.74	1.22	5.74	4.11
MSPWS - SDCMPC2	94.9	48.88	-0.29	1.21	9.52	4.98

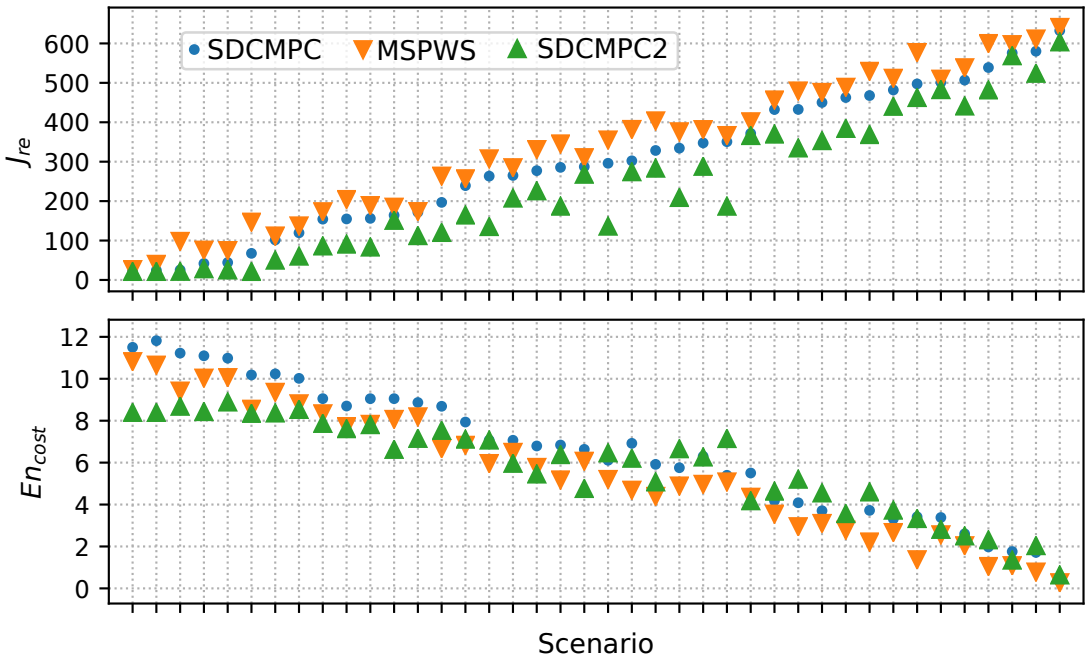

Figure 5.17 – Reconstructed optimization cost rearranged in ascending order of the results obtained by the SDCMPC with an horizon of 7.5 hour

because the latter is very similar to the reconstructed cost J_{re}. To increase the figures clarity, the scenarios are sorted in ascending order of the reconstructed optimization cost for the SDCMPC. This yields an approximate ascending order for the other controllers' cost and approximate descending order for the energy bill. Indeed, the energy bill is negatively correlated with grid unavailability and, therefore, the energy dissatisfaction.

We can see that the SDCMPC2 yields the lowest optimization cost J_{re} for all scenarios, followed by the MSPWS, and then the SDCMPC. For the energy bill, considering the same horizon, the MSPWS's is lower in all the cases compared to the SDCMPC. As for the SDCMPC2's it is respectively lower, higher in 42.5% and 30% of the scenarios compared to both others controllers. However, even for the scenarios where the SDCMPC2 energy cost is worse (higher) than the other's, this is largely compensated by a lower optimization cost hence a lower energy dissatisfaction.

5.7 Conclusion

We have proposed in this chapter a controller that integrates discrete stochastic constraints in the MPC framework. To do so, we have used relaxation techniques within an

Open Loop Feedback Control formulation. The resulting optimization complexity is not much increased compared to a deterministic MPC. On an energy management application, we have compared the new controller to a controller based on the MSPWS. Our controller's very low computational time and memory usage compared to the MSPWS allow a substantial extension of its prediction horizon. The extended horizon results in a significant improvement in the quality of service and the closed-loop optimization cost.

Conclusion

This thesis has investigated how to control a building energy management system for its resilience to rare events. We have mainly focus on grid power outages as types of rare events.

In part I, an introduction to Model Predictive Control (MPC) especially its usage in buildings control and briefs recalls on reliability theory to model defaults have been provided. We have also presented a succinct description of the case study, i.e., the solar building. It consists of four parts: the electrical grid, the storage unit, the renewable energy source, and the building iself considered as the load. Based on a real dataset made available by Ausgrid [1] the sizing of the building's components is explained; then we also introduced an example of a non resilient rule-based controller.

In part II, we have focused on two different issues that we summarise in the following lines.

We firstly explained the design of the classic model predictive controller (CMPC) to manage the energy flow within buildings. Since this controller is entirely passive to the occurrence of an extreme event, we have proposed a more sophisticated controller that we have called the Resilient Model Predictive Controller (ReMPC). The latter is an active controller because it adapts its behaviour given the extreme event's appearance or non-appearance. We have investigated the case of two classes of rare deterministic events: (i) planned events (the starting date and duration of the event is known in advance, and this information is used as an input of the building energy management system) and (ii) unplanned events (no information is given in advance about the occurrence of the default). As it has been shown through a comparison of the ReMPC to three other states of the art controllers (designed for the same purpose), the former outperforms its contenders, i.e., satisfy the building critical energy needs during outages longer.

Secondly, we have investigated a more interesting type of fault. Since we have first considered a deterministic default, we took a more realistic approach. We have supposed

1. Australia's largest electricity distributor

probabilistic information about the grid's state before the occurrence or during an outage. After we formalised the new problem, we have explained why the current existing frameworks, mainly robust optimisation and chance constraints, are not well suited to be used as resolution methods. The multistage stochastic programming method could be used; however, due to the length of the MPC's receding horizon, this leads to a combinatorial explosion of the scenario to consider. We have, therefore, proposed a new method to tackle this problem without reducing the horizon's length. The new method has been used to design a new controller that we have called the stochastic discrete constraint model predictive controller (SDCMPC). We have benchmarked the latter against a controller based on the multistage stochastic programming wait and see (MSPWS). As it has been shown, there is a huge difference in memory usage and computing time, the SDCMPC being better while using the same horizon length. This difference has still stayed remarkable even when we have extended the horizon length for the SDCMPC while we run out of RAM for the simulation with its contender.

Future works

Besides the work that has been presented in this thesis, we propose in the following some ideas of improvement that can be carried as future works.

Uncertainty One of the first assumption in the work is to consider a deterministic building demand and solar production over the future. Even though prediction algorithms have largely improve, the likelihood of error prediction is still present. Since this cannot be avoided, therefore, we propose to consider these uncertainties in the building model so that it can be integrated to the controllers designing. Another type of uncertainty that is worth investigating is when the control computed can not be applied directly to the system due to the asynchronism of both the GPO and the command instant.

Lower level controller The different control strategies that we have developed in this work are all of a higher level type since these cannot directly impinge on the buildings actuators. They provide therefore set points to be utilise by a lower level controller. It follows that our strategies must be combined with others controllers to be fully operational. Although this approach is practical and implementable, an interesting development idea will be to directly consider the actuators' control in the strategies at the cost of increased

complexity.

Hybrid formulation The extreme event that we have consider all along this work is a grid power outage. Since this implies that the value of maximum power generated by the latter varies within an discrete set we propose to shift the modelling of our problem in the hybrid framework. The system could be represented as having two or several modes between which it should switch directly according to the grid's state; hence different objective could be associated with each mode.

Resilient SDCMPC The first controller we have developed is a resilient type in the sense that it can automatically adjust the building's demand during an outage. The second strategy however has focused on integrating probabilistic model of the grid outage in the model. We propose as future work to investigate the possibilities of a resilient SDCMPC which besides integrating the probabilistic grid information should also be able to adjust the building's demand during outage according to the probabilistic information.

Interactions In this work, we have investigated the resilient controller in one building ignoring its surrounding. We think it would be interesting to investigate the decentralized or distributed interactions between several such controllers in a smart city in order to improve the latter global resilience.

Part III

Appendices

Annexe A

Résumé étendu en français

A.1 Introduction [1]

L'une des conséquences les plus apparentes du réchauffement climatique, est la rapide augmentation de la fréquence et des amplitudes des événements météorologiques extrêmes [Wal+14]. À leur tour, ceux-ci, produisent souvent des dégâts sur les lignes de distribution d'électricité. Il en résulte souvent des délestages de longue durée dont les répercussions peuvent s'évaluer en conséquences économiques mais aussi en perte de vie humaines. C'est le cas du Porto Rico où après l'ouragan Maria et les mois de délestages qui en ont suivi, les pertes en vie humaines sont estimées à des milliers [Kis+18].

Limiter les conséquences des évènements extrêmes devient donc primordial pour les pouvoirs publics. La résilience qui se définit comme la capacité d'un système à se préparer et adapter son comportement en présence d'évènements perturbateurs se présente comme l'une des solutions. Plusieurs travaux ont été menés dans ce contexte, afin d'intégrer ou d'adapter les systèmes existant aux contraintes qu'impose la résilience.

Ces travaux pour la plupart, sont axés autour des infrastructures inter-connectées, des systèmes cybers-physiques et des systèmes de grandes tailles et négligent donc les petits systèmes de l'utilisateur. Pourtant, une stratégie résiliente du distributeur d'électricité ne saurait être complètement effective si l'utilisateur, de son côté, par l'intermédiaire du système de gestion d'énergie dans le bâtiment (BEMS [2]), n'implémente pas aussi une certaine stratégie résiliente.

Dans cette thèse, nous nous sommes donc posés la question principale qui est :

1. Résumé du chapitre 1
2. Building Energy Management System

Comment piloter un système énergétique pour améliorer sa résilience aux événements rares ?

Les parties suivantes apportent des éléments de réponse à cette question en se focalisant sur les délestages, un exemple d'évènement rare et en examinant le cas des bâtiments intelligents comme système énergétique.

Ce faisant nos contributions sont les suivantes :

- un état de l'art succinct sur les stratégies de commande résilientes dans les bâtiments ;
- la conception d'une nouvelle stratégie résiliente basée sur le contrôle prédictif, qui vient refermer le gap existant des anciennes stratégies dans le cas des délestages déterministes ;
- la proposition d'une nouvelle méthode pour éviter l'explosion combinatoire (des arbres de scénarios), qu'engendre la prise en compte des évènements extrêmes probabilistes ;
- l'application de la méthode proposée sur un cas d'étude.

A.2 Introduction du MPC et de la sûreté [3]

Dans cette section nous présentons brièvement au lecteur, la théorie de la commande prédictive et de la fiabilité de fonctionnement. Le lecteur intéressé peut se référer à [CA07 ; KC16] pour la première et [RH04 ; BA92] pour la seconde. Ces deux théories sont les socles sur lesquels se basent les stratégies qui sont développées dans les sections suivantes.

A.2.1 Commande prédictive

La méthodologie de la commande prédictive [4] se base sur la stratégie décrite par la figure A.1. Soit un système dynamique décrit par son équation discrète :

$$x(k+1) = f(k, x(k), u(k)) \tag{A.1}$$

3. Résumé du chapitre 2
4. Model Predictive Control (MPC)

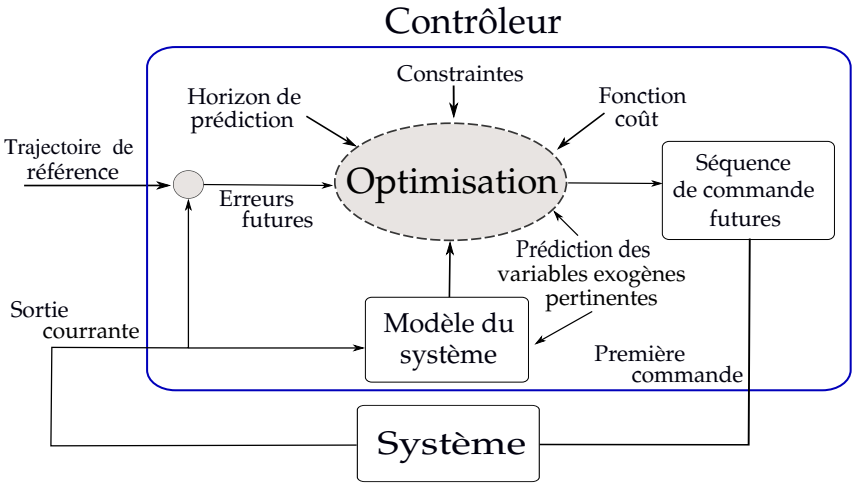

Figure A.1 – Méthodologie de la commande prédictive pour le contrôle d'un système

avec

- k l'index de l'instant présent ;
- $x(k) \in \mathbb{R}^{n_x}$, et $u(k) \in \mathbb{R}^{n_u}$ respectivement les vecteurs d'états et de commande du système (A.1).

Supposition A.1. Nous supposons qu'à chaque instant k le vecteur d'état peut-être soit mesuré, estimé ou observé.

Le système ainsi défini est contraint tel que :

$$\Big(u(k), x(k)\Big) \in \mathbb{D} \subset \mathbb{U} \times \mathbb{X} \text{ avec } \mathbb{U} \subset \mathbb{R}^{n_u} \text{ et } \mathbb{X} \subset \mathbb{R}^{n_x}. \tag{A.2}$$

Notons par $v(k+h|k)$ la prédiction à l'instant k de la variable $v \in \mathbb{R}^{n_v}$ sur un instant futur $k+h$ et par

$$V(k) = \Big[v^T(k|k), v^T(k+1|k), \ldots, v^T(k+H-1|k)\Big]^T \in \mathbb{R}^{n_v.H} \tag{A.3}$$

la trajectoire prédite de v à l'instant k le long de l'horizon de prédiction de longueur H. A chaque instant k, l'évolution du système le long de l'horizon de prédiction est formulée grâce à son équation dynamique. Basé sur cette prédiction et sous les contraintes, un coût de performance donné par

$$J(k) = \sum_{h=0}^{H-1} l_h\Big(x(k+h|k), u(k+h|k)\Big) + V_f\Big(x(k+H|k)\Big) \tag{A.4}$$

avec $l_h : \mathbb{R}^{n_x} \times \mathbb{R}^{n_u} \to \mathbb{R}$, et $V_f : \mathbb{R}^{n_x} \to \mathbb{R}$ respectivement les coûts instantané et terminal, est minimisé. Le problème générique est défini par le problème A.1

Problème A.1 (Problème du contrôle Prédictif).

$$U^*(k) = \underset{u(k|k),\ldots,u(k+H-1|k)}{\arg\min} \quad J(k) \tag{A.5a}$$

$$\text{tel que } \forall h \in \mathbb{N}_0^{H-1}$$

$$\Big(u(k+h|k), x(k+h|k)\Big) \in \mathbb{U} \times \mathbb{X} \tag{A.5b}$$

$$x(k+H|k) \in \mathbb{X}_f \tag{A.5c}$$

$$x(k|k) = x(k) \tag{A.5d}$$

$$x(k+h+1|k) = f\Big(k, x(k+h|k), u(k+h|k)\Big) \tag{A.5e}$$

Grâce au principe de l'horizon glissant, à chaque nouvel instant l'horizon de prédiction est déplacé d'un pas vers l'avant (comme indiqué par la figure A.2) et le problème A.1 est résolu. Le problème ainsi résolu permet d'obtenir une séquence de commande d'entrées $U^*(k)$, dont uniquement le premier élément $u(k|k)$ est appliqué au système.

Définir un problème de contrôle prédictif revient principalement donc à :

1. trouver le modèle décrivant le système à contrôler ;
2. définir la fonction coût qui prend en compte les performances voulues ;
3. décrire les contraintes du système.

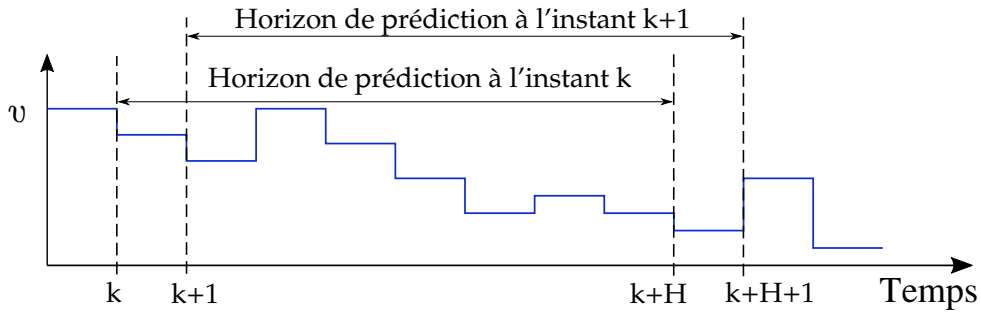

Figure A.2 – Principe de l'horizon glissant

A.2.2 Commande prédictive dans le bâtiment

Modèle du système

Pour que le contrôleur prédictif puisse prédire l'état du système à n'importe quel moment futur, Il est important de définir un modèle mathématique, décrivant le plus fidèlement possible le comportement du processus associé. Nous distinguons trois types de modèles :

1. modèle à boîte blanche : qui sont développés en analysant les principes physiques du système afin d'obtenir des équations dynamiques bien précises. Ils sont donc les plus pertinents pour des stratégies basées sur l'optimisation ;
2. modèle à boîte noire : qui sont aussi connus sous le nom de modèles axés sur les données car ils se basent sur ces dernières (entrées et sorties mesurées) pour approximer via des fonctions mathématiques la dynamique interne du système ;
3. modèle à boîte grise : Une combinaison des deux modèles précédents où une partie de la dynamique interne du système est connue ;

Qu'importe le modèle choisi, il est important de noter qu'au niveau de la commande d'un bâtiment ce dernier peut être considéré de deux manières différentes à savoir :

- une zone unique ; autrement appelé contrôle de haut niveau. Le but ici est de gérer les flux d'énergie dans le bâtiment, afin de déterminer des points ou des signaux de référence énergétiques ;
- un ensemble de zones ; aussi connue sous le nom de contrôle bas niveau. Dans ce cas, l'attention est portée sur la commande des équipements de chaque zone du bâtiment comme le chauffage, l'éclairage, les volets etc ...

Dans cette thèse, nous considérons le bâtiment comme une zone unique ; certes certains travaux combinent les deux représentations [ABG18 ; Gan+20].

Fonction coût

La fonction coût de l'optimisation permet de définir un certain comportement à deux fins principales : la stabilité globale du système (le coût optimal doit être une fonction de Lyapunov) et la performance (maximiser le confort des utilisateurs par exemple). Nous distinguons deux types de fonctions coûts toutes convexes

Tableau A.1 – Types de contraintes. Il est à noter que les contraintes sur l'état $x(k+h|k)$ sont uniquement utilisées à titre d'illustration. Ces contraintes pourraient donc être aussi appliquées soit à l'entrée $u(k+h|k)$ ou sur une combinaison des deux. précédents

Type de contraintes	**Description mathématique**
Linéaires	$Ax(k+h\|k) \leq b$
Quadratiques	$(x(k+h\|k) - \bar{x})^T Q(x(k+h\|k) - \bar{x}) \leq 1,\ Q \succeq 0$
Stochastiques	$A(\boldsymbol{\xi})x(\boldsymbol{\xi}, k+h\|k) \leq b(\boldsymbol{\xi})$
À commutation	Si *condition* alors $A_1 x(k+h\|k) \leq b1$ sinon $A_2 x(k+h\|k) \leq b_2$
Non linéaires	$h(x(k+h\|k)) \leq 0$

- Fonction coût quadratique : Utilisée dans le contrôle prédictif du type traditionnel, où le but est de pénaliser l'écart entre le signal de consigne et celui de sortie (commande de la température d'un bâtiment par exemple).
- Fonction coût linéaire : Utilisée dans le contrôle prédictif du type économique [5], où l'objectif est de minimiser des signaux économiques (minimiser une facture électrique par exemple).

Définition des contraintes

La capacité à facilement définir les contraintes dans la formulation du problème est l'une des forces du contrôle prédictif. Nous distinguons plusieurs types de contraintes qui se résument dans le tableau A.1.

A.2.3 Introduction à la sûreté de fonctionnement

La sûreté de fonctionnement [6] est l'aptitude d'un système à remplir une ou plusieurs fonctions requises dans des conditions données. Cette section introduit ses notions clés qui nous intéressent dans le cadre de cette thèse.

Supposons que l'état aléatoire $\boldsymbol{X}$ dans lequel se trouve un système à un instant t noté $\boldsymbol{X}(t)$ [7] se définit par

5. Economic Model Predictive Control (EMPC)
6. Reliability, Availability, Maintainability, and Safety (RAMS)
7. La convention suivante est adoptée pour le reste du manuscrit : Une variable aléatoire et sa réalisation sont respectivement indiquées par une lettre majuscule en gras et en normal

$$\boldsymbol{X}(t) = \begin{cases} 1 & \text{Si le système fonctionne à l'instant t} \\ 0 & \text{Si le système ne fonctionne à l'instant t} \end{cases} \tag{A.6}$$

Intéressons-nous aux mesures suivantes :

temps jusqu'à la défaillance. Il s'agit du laps de temps entre la mise en marche d'un système (la date de départ est toujours considérée comme étant $t = 0$) et l'instant où la première défaillance se produit ;

fonction de répartition $F(t)$. C'est la probabilité de non fonctionnement à la date t. À la date initiale $t = 0,\ F(t) = 0$ et croît vers $F(t) = 1$ lorsque $t \to \infty$;

fonction de fiabilité $R(t)$. C'est la probabilité de bon fonctionnement à la date t. Elle est le complément de la fonction de répartition de telle sorte qu'à la date initiale $t = 0,\ R(t) = 1$ et croît vers $R(t) = 0$ lorsque $t \to \infty$

$$R(t) = 1 - F(t); \tag{A.7}$$

fonction densité de probabilité. Elle se nomme autrement fonction de distribution et se définit comme la probabilité qu'un défaut se produise dans un intervalle de temps dt donné.

$$f(t) = \frac{d}{dt}F(t) = -\frac{d}{dt}R(t); \tag{A.8}$$

Fonction taux de défaillance instantané $z(t)$. C'est la probabilité qu'un défaut se produise sur un intervalle $dt = t_1 - t$ sachant que le dispositif est en fonctionnement à l'instant t

$$z(t) = \frac{f(t)}{R(t)} \tag{A.9}$$

Les relations mathématiques entre les fonctions de répartition $F(t)$, de fiabilité $R(t)$, de densité de probabilité $f(t)$ et de taux de défaillance instantané $z(t)$ sont données dans le tableau A.2, tandis que la figure A.3 illustre ces relations dans le cas d'une densité de probabilité $f(t)$ normale de moyenne $\mu = 3.5$ et de variance $\sigma^2 = 1$.

La courbe en baignoire

La fonction taux de défaillance caractérisant un système le long de sa vie, se représente par la courbe en forme de baignoire illustrée par la figure A.4. Nous y distinguons trois zones :

Tableau A.2 – Relation mathématique entre $F(t)$, $f(t)$, $R(t)$ et $z(t)$

	$F(t)$	$f(t)$	$R(t)$	$z(t)$
$F(t) =$	-	$\int_0^t f(u)du$	1- R(t)	$1 - \exp\left(-\int_0^t z(u)du\right)$
$f(t) =$	$\frac{d}{dt}F(t)$	-	$-\frac{d}{dt}R(t)$	$z(t)\ \exp\left(-\int_0^t z(u)du\right)$
$R(t) =$	$1 - F(t)$	$\int_t^\infty f(u)du$	-	$\exp\left(-\int_0^t z(u)du\right)$
$z(t) =$	$\frac{dF(t)/dt}{1-F(t)}$	$\frac{f(t)}{\int_t^\infty f(u)du}$	$-\frac{d}{dt}lnR(t)$	-

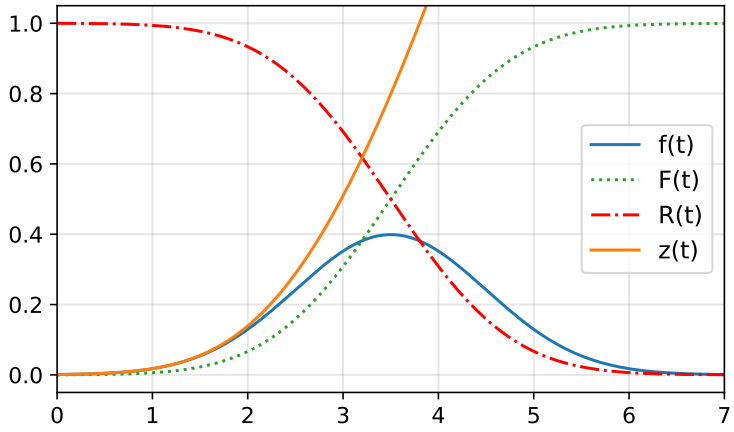

Figure A.3 – Relation entre les fonctions $F(t), R(t)$ et $z(t)$ pour une $f(t)$ loi normale $\mu = 3.5$ et de $\sigma^2 = 1$

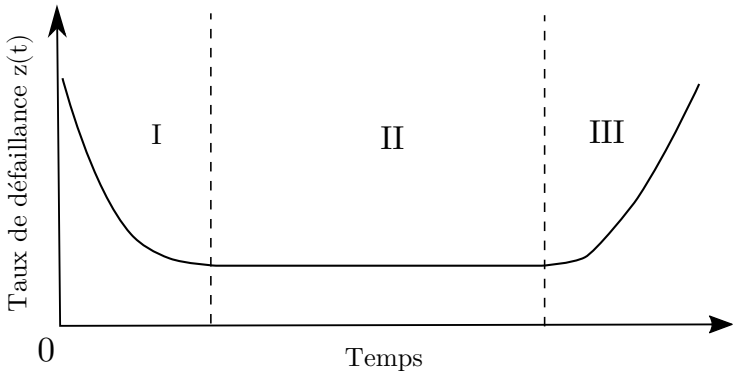

Figure A.4 – Courbe en baignoire

- zone I où se produisent les pannes de jeunesse. $z(t)$ décroît, le système s'améliore ;
- zone II où se produisent des pannes aléatoires dues à des défaillances brutales, le plus souvent imprévisible. $z(t)$ est constant ;
- zone III où se produisent les pannes d'usures dû au vieillissement du système. $z(t)$ croit, le système se dégrade.

Nous nous intéressons ici à la zone II qui modélise les pannes imprévisibles dans un cas où le temps est discret.

Taux de défaillance constant : Distribution géométrique Considérons une épreuve de Bernoulli dont le succès, l'évènement A et dont l'échec l'évènement A^* ont les probabilités suivantes associées

$$\begin{aligned} \Pr[A] &= p \in [0,1] \\ \Pr[A^*] &= 1-p. \end{aligned} \tag{A.10}$$

En supposant une séquence d'épreuve de Bernoulli où les probabilités $\Pr[A]$ et $\Pr[A*]$ sont constantes entre épreuves, le nombre d'expériences avant que le premier succès ne se produise est donné par la distribution géométrique.

En associant un succès à l'instant k ($k^{ième}$ expérience) à une défaillance d'un système, la probabilité de succès devient le taux de défaillance telle que

$$p = z(k) \tag{A.11}$$

et la fonction densité de défaillance discrète se calcule par

$$f(k) = p(1-p)^k, \quad \forall k \in \mathbb{N}_1^\infty. \tag{A.12}$$

A.3 Description de la maison solaire[8]

Pour illustrer les différentes méthodes de gestion à développer, nous décrivons dans cette section le bâtiment utilisé ainsi que le dimensionnent de ses composantes.

8. Résumé du chapitre 3

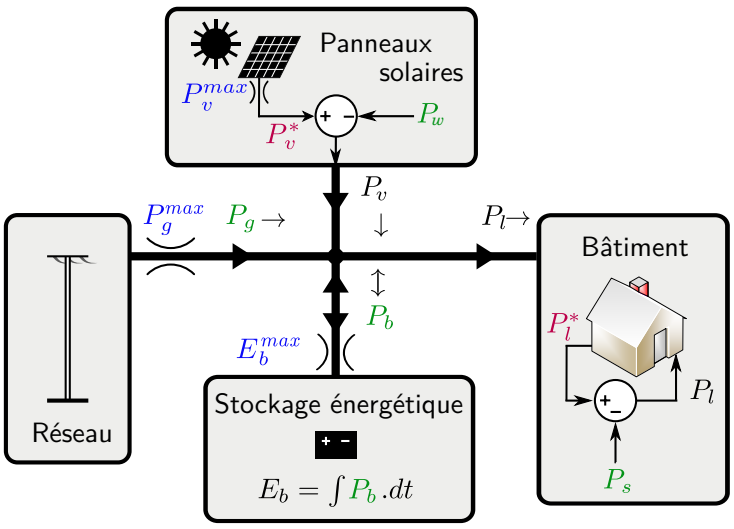

Figure A.5 – Modèle en flux de la maison solaire. Les variables de décision sont en couleur verte, les variables externes en couleur rouge, les variables internes en couleur noir et les variables constantes en couleur bleue

A.3.1 Modèle du bâtiment solaire

Le système énergétique que nous considérons dans nos applications est un bâtiment photovoltaïque décrit par la figure A.5. Ce dernier se compose de 4 parties : Le réseau électrique ; l'ensemble de stockage ; les sources d'énergie renouvelable représentées par des panneaux solaires et le bâtiment.

Réseau électrique : Il s'agit du distributeur d'électricité. La puissance maximale P_g^{max}[kW] qu'il fournit prend deux valeurs suivant sa disponibilité comme suit :

$$P_g^{max} = \begin{cases} P_{g1}^{max} & \text{Lorsque le réseau électrique est disponible} \\ P_{g0}^{max} & \text{Lorsque le réseau électrique est indisponible.} \end{cases} \tag{A.13}$$

La puissance soutirée du réseau à l'instant k $P_g(k)$ est limitée par la puissance maximale souscrite et l'injection sur le réseau dans un but de revente de puissance est interdite :

$$0 \leq P_g(k) \leq P_g^{max}. \tag{A.14}$$

Panneaux solaires : C'est la seconde source d'énergie de puissance nominale P_v^{max}. Sa production $P_v^*(k)$[kW] à un instant donné k est réduite en cas de surproduction par la puissance écrêtée $P_w(k)$[kW], de sorte que la puissance réelle injectée dans le système est

donnée par

$$P_v(k) = P_v^*(k) - P_w(k) \quad \text{avec } 0 \leq P_w(k) \leq P_v^*(k). \tag{A.15}$$

Système de stockage : Il permet de stocker ou de délivrer à chaque instant une puissance $P_b(k)$. L'accumulation de cette dernière au cours du temps permet d'obtenir l'état de charge E_b[kWh]

$$E_b(k+1) = E_b(k) + P_b(k)\Delta_t, \tag{A.16}$$

limité par la capacité du stockage telle que

$$0 \leq E_b(k) \leq E_b^{max}. \tag{A.17}$$

Le bâtiment : L'énergie fournit par les trois parties précédemment décrites permet d'alimenter le bâtiment. Nous différencions entre la puissance qui lui est fournie $P_l(k)$[kw] et celle demandée $P_l^*(k)$[kW], car lorsque cette dernière est supérieure au potentiel du système une partie doit être délestée. Nous définissons donc la puissance délestée $P_s(k)$ de telle sorte que

$$P_l(k) = P_l^*(k) - P_s(k) \quad \text{avec} \quad 0 \leq P_s(k) \leq P_l^*(k). \tag{A.18}$$

Remarque A.1. L'accumulation de la puissance délestée sur une certaine période sera utilisé comme métrique de mesure de la non satisfaction énergétique du bâtiment.

Remarque A.2. Nous définissons le "net load" comme étant la différence entre la puissance demandée par le bâtiment $P_l^*(k)$ et la puissance solaire produite $P_v^*(k)$.

$$P_{nl}^*(k) = P_l^*(k) - P_v^*(k). \tag{A.19}$$

Remarque A.3. Nous définissons le "controlled net load " comme étant la différence entre la puissance fournie au bâtiment et la puissance solaire produite

$$P_{nl}(k) = \underbrace{P_l^*(k) - P_s(k)}_{P_l(k)} - P_v^*(k). \tag{A.20}$$

Les quatre parties décrites ci dessus sont liées entre elles par l'équation de conservation d'énergie décrite par

$$P_g(k) - P_b(k) + \underbrace{P_v^*(k) - P_w(k)}_{P_v(k)} = \underbrace{P_l^*(k) - P_s(k)}_{P_l(k)} \tag{A.21}$$

Données de la maison solaire

Les données en entré du bâtiment, spécifiquement la puissance demandée P_l^* et celle solaire P_v^* sont extraites de la base de donnée "Solar home electricity data"[Com ; Rat+17], en libre accès du fournisseur d'électricité Australien Ausgrid. Elle contient la demande et la production enregistrées à intervalles de temps réguliers $\Delta_t = 30$ mn de 300 clients sélectionnés aléatoirement sur la période allant du 1^{er} Juillet 2010 au 30 Juin 2013.

Nous utilisons directement la demande de chaque bâtiment comme telle mais procédons à une mise à l'échelle de la puissance solaire produite $P_v^*(k)$ telle que

$$\begin{aligned} P_v^*(k) =& P_v^{max} \times P_v^{1k} \\ =& P_v^{max} \times \frac{GP(k)_n}{PN_n} \end{aligned} \tag{A.22}$$

avec P_v^{1k} la production d'un panneau solaire de 1kWhc [9], $GP(k)_n$ et PN_n respectivement la puissance réelle produite et la puissance nominale de l'installation photovoltaïque du client n

Nous divisons la base de données en 2 parties : les données d'entraînement (du 1^{er} Juillet 2011 au 30 Juin 2012) et les données d'évaluation (du 1^{er} Juillet 2010 au 30 Juin 2011 et du 1^{er} Juillet 2012 au 30 Juin 2011).

A.3.2 Dimensionnent des éléments

Supposons que le dimensionnnement optimal est celui qui minimise le coût global (C_{glob}) de l'installation qui est égal à la somme du coût d'investissement initial (C_{inv}) et du coût opérationnel (C_{ope}),

$$C_{glob} = \begin{cases} C_{inv} &= c_E E_b^{max} + c_P P_v^{max} \\ + & \\ C_{ope} &= T_{life} \times \langle c_g P_g \rangle. \end{cases} \tag{A.23}$$

— C_{inv} est proportionnel à P_v^{max} et E_b^{max}, $c_E = 0.5$k€/kWh étant donné qu'un Tesla Powerwall [10] de 14 kWh coûte environ 7k€[Car17] et $c_P = 2$k€/kWc [inf15] ;

9. kWhc : kWh crête
10. Stockage énergétique de la marque Tesla

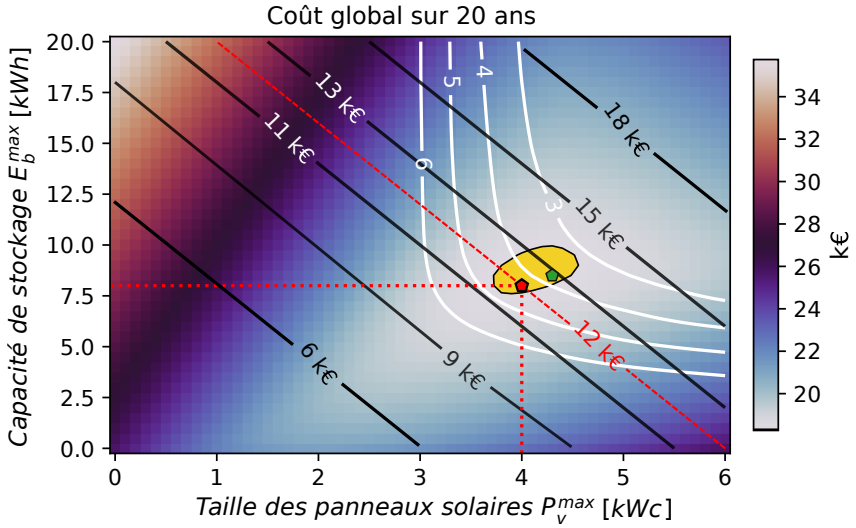

Figure A.6 – Coût Global dimensionnement

— C_{ope} est proportionnel à la facture électrique moyenne journalière $\langle c_g P_g \rangle$ du bâtiment multipliée par la durée de vie $T_{life} = 20$ ans (converti en jours) et en supposant que $c_g = 0.2$€/kWh.

Pour en arriver au dimensionnement choisi (8kWh, 4kWc) une étude paramétrique est menée sur la puissance nominale des panneaux solaires et de la capacité du stockage : $E_b^{max}(k) \in \{0 : 0.5 : 20\}$[kWh] et $P_v^{max} \in \{0 : 0.2 : 6\}$ [kWp].

Pour chaque paire de valeurs, le problème de contrôle du bâtiment est simulé en utilisant une loi de gestion heuristique. La figure A.6 illustre le coût global associé à chaque paire ainsi défini. Les isoclines diagonales y indiquent le coût d'investissement initial et celles blanches indiquent la consommation journalière moyenne.

Le choix du dimensionnement optimal peut se faire de deux manières différentes :

1. minimiser directement le coût global ;
2. mixer un coût d'investissement initial et minimiser le coût global associé.

Sur la figure A.6 le résultat de la première stratégie est indiqué par le pentagone vert. Dans son voisinage près à $1,5\%$ (zone délimitée en jaune) se trouve le dimensionnement que nous avons choisi (pentagone rouge) en suivant la seconde stratégie pour un coût d'investissement initial de 12k€.

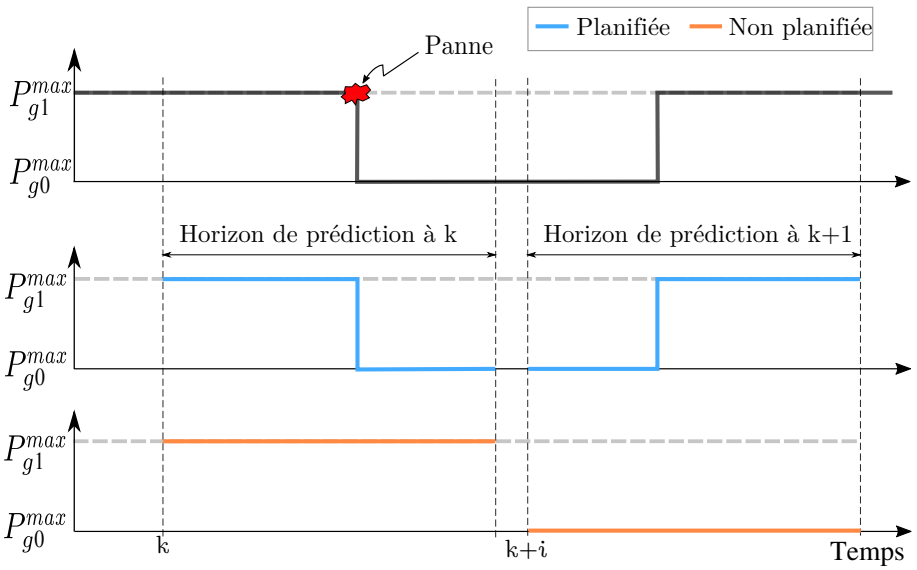

Figure A.7 – Prévision de l'état du réseau électrique dans le cas des pannes planifiées et non planifiées

A.4 Contrôleur énergétique résilient : Panne déterministe [11]

Dans cette section nous introduisons la notion de résilience afin de concevoir un contrôleur résilient pour la commande des bâtiments photovoltaïques. Nous concevons le contrôleur résilient basé sur la famille des contrôleurs prédictifs dans le cas d'un évènement déterministe, qui est le délestage électrique. Il en existe deux types définis ci dessous.

Définition A.1. Panne non planifiée [12] Il s'agit des pannes pour lesquelles aucune information n'est communiquée à la stratégie de commande.

Définition A.2. Panne planifiée [13] Il s'agit des pannes pour lesquelles toutes les informations associées sont communiquées à la stratégie de commande.

Les informations se réfèrent à la date de début et de fin de la panne. La figure A.7 illustre la prévision de l'état du réseau utilisé par le contrôleur dans le cas des pannes planifiées et non planifiées.

11. Résumé du chapitre 4
12. Unplanned Grid Power Outage (UGPO)
13. Planned Grid Power Outage (PGPO)

A.4.1 Objectifs de contrôle

En fonctionnement nominal (lorsqu'il n'y a pas de panne) la commande d'un bâtiment intelligent à deux objectifs :

1. minimiser la facture électrique ;
2. maximiser le confort des utilisateurs (qui revient à minimiser l'énergie délestée).

Mathématiquement, à chaque instant k ils s'écrivent respectivement :

$$C_G(k) = \sum_{h=0}^{H-1} c_g(k+h) P_g(k+h|k), \quad \forall\, k \in \mathbb{N}_1^N \tag{A.24}$$

$$C_S(k) = \sum_{h=0}^{H-1} c_s(k+h) P_s(k+h|k), \quad \forall\, k \in \mathbb{N}_1^N \tag{A.25}$$

avec $c_g(k+h)$ le coût de l'électricité à l'instant $k+h$, $c_s(k+h)$ un coût virtuel de délestage à l'instant $k+h$, H l'horizon du contrôleur prédictif et N l'horizon du problème.

Afin d'éviter de gaspiller l'énergie gratuite fournie par les panneaux solaires, nous minimisons aussi la puissance écrêtée qui s'écrit comme

$$C_W(k) = \sum_{h=0}^{H-1} c_w(k+h) P_w(k+h|k), \quad \forall\, k \in \mathbb{N}_1^N \tag{A.26}$$

avec $c_w(k+h)$ un coût virtuel d'écrêtage à l'instant $k+h$.

A.4.2 Contrôleur classique prédictif (CMPC [14])

Le coût d'optimisation du contrôleur classique se définit par une somme pondérée, par linéarisation scalaire [Nog15] des coûts précédemment définis.

$$J_{CLAS}(k) = C_G(k) + C_C(k) + C_S(k) \tag{A.27}$$

avec

$$c_w(k+h) = c_s(k+h) \tag{A.28}$$

$$c_w(k+h) \gg c_g(k+h). \tag{A.29}$$

14. CMPC : Classical Model Predictive Controller

Nous définissons le problème du contrôleur classique suivant

Problème A.2 (**Contrôle classique**).

$$\min_{\{P_g,P_b,P_s,P_w\}(k+h|k)} \quad J_{CLAS}(k) \tag{A.30a}$$

$$\text{s.t.} \forall h \in \mathbb{N}_0^{H-1},\ 0 \leq P_g(k+h|k) \leq P_g^{max} \tag{A.30b}$$

$$0 \leq P_w(k+h|k) \leq P_v^*(k+h) \tag{A.30c}$$

$$0 \leq P_s(k+h|k) \leq P_l^*(k+h) \tag{A.30d}$$

$$0 \leq E_b(k+h|k) \leq E_b^{max} \tag{A.30e}$$

$$P_v(k+h|k) = P_v^*(k+h) - P_w(k+h|k) \tag{A.30f}$$

$$P_l(k+h|k) = P_l^*(k+h) - P_s(k+h|k) \tag{A.30g}$$

$$E_b(k+h+1|k) = E_b(k+h|k) + P_b(k+h|k)\Delta_t \tag{A.30h}$$

$$P_g(k+h|k) - P_b(k+h|k) + P_v(k+h|k) = P_l(k+h|k) \tag{A.30i}$$

avec [15]

$$c_s(k) > c_s(k+1) > \ldots > c_s(k+H-1); \tag{A.31}$$

$$c_w(k) > c_w(k+1) > \ldots > c_w(k+H-1); \tag{A.32}$$

$$c_s(k+H-1) \gg max\Big[c_g(k+h), \quad \forall\, h \in \mathbb{N}_0^{H-1}.\Big] \tag{A.33}$$

le contrôleur ainsi décrit ne prend pas en compte l'apparition des pannes électriques. Pour ce faire nous concevons le contrôleur résilient ci dessous décrit.

A.4.3 Contrôleur résilient prédictif (ReMPC [16])

Durant les pannes de réseau électrique, le bâtiment accepte une réduction de sa demande énergétique telle que la nouvelle puissance demandée ; la puissance critique demandée P^c est proportionelle à la puissance demandée en période nominale et se calcule par :

$$P^c(k+h) = \alpha(k+h)P_l^*(k+h), \quad \text{avec} \quad \alpha(k+h) \in [0,\ 1], \tag{A.34}$$

le coefficient de confort. Lorsque α prend respectivement les valeurs 0 et 1 la demande critique est nulle ou égale à la demande nominale.

15. Le lecteur est prié de se référer au 4 pour plus d'explications sur les pondérations suivantes.
16. ReMPC : Resilient MPC

Nous définissons la contrainte

$$P_l^*(k+h) - P_s(k+h|k) \geq P^c(k+h). \tag{A.35}$$

qui exprime la prise en compte de la puissance critique lors des pannes de réseau. IL est à noter que lorsque le stockage est vide, la puissance critique ne pourra pas être satisfaite ; de ce fait nous introduisons la puissance critique délestée qui relaxe la contrainte précédente comme suit

$$P_l^*(k+h) - P_s(k+h|h) \geq P^c(k+h) - P_s^c(k+h|h), \tag{A.36}$$

avec

$$0 \leq P_s^c(k+h|h) \leq P^c. \tag{A.37}$$

Nous proposons de minimiser le coût de délestage critique donné par

$$C_S^C(k) = \sum_{h=0}^{H-1} c_s^c(k+h) P_s^c(k+h|k), \quad \forall\, k \in \mathbb{N}_1^N, \tag{A.38}$$

et définissons le coût global du contrôleur résilient comme

$$J_{ReMPC} = \underbrace{C_G(k) + C_C(k) + C_S(k)}_{J_{CLAS}(k)} + C_S^C(k). \tag{A.39}$$

Le problème du contrôleur résilient s'écrit :

Problème A.3 (Contrôleur résilient prédictif).

$$\min_{\{P_g, P_b, P_s, P_w, P_s^c\}(k+h|k)} \quad J_{ReMPC}(k) \tag{A.40}$$
$$\text{s.t.} \forall h \in \mathbb{N}_0^{H-1},\ \text{(A.30b)}, \text{(A.30c)}, \ldots, \text{(A.30i)}, \text{(A.36)}, \text{(A.37)}$$

A.4.4 Métriques de comparaison

Nous définissons les métriques suivantes :

— Le ratio de satisfaction L_{sr} [17]

$$L_{sr} = \frac{P_l}{P_l^*}. \tag{A.41}$$

17. Load satisfaction ratio

En période de panne, la puissance fournie doit être au minimum égale à la puissance critique, $P_l = P^c$ et nous définissons de ce fait le ratio de satisfaction critique L^c_{sr} [18]

$$L^c_{sr} = \frac{P^c}{P^*_l}. \tag{A.42}$$

— La fraction de temps (en pourcentage de la durée totale des pannes) durant laquelle le ratio de satisfaction L_{sr} est resté dans un certain intervalle

◇ τ^- : Lorsque $P_l \in [0, P^c[$ ou $L_{sr} \in [0, L^c_{sr}[$;

◇ τ^+ : Lorsque $P_l \in [P^c, P^*_l[$ ou $L_{sr} \in [L^c_{sr}, 1[$;

◇ τ^* : Lorsque $P_l = P^*_l$ ou $L_{sr} = 1$;

— La facture d'électricité En_{cost} [€]

$$En_{cost} = \sum_{k=1}^{N} c_g(k) P_g(k) \Delta_t \tag{A.43}$$

Nous ajoutons à ces nouvelles métriques l'énergie totale tirée du réseau électrique P_g, l'énergie totale délestée P_s et celle gaspillée P_w.

A.4.5 Simulations et résultats

Réglages de simulations

Dans les simulations, nous comparons en premier le ReMPC et le CMPC. Après s'en suit la comparaison entre le ReMPC et deux autres stratégies de contrôle résilientes : le *Smart Strategy controller* et le *Power save contrôleur* décrits dans [Gha+15 ; Jon+16b]. En vue de simplification et de lisibilité le premier est renommé RBC-R [19] et le second RBCPSC-R [20]. Ces deux contrôleurs sont principalement basés sur la stratégie heuristique décrite en section 3.3 en plus de quelques autres règles que nous expliquons ci dessous.

Le RBC-R maintient un niveau de stockage minimum E^{min}_b tant que le réseau est disponible. Par contre dès qu'une panne se produit, cette restriction est levée. Le RBCPSC-R se comporte pareillement que le RBC-R en cas de fonctionnement nominal. La différence apparaît en cas de panne électrique où, en plus de lever la restriction sur le stockage

18. Critical load satisfaction ratio
19. Rule Based Controller with Reserve
20. Rule Based Power Save Controller with Reserve

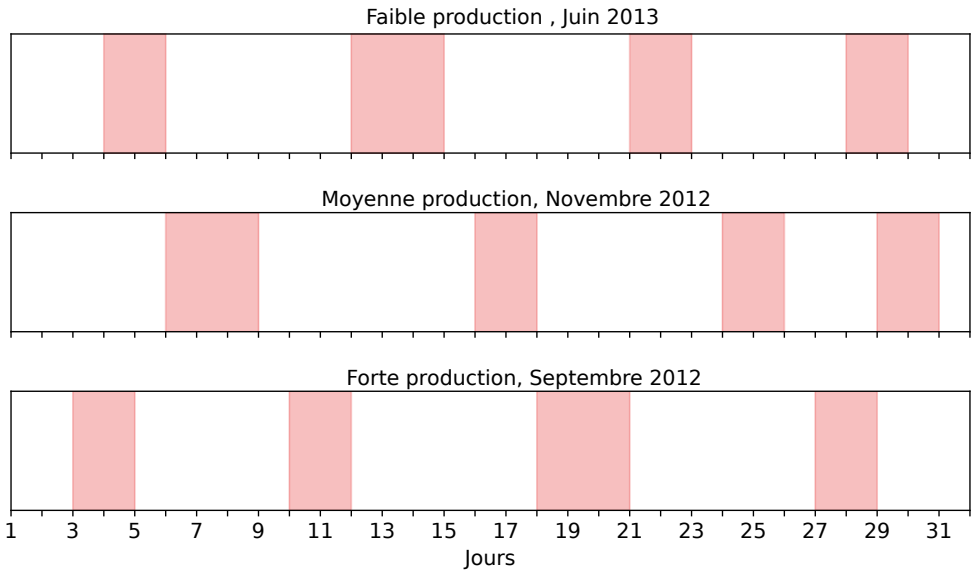

Figure A.8 – Les Mois de simulation et les jours de pannes

minimum, la stratégie réduit directement la puissance fournie au bâtiment à la puissance critique. Nous considérons les réserves de $20\%E_b^{max}$ et $30\%E_b^{max}$.

Afin de voir le comportement des contrôleurs en situation différentes, nous simulons sur trois périodes de production solaire faible (Juin 2013, 127kWh), moyenne (Novembre 2013, 208 kWh) et forte (Septembre 2012, 285kWh). La figure A.8 illustre ces différents mois avec les périodes de pannes représentées en rouge. Le total d'énergie demandé par le bâtiment durant ces périodes est 234kWh, 239kWh and 242kWh pour les mois respectifs de Juin 2013, Novembre et Septembre 2012.

Nous supposons que les pannes planifiées ou non commencent le premier jour à 00h et se terminent le dernier jour à 23h59.

Le coût de l'électricité est variable dans la journée tel que

$$c_g = \begin{cases} c_{nuit} = 0,1€/\text{kWh} & \text{en heure creuse : } 00h \text{ à } 05h59 \\ c_{jour} = 0,2€/\text{kWh} & \text{en heure pleine : } 00h \text{ à } 05h59 \end{cases} \tag{A.44}$$

Nous considérons un horizon de prédiction (H=48 ; 24h) et le coefficient de confort en cas de panne est donné par $\alpha = 0,5$ de telle sorte que, la puissance critique demandée est

la moitié de celle nominale,

$$P^c(k+h) = \underbrace{0,5}_{\alpha} P_l^*(k+h) \tag{A.45}$$

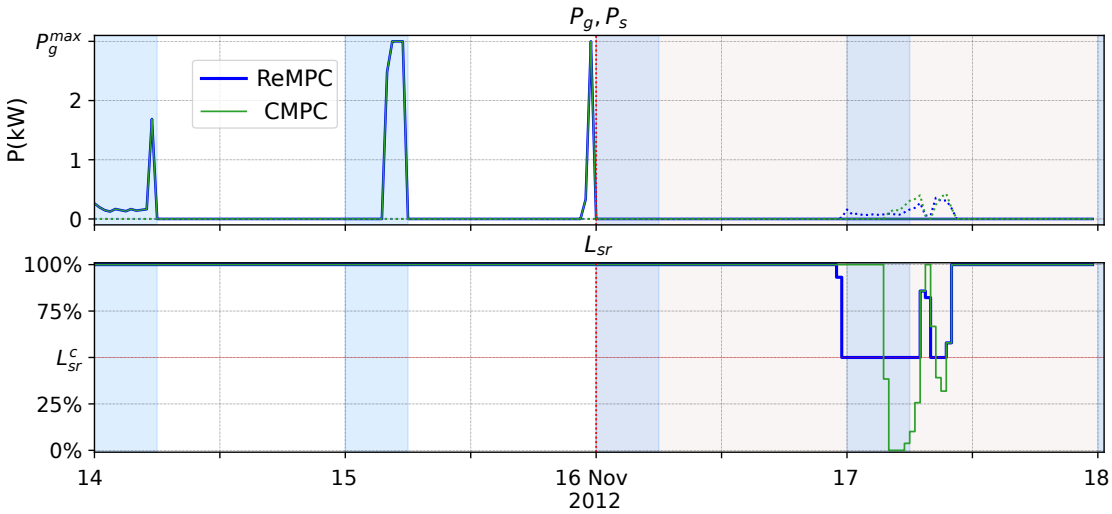

Figure A.9 – ReMPC (bleue) vs CMPC (verte), panne planifiée : Courbes d'évolution de P_g, P_s (1ère sous figure) et de L_{sr} (2nd sous figure) pour 4 jours de simulation

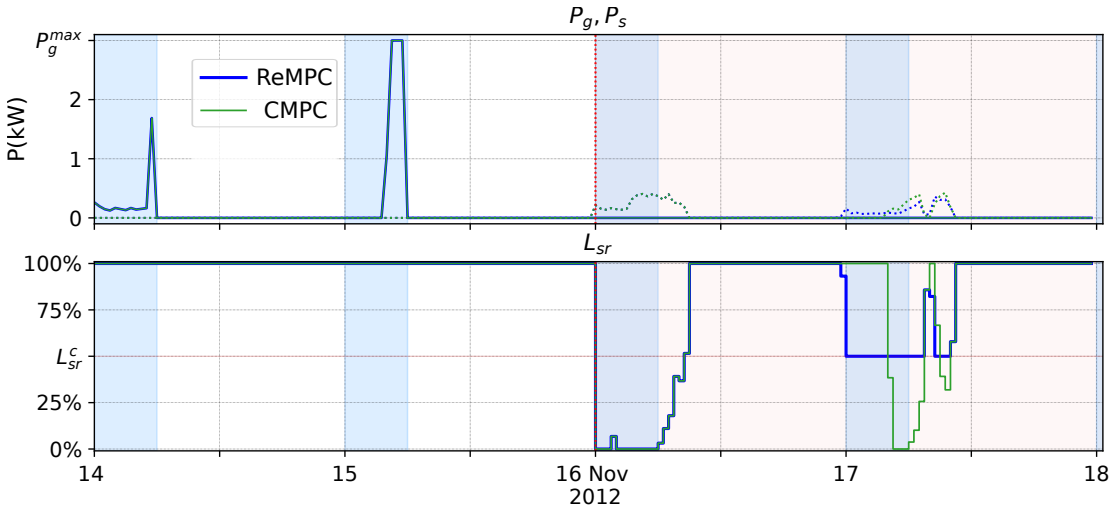

Figure A.10 – ReMPC (bleue) vs CMPC (verte), panne non planifiée : Courbes d'évolution de P_g, P_s (1ère sous figure) et de L_{sr} (2nd sous figure) pour 4 jours de simulation

Tableau A.3 – Performances du ReMPC et du RBCPS-R

		ReMPC						**RBCPS-R**					
Scénario	Réserve bat	$P_g \mid En_{cost}$	P_s	P_w	τ^-	τ^+	τ^*	$P_g \mid En_{cost}$	P_s	P_w	τ^-	τ^+	τ^*
Faible Prod	20%	83,6 | 9,04	24,6	0	10,9	47,4	41,7	73.6 | 12,8	37,7	4,9	10,9	89,1	
	30%	88,4 | 10,3	21,8	1,2	9,0	43,3	47,7	76,1 | 13,3	37,0	6,4	9,0	90,9	
Moy Prod	20%	31,7 | 3,35	14,9	15,8	3	24,1	72,9	24,8 | 4,1	37,7	28,4	2,1	97,9	0
	30%	35,5 | 4,00	13,3	17,9	1,4	22,4	76,2	29,5 |4,9	37,1	32,4	0	100	
Forte Prod	20%	11,1 | 1,18	0	49,9	0	0	100	11,2 | 1,5	35,9	85,4	0	100	
	30%	15,6 | 1,71		54,4				16,1 |2,3		90,4			

Résultats de simulations

Sur toutes les figures utilisées dans les explications, les périodes d'heures creuse sont marquées en bleue clair.

ReMPC vs CMPC : Les figures A.10 et A.9 illustrent dans le cas des deux types de pannes l'évolution de L_{sr}, P_g, et P_{nl}.

Nous constatons que les deux contrôleurs se comportent pareillement en période de fonctionnement nominale, ils puisent de l'énergie du réseau uniquement durant les heures creuses, hormis vers la fin de la journée du 15 Novembre 2012. Ce changement de comportement est dû à la prise en compte de l'information de panne planifiée qui permet d'éviter aux deux contrôleurs d'aller en dessous du ratio de satisfaction critique L_{sr}^c. En début de la journée du 17 Novembre, le ReMPC descend automatiquement son niveau de satisfaction à L_{sr}^c ; tandis que le CMPC continue de satisfaire toute la demande malgré la période de panne électrique. Plus tard dans la journée, ceci le conduit à descendre en dessous de L_{sr}^c pendant que le ReMPC y reste fixé. En général, pour toutes les simulations sur les trois périodes de production photovoltaïque le ReMPC satisfait pendant plus longtemps la demande critique ce qui lui permet de passer moins de temps à τ^-. En matière de coût de la facture, de l'énergie gaspillée et de l'énergie délestée les deux contrôleurs ont néanmoins les mêmes performances.

ReMPC vs RBCPS-R : Le RBCPS-R n'étant pas capable de considérer l'information de planification de panne, nous réalisons la comparaison dans le cas des pannes non planifiées. Nous ajoutons aussi au ReMPC la contrainte de réserve d'énergie dans le stockage en période de fonctionnement nominale. Le tableau A.3 illustre les résultats associés pour les 3 périodes de test utilisées.

En considérant l'énergie tirée du réseau, nous constatons que le ReMPC consomme plus que son adversaire mais en payant une facture moindre. Ceci est dû au fait qu'il tire la plus part de son énergie en période creuse, tandis que le RBCPS-R le fait indifféremment de la période. Lorsqu'on se focalise sur la fraction de temps passée à fournir moins de la charge critique τ^-, nous avons à la virgule près les mêmes performances. Mais en se référant à τ^+ et τ^-, force est de constater que le RBCPS-R passe le plus clair du temps à satisfaire exactement la puissance critique demandée, alors que le ReMPC en satisfait largement plus. Il en résulte que l'énergie gaspillée du ReMPC est moindre que celle du RBCPS-R. De tout ce qui précède nous pouvons tirer comme conclusion que le le ReMPC

est meilleur que le RBCPS-R.

A.5 Contrôleur énergétique stochastique : Panne probabiliste [21]

Dans la section précédente nous avons discuté des pannes déterministes, l'information de panne ou de non panne est complètement connue. Dans cette section nous nous focalisons sur des pannes stochastiques ; la contraintes modélisant l'état du réseau prends ses valeurs dans un ensemble discret dont la distribution est connue.

A.5.1 Énoncé du problème

Description du système

Considérons le problème du MPC générique (A.1) où nous rappelons que les contraintes sur la commande sont exprimées comme suit

$$u(k+h|k) \ \in \ \mathbb{U}. \tag{A.46}$$

Supposons que (A.46) peut se diviser en deux groupes de contraintes sur la commande,

- n_d contraintes déterministes :

$$D_d u(k+h|k) \leq d, \tag{A.47}$$

  avec $D_d \in \mathbb{R}^{n_d \times n_u}$, et $d \in \mathbb{R}^{n_d}$ un vecteur colonne.

- n_s contraintes stochastiques :

$$e_i^T u(k+h|k) \leq \boldsymbol{\xi}_i(k+h|k), \ \ \forall i \in \mathbb{N}_1^{n_s} \tag{A.48}$$

Supposition A.2. $\forall i \in \mathbb{N}_1^{n_s}$, la variable aléatoire $\boldsymbol{\xi_i}(k+h|k)$ appartient à un ensemble discret définit comme suit :

$$\Xi_i = \{\xi_{1,i}, \xi_{2,i}, ... \xi_{N_i,i}\}, \tag{A.49}$$

21. Résumé du chapitre 5

avec $N_i = \text{card}\{\Xi_i\}$ et ses éléments pouvant s'arranger comme suit

$$\xi_{1,i} < \xi_{2,i} < \ldots < \xi_{N_i,i}; \quad \forall i \in \mathbb{N}_1^{n_s}. \tag{A.50}$$

Supposition A.3. À l'instant indexé par $(k+h|k)$, pour tout $i \in \mathbb{N}_1^{n_s}$, pour toutes les réalisations de la variable aléatoire $\boldsymbol{\xi_i}(k+h|k)$ et pour tout $x(k+h|k) \in \mathbb{X}$, il existe un $u(k+h|k)$ qui satisfait (A.47) and (A.48) tel que $x(k+h+1|k) \in \mathbb{X}$.

Supposition A.4. À chaque instant $(k+h|k)$ les sources d'incertitudes sont totalement indépendantes l'une de l'autre.

A.5.2 Formulation du problème

Basé sur la sous section précédente, nous pouvons écrire le problème contrôleur prédictif stochastique suivant

Problème A.4 (**Contrôleur prédictif stochastique**).

$$J_s^*\Big(x(k)\Big) = \min_{u(k|k),\ldots,u(k+H-1|k)} \quad \sum_{h=0}^{H-1} l_h\Big(x(k+h|k), u(k+h|k)\Big) + V_f\Big(x(k+H|k)\Big) \tag{A.51a}$$

$$\begin{aligned}
&\text{s.t. } \forall h \in \mathbb{N}_0^{H-1} \\
&D_d u(k+h|k) \leq d && \text{(A.51b)}\\
&e_i^T u(k+h|k) \leq \boldsymbol{\xi}_i(k+h|k) \ , \forall i \in \mathbb{N}_1^{n_s} && \text{(A.51c)}\\
&x(k+h|k) \in \mathbb{X} && \text{(A.51d)}\\
&x(k+H|k) \in \mathbb{X}_f && \text{(A.51e)}\\
&x(k|k) = x(k) && \text{(A.51f)}\\
&x(k+h+1|k) = f\Big(k, x(k+h|k), u(k+h|k)\Big) && \text{(A.51g)}
\end{aligned}$$

Nous faisons les suppositions suivantes :

Supposition A.5. $l_h(\cdot)$ et $V_f(\cdot)$ sont des fonctions convexes

Supposition A.6. À l'instant initial de l'horizon de prédiction indexé par $(k|k)$, pour tout $i \in \mathbb{N}_1^{n_s}$, la réalisation de la variable aléatoire $\boldsymbol{\xi}_i(k|k)$ est connue et pour le reste de

l'horizon de prédiction, $\Big\{(h = 1, \ldots, H-1)|k\Big\}$, la probabilité marginale

$$\Pr\Big[\boldsymbol{\xi}_i(k+h) = \xi_{n_i,i} \,|\, \boldsymbol{\xi}_i(k|k)\Big] = \pi_{n_i,i}(k+h|k) \tag{A.52}$$

avec $n_i \in \mathbb{N}_1^{N_i}$, est aussi connue.

Notons que le **problème A.4** est mal défini car nous n'avons pas encore formellement donné une signification à l'inégalité stochastique (A.51c). Dans la littérature, basé sur des suppositions, l'optimisation robuste RO [22] [ALA09] et celle probabiliste [23] [Pré95] sont utilisées pour y trouver une définition formelle [24].

Chacune de ces méthodes à ses inconvénients dans notre cas d'application. Nous proposons donc dans la suite une stratégie pour pallier à l'inconvénient principal (explosion combinatoire) de l'optimisation stochastique multi stages (MSP [25]), une méthode dérivée de l'optimisation probabiliste.

A.5.3 Contrôleur prédictif à contraintes stochastiques discrètes (SDCMPC) [26]

Nous développons un contrôleur qui ne souffre pas de l'explosion combinatoire. Pour ce faire nous proposons de relaxer (A.51c) en utilisant des variables de relaxation qui contrairement à u, peuvent dépendre de $\boldsymbol{\xi}_i(k+h|k)$. En faisant ceci, les variables de relaxation deviennent des variables aléatoires. La contrainte relaxée s'écrit :

$$\begin{aligned} \forall h \in \mathbb{N}_1^{H-1};\quad \forall i \in \mathbb{N}_1^{n_s}\ ; e_i^T u(k+h|k) - \boldsymbol{y}_i(k+h|k) &\leq \boldsymbol{\xi}_i(k+h|k) \\ \boldsymbol{y}_i(k+h|k) &\geq 0. \end{aligned} \tag{A.53}$$

Chaque variable de relaxation $\boldsymbol{y}_i$ est aléatoire car sa valeur optimale est fonction de sa borne supérieure $\boldsymbol{\xi}_i$.

Nous pénalisons la violation de la contrainte ainsi définie dans la fonction coût du problème d'optimisation. Le nouveau coût à optimiser est donc la somme entre la fonction

22. RO : Robust Optimisation
23. Probabilistic programming
24. Le lecteur est prié de se référer à la version anglaise pour un état de l'art de ces méthodes
25. MSP : Multistage Stochastic Programming
26. SDCMPC : Stochastic Discrete Constraint Model Predictive Controller

coût du problème (A.4) et d'un nouveau terme relatif à la pénalisation tel que

$$J_{SDCMPC}\Big(x(k), y\Big) = J_s\Big(x(k)\Big) + J_y(k), \tag{A.54}$$

avec

$$J_y(k) = E\left[\sum_{h=1}^{H-1}\sum_{i=1}^{n_s} c_i \boldsymbol{y}_i(k+h)\right], \tag{A.55}$$

l'espérance du coût de pénalisation de toutes les variables aléatoires $\boldsymbol{y}_i(k+h)$ sur l'horizon de prédiction excepté le premier instant (A.6) et c_i la valeur de la pénalisation associée à l'utilisation de $\boldsymbol{y}_i$.

Problème déterministe équivalent

Nous formulons le problème déterministe équivalent en introduisant les variables

$$y_{1,i}(k+h|k),\ \ldots\ , y_{N_i-1,i}(k+h|k) \tag{A.56}$$

toutes positives et qui sont les différentes valeurs prises par $\boldsymbol{y}_i(k+h|k)$ pour tous les éléments exceptés le dernier sur l'espace probabiliste de $\boldsymbol{\xi_i}$ à l'instant $(k+h|k)$. La contrainte stochastique devient donc une liste de contraintes déterministe

$$\forall i \in \mathbb{N}_1^{n_s};\ \forall h \in \mathbb{N}_1^{H-1} \quad \begin{cases} e_i^T u(k+h|k) - y_{1,i}(k+h|k) \leq \xi_{1,i}; \\ \vdots \\ e_i^T u(k+h|k) - y_{N_i-1,i}(k+h|k) \leq \xi_{N_i-1,i}; \\ e_i^T u(k+h|k) \leq \xi_{N_i,i}. \end{cases} \tag{A.57}$$

Il est à noter que la dernière contrainte n'est pas relaxée car dans notre application il est plus judicieux de l'interdire. Nous avons donc

$$y_{N_i,i}(k+h|k) = 0 \tag{A.58}$$

afin que la N_i ^{ème} contrainte soit dure. Avec ces développements nous pouvons réécrire,

$$\begin{aligned} J_{\boldsymbol{y}}(k) &= \sum_{h=1}^{H-1}\sum_{i=1}^{n_s} c_i \mathrm{E}\Big[\boldsymbol{y}_i(k+h|k)\Big] \\ &= \sum_{h=1}^{H-1}\sum_{i=1}^{n_s}\sum_{n_i=1}^{N_i-1} c_i \pi_{n_i,i}(k+h|k) y_{n_i,i}(k+h|k). \end{aligned} \tag{A.59}$$

Nous définissons donc le problème final comme

Problème A.5 (**Contrôleur prédictif à contraintes stochastiques discrètes**)**.**

$$J^*_{SDCMPC}\Big(x(k), y\Big) = \min_{\substack{u(k|k),\,\dots\,,u(k+H-1|k)\\ y(k+1|k),\,\dots\,,y(k+H-1|k)}} \quad \Bigg\{ J_{\boldsymbol{y}}(k) + V_f\Big(x(k+H|k)\Big) + \sum_{h=0}^{H-1} l_h\Big(x(k+h|k), u(k+h|k)\Big) \Bigg\} \tag{A.60a}$$

s.t. :

$\forall h \in \mathbb{N}_0^{H-1}$

$$x(k+h+1|k) = f\Big(k, x(k+h|k), u(k+h|k)\Big) \tag{A.60b}$$

$$D_d u(k+h|k) \leq d \tag{A.60c}$$

$$x(k+h|k) \in \mathbb{X} \tag{A.60d}$$

$$x(k+H|k) \in \mathbb{X}_f \tag{A.60e}$$

$$x(k|k) = x(k) \tag{A.60f}$$

$\forall h \in \mathbb{N}_1^{H-1}, \;\; \forall i \in \mathbb{N}_1^{n_s}$

$$e_i^T u(k+h|k) \leq \xi_{N_i,i} \tag{A.60g}$$

$$\forall n_i \in \mathbb{N}_1^{N_i-1}, \; \xi_{n_i,i} \geq e_i^T u(k+h|k) - y_{n_i,i}(k+h|k) \tag{A.60h}$$

$$\forall n_i \in \mathbb{N}_1^{N_i-1}, \; y_{n_i,i} \leq 0 \tag{A.60i}$$

Remarque : Considérons le problème (A.4). Le nombres de variables utilisées pour résoudre celui ci en utilisant l'optimisation stochastique multi-stage est donnée par

$$(n_x + n_u)\Big[1 + \sum_{h=1}^{H-1} \Big(\prod_{i=1}^{n_s} N_i\Big)^h\Big] \tag{A.61}$$

tandis que avec le SDCMPC notre méthode, nous avons

$$n_x + n_u + (H-1)\Big(n_x + n_u + \sum_{i=1}^{n_s}(N_i - n_s)\Big) \tag{A.62}$$

Nous remarquons une réduction immense du nombre de variables d'une croissance exponentielle à une croissance linéaire en fonction de l'horizon de prédiction.

L'autre avantage de notre méthodologie est qu'elle est applicable pour tous types de variables aléatoire dès que la probabilité marginale d'apparition de ce dernier $\pi_{n_i,i}(\cdot|k)$

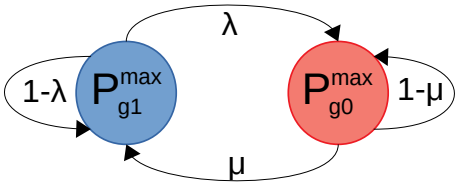

Figure A.11 – Chaîne de Markov modélisant l'état du réseau électrique

peut être calculée.

A.5.4 Modélisation de l'état du réseau électrique

Supposons que la puissance maximum du réseau électrique à chaque instant est P_{g1}^{max} ou P_{g0}^{max} respectivement lorsque le réseau est disponible ou pas. la puissance soutirée du réseau à chaque instant k est donc la variable aléatoire que nous nommons $\boldsymbol{P_g^{max}}(k)$.

Nous modélisons l'évolution du processus associé par la chaîne de Markov MC [BA92] à deux états illustrée par la figure A.11. λ $(0 \leq \lambda \leq 1)$ et μ $(0 \leq u \leq 1)$ sont les *taux de défaut* et *taux de réparation* du réseau électrique. La matrice de transition de pas unitaire représentant la chaîne de Markov se définit par

$$T = \begin{bmatrix} 1-\lambda & \lambda \\ \mu & 1-\mu \end{bmatrix}. \tag{A.63}$$

Notons par $\Pi^{k+h|k}$ le vecteur de transition probabiliste à h-pas du processus à partir de l'instant k

$$\Pi^{k+h|k} = \begin{bmatrix} \pi_1(k+h|k) & \pi_0(k+h|k) \end{bmatrix}. \tag{A.64}$$

Il se calcul avec les équation de *Chapman–Kolmogorov* tel que :

$$\Pi^{k+h|k} = \Pi^k T^h \quad \forall h \geq 1, \quad \text{avec } \Pi^{k|k} = \Pi^k \tag{A.65}$$

Puisque l'état du réseau est connu à l'instant initial (supposition A.6), le vecteur de transition probabiliste initial Π^k prend la valeur [1 0] lorsque le réseau est disponible et [0 1] dans le cas contraire.

A.5.5 Cas d'application

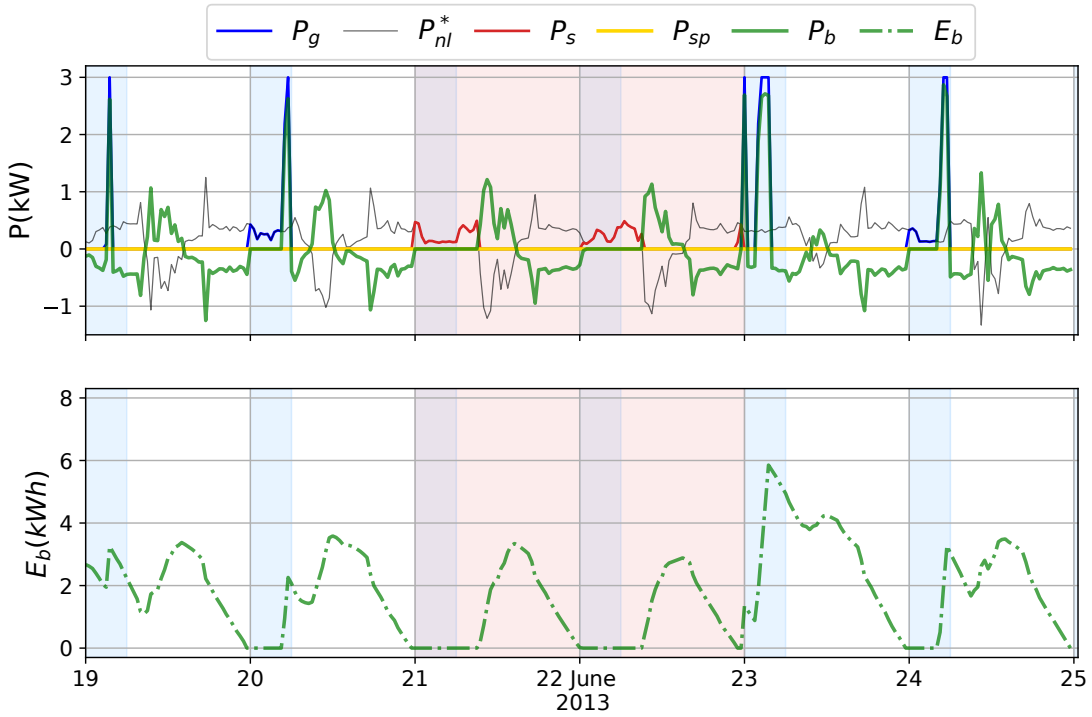

Figure A.12 – SDCMPC : taux de défaillance faible $\lambda = 10^{-15}$

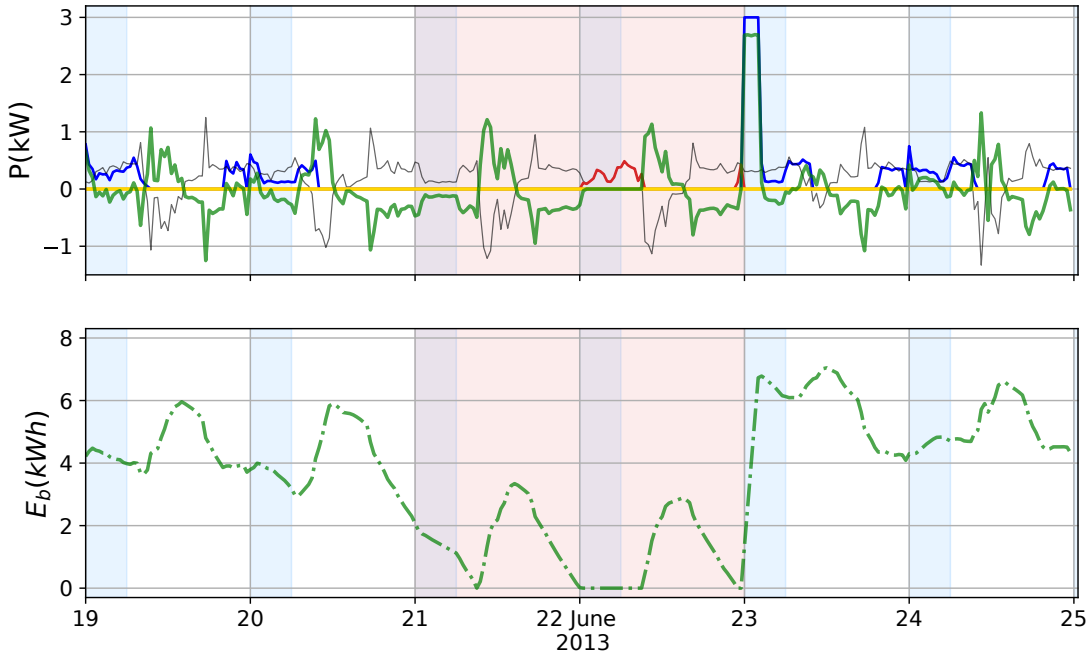

Figure A.13 – SDCMPC : taux de défaillance élevé $\lambda = 0.99$

Nous considérons le bâtiment décrit en section A.3. Pour le problème qui en découle, nous avons une seule inégalité stochastique, donc $n_s = 1$. Ceci implique $i = 1$ et $c_i = c$. Puisque la seule variable aléatoire ne peut prendre que deux valeurs, il en suit que $N_i = N_1 = 2$.

Taux de défaillances extrêmes

Nous nous intéressons en premier aux taux de défaillance extrêmes ($\lambda = 10^{-15}$, $\lambda = 0.99$) en gardant constant le taux de réparation $\mu = 10^{-2}$. Nous réalisons deux types de simulations par taux de défaillance : l'une avec panne et la seconde sans pour la période de faible production photovoilataïque. Le tableau A.4 résume les performances du contrôleur tandis que les figures A.12, A.13 illustrent l'évolution des variables de contrôle durant la période allant du 19 au 25 Juin 2013.

En se référant à cette figure nous constatons que pour un faible taux de panne le contrôleur consomme sur le réseau électrique uniquement durant la nuit, tandis que la consommation se fait à n'importe quel moment avec un taux de défaillance élevé. De surcroît, dans le premier cas, au moment de la panne, la batterie est vide et induit donc un délestage durant les premières heures du 21 Juin. Dans le second cas ce délestage ne se produit pas car la batterie n'est pas vide au moment de la panne. Sur toute la simulation, Le tableau A.4 montre que la même quantité d'énergie est tirée du réseau tant qu'il n'y a pas de pannes, mais avec des factures différentes. Lorsqu'il y a des pannes par contre, l'énergie délestée avec un taux de défaillance élevé est plus faible par rapport à celui dans le cas du taux de défaillance faible. Ceci puisque la consommation sur le réseau est plus importante dans le premier cas.

Tableau A.4 – Performances du SDCMPC pour les taux de défaillances faible et élevé

	Sans pannes			**Avec pannes**		
λ	$P_g \mid En_{cost}$	P_s	P_w	$P_g \mid En_{cost}$	P_s	P_w
Low	106.6 | 10.66	0	0	79.1 | 07.91	27.6	0
High	106.6 | 17.67			91.1 | 13.56	15.6	

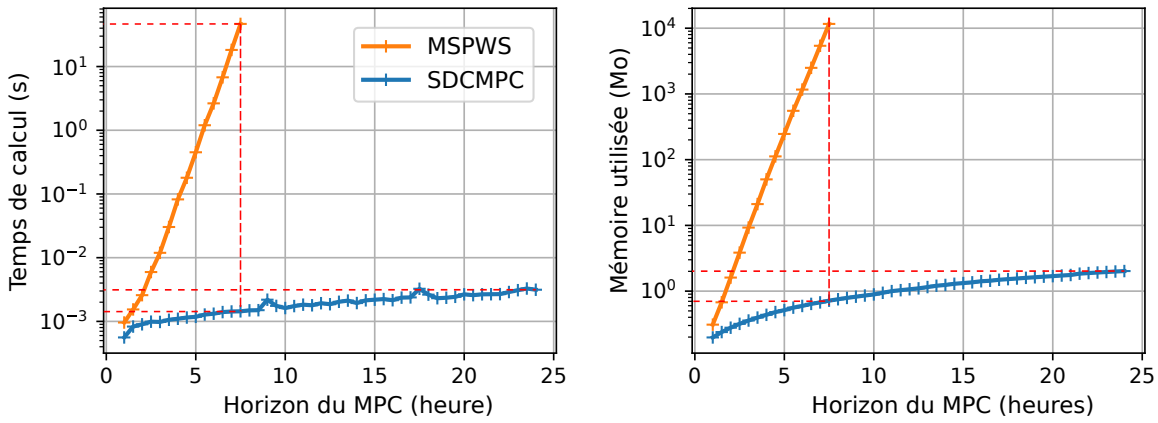

Figure A.14 – Évolution de l'utilisation de la mémoire RAM et du temps de calcul en fonction de l'horizon de prédiction

SDCMPC vs. MSPWS [27]

Comparaison des coûts de calcul Nous comparons l'utilisation de la mémoire RAM et du temps de calcul lors des simulations utilisant le SDCMPC et MSPWS. Pour ce faire, nous réalisons une simulation en fonction de l'horizon de prédiction avec chaque contrôleur. La simulation est menée en boucle ouverte car nous pouvons extrapoler les résultats obtenus en boucle fermée. Les résultat de la simulation sont montrés par la figure A.12.

Il est à noter que nous n'avons pas pu effectuer des simulations pour un horizon de prédiction plus grand que 7h30 min dans le cas du MSPWS car l'ordinateur était à court de mémoire RAM. La figure souligne les résultats des équations (A.61, A.62). Nous pouvons facilement conclure que le SDCMPC à de meilleures performances en temps de calcul et en utilisation de mémoire comparé au MSPWS

Simulation de Monté carlo En utilisant un taux de défaillance et de réparation constant, $\mu = \lambda = 10^{-2}$ pour la chaîne de markov décrivant les états du réseau, et $c_1 = 10^2$ nous avons créés 40 scénarios de disponibilité du réseau, chacun sur une période de 10 jours. La date de départ de chaque scénario est choisi aléatoirement entre les 80 jours décrit comme suit :

- jour 1 à 30 : 1 - 30 Juin 2013 ;
- jour 31 à 60 : 1 - 30 Novembre 2012 ;

27. Le lecteur est prié de se référer à la version anglaise pour une description de ce contrôleur

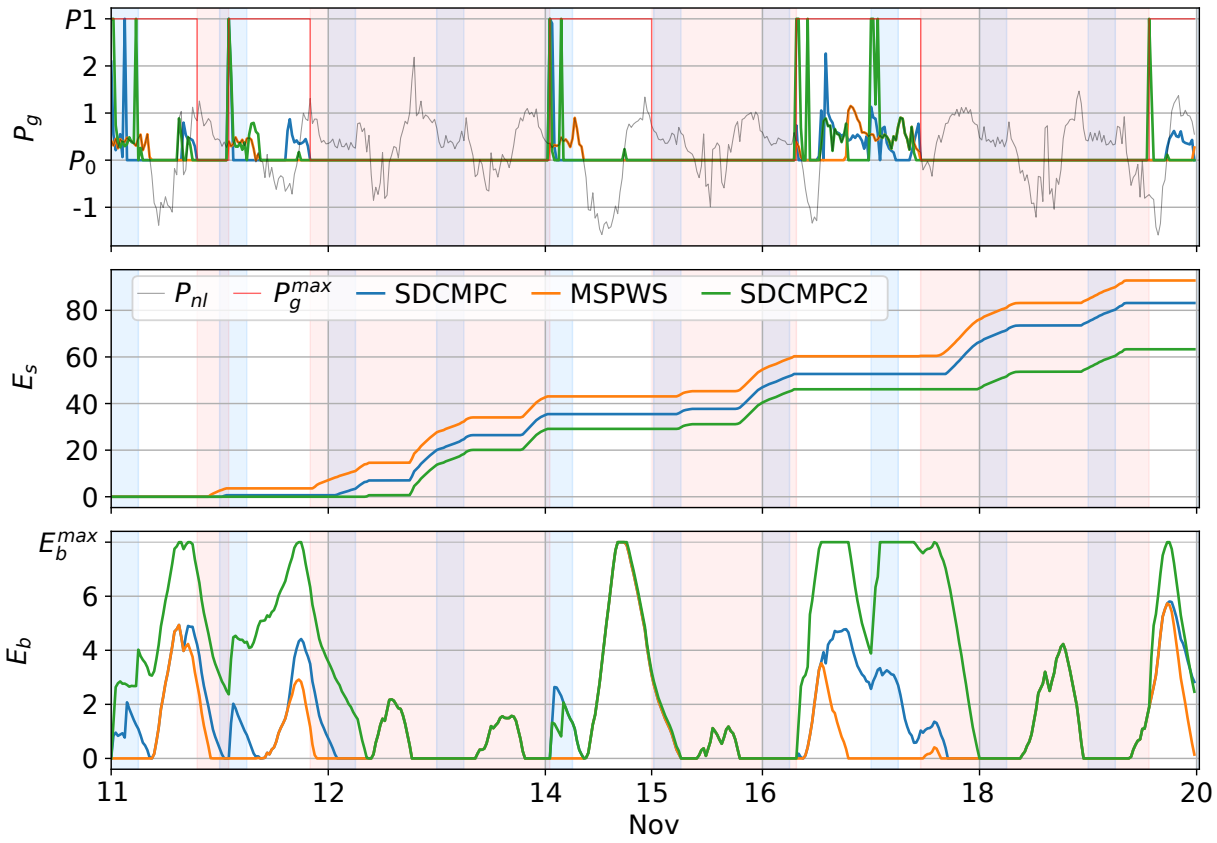

Figure A.15 – Exemple d'un scénario de simulation de Monté Carlo

- our 61 à 80 : 1 - 20 Septembre 2012.

Nous simulons le SDCMPC et le MSPWS avec un horizon de 7h30mn et le SDCMPC avec un horizon étendu de 24h (SDCMPC2). Nous considérons les indices de performances suivants,

- la facture d'électricité défini par A.43 ;
- l'énergie cumulée délestée E_s[kWh] ;

$$E_s = \sum_{k=1}^{N} P_s(k)\Delta_t; \tag{A.66}$$

- le coût d'optimisation reconstruit ;

$$J_{re} = \sum_{k=1}^{N} \begin{bmatrix} c_g(k) & c_w(k) & 0 & c_s(k) \end{bmatrix} u(k) \tag{A.67}$$

Tableau A.5 – Performances des contrôleurs pour 100 simulations de monté carlo

	J_{re}		En_{cost}		E_s	
	Mean	Std	Mean	Std	Mean	Std
MSPWS - SDCMPC	36.75	22.54	-1.03	0.47	3.78	2.29
SDCMPC - SDCMPC2	58.15	40.24	0.74	1.22	5.74	4.11
MSPWS - SDCMPC2	94.9	48.88	-0.29	1.21	9.52	4.98

La figure A.15 illustre l'évolution des variables qui nous intéressent sur l'un des scénarios. En particulier La seconde sous figure indique l'évolution de l'énergie délestée cumulée pour chacun des contrôleurs. Nous comparons les différences de moyennes des indices de performances des contrôleurs deux a deux. Le tableau A.5, montre la moyenne et l'écart type de ces différences sur tous les scénarios. Nous pouvons en conclure que, le SDCMPC2 est meilleur en moyenne comparé aux autres. Ceci est dû à son plus grand horizon de prédiction qui lui permet d'avoir une meilleure anticipation du futur et de consommer une grande partie de ses besoins énergétiques sur le réseau en période d'heures creuses.

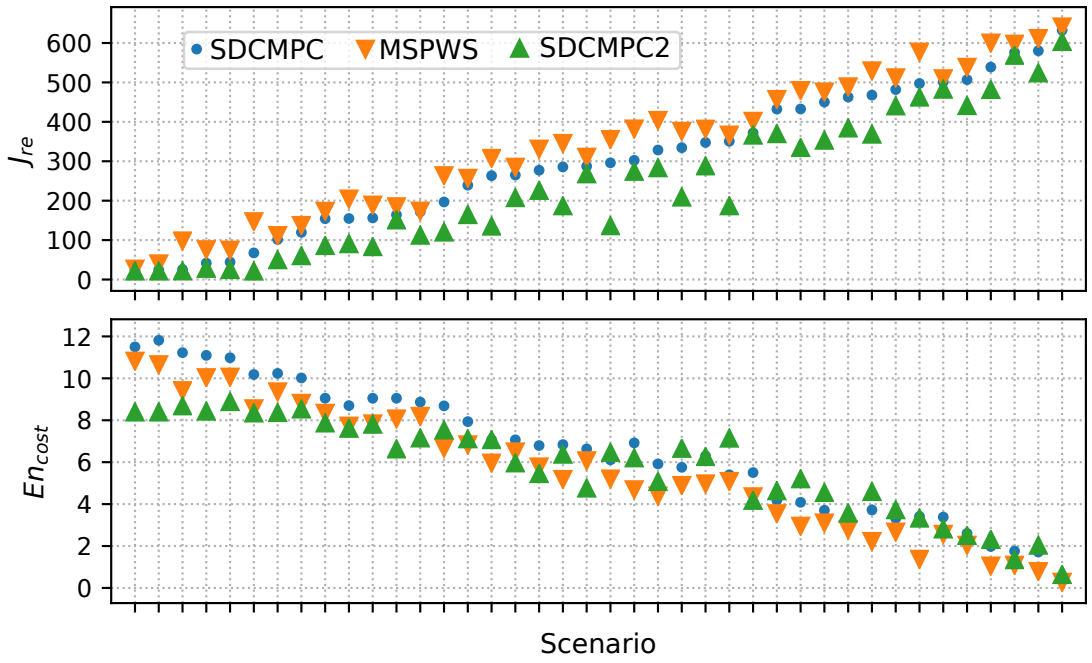

Figure A.16 – Performances des contrôleurs en fonction du scénario de Monté carlo

La figure A.16 montre les valeurs du coût reconstruit (similaire à l'énergie délestée cumulée) et de la facture d'électricité pour chaque scénario et contrôleur. Nous y voyons que le SDCMPC2 produit le plus faible coût d'optimisation J_{re} pour tous les scénarios, suivi du MSPWS, et du SDCMPC. Concernant la facture d'électricité, à même horizon de prédiction le MSPWS a un coût moindre devant le SDCMPC. Quant au coût du SDCMPC2 il est plus bas dans 42.5% et plus grand dans 30% des cas comparé aux deux autres. Nous pouvons donc en conclure qu'il est meilleure que le SDCMPC

A.6 Conclusion

Cette thèse a été dédié au développement et à l'évaluation de stratégies de commandes d'un système énergétique intégrant l'apparition d'évènements rares dans un but d'adaptation lors de la présences de ceux-ci. Nous avons focalisé notre attention sur les bâtiments intelligents connectés au réseau électrique, disposant de sources d'énergie renouvelables et avons considéré les pannes de réseau comme évènement extrêmes.

Il a été élaboré un contrôleur prédictif résilient déterministe. Ceci parce qu'il prend en compte une information complète sur l'apparition de la panne électrique : soit la date d'arrivée est connue parfaitement ou pas du tout. Il a été montré que le contrôleur peut s'adapter aux besoins de l'utilisateur en modifiant automatiquement l'énergie fourni au bâtiment lors des périodes de pannes électrique. Les comparaison avec d'autres contrôleurs on témoignés de la bonne performance du nouveau contrôleur.

La prise en compte de modèles de pannes probabilistes et plus réalistes a démontré que les méthodes de résolutions actuelles ont toutes des limites dans notre cas d'application. Spécifiquement le multistage stochastic programming qui souffre d'une explosion combinatoire en fonction de la taille de l'horizon et du nombre d'éléments dans l'espace probabiliste des variables aléatoires. Ceci nous à conduit à l'élaboration d'une méthodologie permettant de réduire d'une croissance exponentielle à une croissance linéaire le nombre de variables à considérer pour résoudre le problème. La comparaison sur un cas d'application avec des simulations de monté carlo à prouvé l'efficacité de la nouvelle stratégie.

Appendix B

Coding

Laptop characteristics

Os	Ubuntu 18.04.5 LTS, 64bits
Memory	15.5Gib
Processor	Intel® Core™i7-8750H CPU @ 2.20GHz × 12
Graphics	Intel® UHD Graphics 630 (CFL GT2)

Programming language

For all the simulation carried out in this thesis we have used mostly used the languages Matlab and Julia.

Optimisation solver	GLPK
Performances comparison package	BenchmarkTools [Rev15]

GitHub repository

All the code associated to the writing of this thesis is available freely at PhD-Simulations [A21]

BIBLIOGRAPHY

[A21] Jesse James PRINCE A., *Phd-Simulations*, [Online; accessed 17-Mars-2021], 2021, URL: https://github.com/pajjaecat/PhD-Simulations.

[Abe+20] Ahad Abessi et al., « Sustainable and Resilient Smart House Using the Internal Combustion Engine of Plug-in Hybrid Electric Vehicles », *in*: *Sustainability* 12.*15* (July 2020), p. 6046.

[ABG17] Amanda Abreu, Romain Bourdais, and Hervé Guéguen, « Inter-Layer Interactions in Hierarchical MPC for Building Energy Management Systems », *in*: *IFAC-PapersOnLine* 50.*1* (July 2017), pp. 12027–12032.

[ABG18] Amanda Abreu, Romain Bourdais, and Hervé Guéguen, « Hierarchical Model Predictive Control for Building Energy Management of Hybrid Systems », *in*: *Conference on Analysis and Design of Hybrid Systems ADHS*, vol. 51, 16, Oxford, United Kingdom, July 2018, pp. 235–240, DOI: 10.1016/j.ifacol.2018.08.040, URL: https://hal.archives-ouvertes.fr/hal-01875397.

[Ada+18] Lukas Adam et al., « Solving joint chance constrained problems using regularization and Benders' decomposition », *in*: (July 2018).

[Adm17] U.S. Energy Information Administration, *Hurricane Irma cut power to nearly two-thirds of Florida's electricity customers*, [Online; accessed 10-January-2021], 2017, URL: https://www.eia.gov/todayinenergy/detail.php?id=32992.

[Age20] International Energy Agency, *Explore Historical data and forecasts for all renewables sectors and technologies*, [Online; accessed 27-January-2021], 2020, URL: https://www.iea.org/articles/renewables-2020-data-explorer?mode=market&region=World&product=PV+by+segment.

[Ahm+16] Maytham S. Ahmed et al., « Artificial neural network based controller for home energy management considering demand response events », *in*: *2016 International Conference on Advances in Electrical, Electronic and Systems Engineering (ICAEES)*, IEEE, Nov. 2016.

[AJ14] Abdul Afram and Farrokh Janabi-Sharifi, « Theory and applications of HVAC control systems – A review of model predictive control (MPC) », *in*: *Building and Environment* 72 (2014), pp. 343–355, ISSN: 0360-1323, URL: http://www.sciencedirect.com/science/article/pii/S0360132313003363.

[ALA09] Ben-tal A., El Ghaoui L., and Nemirovski A., *Robust Optimization*, ed. by Princeton University press, Princeton Series in APPLIED MATHEMATICS, 2009.

[BA92] Roy Billinton and Ronald N. Allan, *Reliability Evaluation of Engineering Systems*, ed. by Springer Science+Business Media New York, Springer US, 1992.

[Baz61] Igor Bazovsky, *Reliability Theory and Practice*, ed. by Prentice Hall, 1961.

[BBC11] Dimitris Bertsimas, David B. Brown, and Constantine Caramanis, « Theory and Applications of Robust Optimization », *in*: *SIAM Review* 53.*3* (Jan. 2011), pp. 464–501, DOI: 10.1137/080734510.

[BG10] Dimitris Bertsimas and Vineet Goyal, « On the Power of Robust Solutions in Two-Stage Stochastic and Adaptive Optimization Problems », *in*: *Mathematics of Operations Research* 35.*2* (May 2010), pp. 284–305, DOI: 10.1287/moor.1090.0440.

[BHJ15] Faeze Brahman, Masoud Honarmand, and Shahram Jadid, « Optimal electrical and thermal energy management of a residential energy hub, integrating demand response and energy storage system », *in*: *Energy and Buildings* 90 (Mar. 2015), pp. 65–75.

[BI12] Ioan Viorel Banu and Marcel Istrate, « Modeling of maximum power point tracking algorithm for photovoltaic systems », *in*: *2012 International Conference and Exposition on Electrical and Power Engineering*, IEEE, Oct. 2012.

[BI17] Ioan Viorel Banu and Marcel Istrate, *Modeling of Maximum Power Point Tracking Algorithm for Photovoltaic Systems*, 2017.

[Bir04] Alessandro Birolini, *Reliability Engineering*, Springer Berlin Heidelberg, 2004, DOI: 10.1007/978-3-662-05409-3.

[BM99] Alberto Bemporad and Manfred Morari, « Robust model predictive control: A survey », *in*: *Robustness in identification and control*, ed. by A. Garulli and A. Tesi, London: Springer London, 1999, pp. 207–226, ISBN: 978-1-84628-538-7.

[Bou+19] Mathieu Bourdeau et al., « Modeling and forecasting building energy consumption: A review of data-driven techniques », *in*: *Sustainable Cities and Society* 48 (July 2019), p. 101533.

[BPH65] Richard E. Barlow, Frank Proschan, and Larry C. Hunter, *Mathematical theory of reliability*, John Wiley & Sons Inc, 1965.

[Bra90] J E Braun, « Reducing energy costs and peak electrical demand through optimal control of building thermal storage », *in*: *ASHRAE Transactions (American Society of Heating, Refrigerating and Air-Conditioning Engineers); (United States)* 96:2 (Jan. 1990), ISSN: 0001-2505, URL: https://www.osti.gov/biblio/5163170.

[BYH15] L. Bram, Ihsan Yamkoglu, and Dick den Hertog, « A Practical Guide to Robust Optimization », *in*: *Omega* 53 (2015), pp. 124–137, ISSN: 0305-0483.

[CA07] Eduardo F. Camacho and Carlos Bordons Alba, eds., *Model Predictive Control*, 2nd, Springer-Verlag London, 2007.

[Car17] Kris Carlon, *Tesla Powerwall: Everything you need to know*, https://dgit.com/tesla-powerwall-specs-price-battery-51137/, Accessed: 2020-10-02, 2017.

[CC59] A. Charnes and W. W. Cooper, « Chance-Constrained Programming », *in*: *Management Science* 6.*1* (1959), pp. 73–79, DOI: 10.1287/mnsc.6.1.73.

[CC62] A. Charnes and W. W. Cooper, « Chance Constraints and Normal Deviates », *in*: *Journal of the American Statistical Association* 57.*297* (1962), pp. 134–148, ISSN: 01621459.

[CC63] A. Charnes and W. W. Cooper, « Deterministic Equivalents for Optimizing and Satisficing under Chance Constraints », *in*: *Operations Research* 11.*1* (1963), pp. 18–39, ISSN: 0030364X, 15265463, URL: http://www.jstor.org/stable/168141.

[CCS58] A. Charnes, W. W. Cooper, and G. H. Symonds, « Cost Horizons and Certainty Equivalents: An Approach to Stochastic Programming of Heating Oil », *in*: *Management Science* 4.*3* (1958), pp. 235–263, ISSN: 00251909, 15265501, URL: http://www.jstor.org/stable/2627328.

[Chr+07] Panagiotis D. Christofides et al., « Smart plant operations: Vision, progress and challenges », *in*: *AIChE Journal* 53.*11* (2007), pp. 2734–2741.

[Com] Ausgrid Company, *Data to share: Solar home electricity data*, Accessed: 2020-06-28, URL: https://www.ausgrid.com.au/Industry/Our-Research/Data-to-share/Solar-home-electricity-data.

[CPS18] Marco Cococcioni, Massimo Pappalardo, and Yaroslav D. Sergeyev, « MCoMPa2018 Lexicographic multi-objective linear programming using grossone methodology: Theory and algorithm », *in*: *Applied Mathematics and Computation* 318 (Feb. 2018), pp. 298–311.

[CRA18] Karim Chabirand, Taouba Rhouma, and Mohamed Naceur Abdelkrim, « A Framework for Attack Resilient Industrial Control Systems: Attack Detection and Controller Reconfiguration », *in*: *Proceedings of the IEEE* 106 (1 2018), pp. 113–128.

[CRC14] Robert Corson, Ronald Regan, and Scott Carlson, *Implementing energy storage for peak-load shifting*, https://www.csemag.com/articles/implementing-energy-storage-for-peak-load-shifting/, Accessed: 2020-09-08, 2014.

[Dav+12] Jim Davis et al., « Smart manufacturing, manufacturing intelligence and demand-dynamic performance », *in*: *Computers & Chemical Engineering* 47 (2012), FOCAPO 2012, pp. 145–156, ISSN: 0098-1354, URL: http://www.sciencedirect.com/science/article/pii/S0098135412002219.

[Dav52] D. J. Davis, « An Analysis of Some Failure Data », *in*: *Journal of the American Statistical Association* 47.*258* (1952), pp. 113–150, ISSN: 01621459, URL: http://www.jstor.org/stable/2280740.

[Deb14] Kalyanmoy Deb, « Multi-objective Optimization », *in*: *Search Methodologies: Introductory Tutorials in Optimization and Decision Support Techniques*, Boston, MA: Springer US, 2014, pp. 403–449.

[Dre64] Stuart E. Dreyfus, « Some Types of Optimal Control of Stochastic Systems », *in*: *Journal of the Society for Industrial and Applied Mathematics Series A Control* vol.2.*No. 1* (1964), pp. 120–134.

[EDC14] Matthew Ellis, Helen Durand, and Panagiotis D. Christofides, « A tutorial review of economic model predictive control methods », *in*: *Journal of Process Control* 24.*8* (Aug. 2014), pp. 1156–1178.

[Eng07] Sebastian Engell, « Feedback control for optimal process operation », *in*: *Journal of Process Control* 17.*3* (Mar. 2007), pp. 203–219.

[Eps58] Benjamin Epstein, *The exponential distribution and its role in life testing*, tech. rep., Departement of Mathematics, Wayne state University,Detroit Michigan, 1958.

[ES53] Benjamin Epstein and Milton Sobel, « Life Testing », *in*: *Journal of the American Statistical Association* 48.*263* (Sept. 1953), pp. 486–502, DOI: 10.1080/01621459.1953.10483488.

[FPZ15] Yiping Fang, Nicola Pedroni, and Enrico Zio., « Optimization of Cascade-Resilient Electrical Infrastructures and its Validation by Power Flow Modeling », *in*: *Risk Analysis* 35 (4 2015), pp. 594–607.

[Gan+19] Hari S. Ganesh et al., « A model-based dynamic optimization strategy for control of indoor air pollutants », *in*: *Energy and Buildings* 195 (July 2019), pp. 168–179.

[Gan+20] Hari S. Ganesh et al., « Indoor air quality and energy management in buildings using combined moving horizon estimation and model predictive control », *in*: *Journal of Building Engineering* (July 2020), p. 101552.

[GG10] D. Gyalistras and M Gwerder, *Use of Weather and Occupancy Forecasts ForOptimal Building Climate Control (OptiControl):Two Years Progress Report*, tech. rep., 2010.

[GGN04] A. Ben-Tal A. Goryashko, E. Guslitzer, and A. Nemirovski, « Adjustable robust solutions of uncertain linear programs », *in*: *Springer* (2004), pp. 351–376.

[Gha+15] Hamed Ghasemieh et al., « Energy Resilience Modeling for Smart Houses », *in*: *Proceedings of the 45th Annual IEEE/IFIP International Conference on Dependable Systems and Networks, DSN 2015* 45 (2015), pp. 275–286.

[GKW18] Angelos Georghiou, Daniel Kuhn, and Wolfram Wiesemann, « The decision rule approach to optimization under uncertainty: methodology and applications », *in*: *Computational Management Science* 16.*4* (Nov. 2018), pp. 545–576, DOI: 10.1007/s10287-018-0338-5.

[GOL98] Laurent El Ghaoui, Francois Oustry, and Hervé Lebret, « Robust Solutions to Uncertain Semidefinite Programs », *in*: *SIAM Journal on Optimization* 9.*1* (Jan. 1998), pp. 33–52, DOI: 10.1137/s1052623496305717.

[GRB20] Ninad Kiran Gaikwad, Naren Srivaths Raman, and Prabir Barooah, « Smart Home Energy Management System for Power System Resiliency », *in*: *2020 IEEE Conference on Control Technology and Applications (CCTA)*, Aug. 2020, pp. 1072–1079.

[GX19] Xinbo Geng and Le Xie, « Data-driven Decision Making with Probabilistic Guarantees (Part 1): A Schematic Overview of Chance-constrained Optimization », *in*: (Mar. 2019), Review on chance constrained programing methodes.

[Hae+18] Pierre Haessig et al., « Gestion d'énergie avec entrées incertaines : quel algorithme choisir ? Benchmark open source sur une maison solaire », *in*: *Symposium de Génie Électrique (SGE 2018), Nancy , France*, 2018.

[Hen02] R. Henrion, « On the Connectedness of Probabilistic Constraint Sets », *in*: *Journal of Optimization Theory and Applications* 112.*3* (Mar. 2002), pp. 657–663.

[Hen07] R. Henrion, « Structural properties of linear probabilistic constraints† », *in*: *Optimization* 56 (Aug. 2007), pp. 425–440, DOI: 10.1080/02331930701421046.

[I63] Propoi A. I., « Use of linear programming methods forsynthesizing sampled-data automatic systems », *in*: *Automatic RemoteControl* 24.*7* (1963), pp. 837–844.

[inf15] Photovoltaique info, *Photovoltaique info: Couts d'investissement*, http://www.photovoltaique.info/Couts-d-investissement.html, Accessed: 2018-10-02, 2015.

[Ise82] H. Isermann, « Linear lexicographic optimization », *in*: *Operations-Research-Spektrum* 4.*4* (Dec. 1982), pp. 223–228, ISSN: 1436-6304.

[Jon+16a] M. R. Jongerden et al., « Assessing the cost of energy independence », *in*: *2016 IEEE International Energy Conference (ENERGYCON)*, Apr. 2016, pp. 1–6.

[Jon+16b] Marijn R. Jongerden et al., « Does Your Domestic Photovoltaic Energy System Survive Grid Outages? », *in*: *Energies* 9.*9* (2016), ISSN: 1996-1073, URL: http://www.mdpi.com/1996-1073/9/9/736.

[Jul+20] Cattiaux Julien et al., *Weather Extremes and Climate Change, Encyclopedia of the Environment*, https://www.encyclopedie-environnement.org/en/climate/extreme-weather-events-and-climate-change/, Accessed: 2020-08-02, 2020.

[KC13] Marina Krotofil and Alvaro A. Cardenas, « Resilience of Process Control Systems to Cyber-Physical Attack », *in*: *Secure IT Systems. NordSec 2013. Lecture Notes in Computer Science*, Springer, Berlin, Heidelberg, 2013, pp. 166–182, DOI: https://doi.org/10.1007/978-3-642-41488-6_12.

[KC16] Basil Kouvaritakis and Mark Cannon, *Model Predictive Control,classical, robust and stochastic*, Springer International Publishing, 2016, DOI: 10.1007/978-3-319-24853-0.

[Kha+17] Albina Khakimova et al., « Optimal energy management of a small-size building via hybrid model predictive control », *in*: *Energy and Buildings* 140 (Apr. 2017), pp. 1–8.

[Kis+18] Nishant Kishore et al., « Mortality in Puerto Rico after Hurricane Maria », *in*: *New England Journal of Medicine* 379.*2* (July 2018), pp. 162–170, DOI: 10.1056/nejmsa1803972.

[KLS17] Przemyslaw Komarnicki, Pio Lombardi, and Zbigniew Styczynski, *Electric Energy Storage Systems*, Springer Berlin Heidelberg, 2017.

[Lam12] Mohamed Yacine Lamoudi, « Distributed model predictive control for energy management in buildings », Theses, Université de Grenoble, Nov. 2012, URL: https://tel.archives-ouvertes.fr/tel-00793614.

[LEC13] Liangfeng Lao, Matthew Ellis, and Panagiotis D. Christofides, « Economic Model Predictive Control of Transport-Reaction Processes », *in*: *Industrial & Engineering Chemistry Research* 53.*18* (June 2013), pp. 7382–7396.

[LG17] Francesco Liberati and Alessandro Di Giorgio, « Economic Model Predictive and Feedback Control of a Smart Grid Prosumer Node », *in*: *Energies* 11.*1* (Dec. 2017), p. 48.

[Luc+14] Sergio Lucia et al., « Handling uncertainty in economic nonlinear model predictive control: A comparative case study », *in*: *Journal of Process Control* 24.*8* (2014), Economic nonlinear model predictive control, pp. 1247–1259, ISSN: 0959-1524.

[LW14] Xiwang Li and Jin Wen, « Review of building energy modeling for control and operation », *in*: *Renewable and Sustainable Energy Reviews* 37 (Sept. 2014), pp. 517–537.

[Mal+17] Naresh Malla et al., « Resilience of Electrical Power Delivery System in Response to Natural Disasters », *in*: *7th International Conference on Power Systems (ICPS)* (2017).

[Mar+17] Mousa Marzband et al., « Optimal energy management system based on stochastic approach for a home Microgrid with integrated responsive load demand and energy storage », *in*: *Sustainable Cities and Society* 28 (Jan. 2017), pp. 256–264.

[May+00] D.Q. Mayne et al., « Constrained model predictive control: Stability and optimality », *in*: *Automatica* 36.*6* (June 2000), pp. 789–814.

[NCW19] H. A. Nasir, A. Care, and E. Weyer, « A Scenario-Based Stochastic MPC Approach for Problems With Normal and Rare Operations With an Application to Rivers », *in*: *IEEE Transactions on Control Systems Technology* 27.*4* (2019), pp. 1397–1410.

[Nog15] V. D. Noghin, « Linear scalarization in multi-criterion optimization », *in*: *Scientific and Technical Information Processing* 42.*6* (Dec. 2015), pp. 463–469.

[Pac+18] François Pacaud et al., « Stochastic optimal control of a domestic microgrid equipped with solar panel and battery », *in*: (Jan. 2018).

[Pap88] M. Papageorgiou, « Certainty equivalent open-loop feedback control applied to multireservoir networks », *in*: *IEEE Transactions on Automatic Control* 33.*4* (1988), pp. 392–399.

[Par+15] A. Parisio et al., « An MPC-based Energy Management System for multiple residential microgrids », *in*: *2015 IEEE International Conference on Automation Science and Engineering (CASE)*, 2015, pp. 7–14.

[PP91] M. V. F. Pereira and L. M. V. G. Pinto, « Multi-stage stochastic optimization applied to energy planning », *in*: *Mathematical Programming* 52.*1* (1991), pp. 359–375.

[Pré70] András Prékopa, « On Probabilistic Constrained Programming », *in*: *Proceedings of the Princeton Symposium on Mathematical Programming*, Princeton University Press, 1970, pp. 113–138.

[Pré95] András Prékopa, *Stochastic Programming*, Springer, Dordrecht, 1995, ISBN: 978-90-481-4552-2.

[Prí+13] Samuel Prívara et al., « Building modeling as a crucial part for building predictive control », *in*: *Energy and Buildings* 56 (Jan. 2013), pp. 8–22.

[Pri+19] Jesse-James Prince Agbodjan et al., « Resilience in energy management system: A study case », *in*: *IFAC-PapersOnLine* 52.*4* (2019), IFAC Workshop on Control of Smart Grid and Renewable Energy Systems CSGRES 2019, pp. 395–400, ISSN: 2405-8963, URL: http://www.sciencedirect.com/science/article/pii/S2405896319305798.

[PVB98] András Prékopa, Béla Vizvári, and Tamás Badics, « Programming Under Probabilistic Constraint with Discrete Random Variable », *in*: *New Trends in Mathematical Programming: Homage to Steven Vajda*, ed. by Franco Giannessi, Sándor Komlósi, and Tamás Rapcsák, Boston, MA: Springer US, 1998, pp. 235–255, ISBN: 978-1-4757-2878-1, DOI: 10.1007/978-1-4757-2878-1_18, URL: https://doi.org/10.1007/978-1-4757-2878-1_18.

[RA09] James B. Rawlings and Rishi Amrit, « Optimizing Process Economic Performance Using Model Predictive Control », *in*: *Nonlinear Model Predictive Control: Towards New Challenging Applications*, ed. by Lalo Magni, Davide Martino Raimondo, and Frank Allgöwer, Berlin, Heidelberg: Springer Berlin Heidelberg, 2009, pp. 119–138, ISBN: 978-3-642-01094-1.

[RAB12] James Rawlings, David Angeli, and Cuyler Bates, « Fundamentals of economic model predictive control », *in*: Dec. 2012, pp. 3851–3861, ISBN: 978-1-4673-2065-8.

[Rak15] Savsa Raković, « Robust Model-Predictive Control », *in*: *Encyclopedia of Systems and Control*, ed. by John Baillieul and Tariq Samad, London: Springer London, 2015, pp. 1225–1233, ISBN: 978-1-4471-5058-9, DOI: 10.1007/978-1-4471-5058-9_2, URL: https://doi.org/10.1007/978-1-4471-5058-9_2.

[Rat+17] Elizabeth L. Ratnam et al., « Residential load and rooftop PV generation: an Australian distribution network dataset », *in*: *International Journal of Sustainable Energy* 36.*8* (2017), pp. 787–806, DOI: 10.1080/14786451.2015.1100196.

[RCA16] Taouba Rhouma, Karim Chabir, and Mohamed Naceur Abdelkrim, « Resilient Control for Networked Control Systems Subject to Cyber/Physical Attacks », *in*: *International Journal of Automation and Computing* (2016).

[Rev15] Jarrett Revels, *BenchmarkTools*, [Online; accessed 17-January-2021], 2015, URL: https://github.com/JuliaCI/BenchmarkTools.jl.

[RH04] Marvin Rausand and Arnljot Hoyland, *System Reliability theory Models, Statistical Methods, and Applications*, Wiley Interscience, 2004.

[RH11] Jakob Rehrl and Martin Horn, « Temperature control for HVAC systems based on exact linearization and model predictive control », *in*: Sept. 2011, pp. 1119–1124.

[Roc+14] R. Roche et al., « A model and strategy to improve smart home energy resilience during outages using vehicle-to-home », *in*: *2014 IEEE International Electric Vehicle Conference (IEVC)*, Dec. 2014, pp. 1–6.

[SB17] Hunyoung Shin and Ross Baldick, « Plug-In Electric Vehicle to Home (V2H) Operation Under a Grid Outage », *in*: *IEEE Transactions on Smart Grid* 8.*4* (July 2017), pp. 2032–2041.

[SE12] J.J. Siirola and T.F. Edgar, « Process energy systems: Control, economic, and sustainability objectives », *in*: *Computers & Chemical Engineering* 47 (Dec. 2012), pp. 134–144.

[SEB16] Omar Santander, Ali Elkamel, and Hector Budman, « Economic model predictive control of chemical processes with parameter uncertainty », *in*: *Computers & Chemical Engineering* 95 (2016), pp. 10–20, ISSN: 0098-1354, URL: http://www.sciencedirect.com/science/article/pii/S009813541630271X.

[Ser+18] Gianluca Serale et al., « Model Predictive Control (MPC) for Enhancing Building and HVAC System Energy Efficiency: Problem Formulation, Applications and Opportunities », *in*: *Energies* 11.*3* (Mar. 2018), p. 631.

[Soy73] A. L. Soyster, « Technical Note—Convex Programming with Set-Inclusive Constraints and Applications to Inexact Linear Programming », *in*: *Operations Research* 21.*5* (Oct. 1973), pp. 1154–1157, DOI: 10.1287/opre.21.5.1154.

[spe18] IEEE spectrum, *Rebuilding Puerto Rico's Power Grid: The Inside Story*, [Online; accessed 10-January-2021], 2018, URL: https://spectrum.ieee.org/energy/policy/rebuilding-puerto-ricos-power-grid-the-inside-story.

[Szé88] T Széntai, « A computer code for solution of probabilistic-constrained stochastic programming problems », *in*: *Numerical techniques for stochastic optimization* 10.*1* (1988), pp. 229–235.

[The13] Office of the Press Secretary The White House, *US esidential policy directive/PPD-21*, [Online; accessed 10-January-2021], 2013, URL: https://obamawhitehouse.archives.gov/the-press-office/2013/02/12/presidential-policy-directive-critical-infrastructure-security-and-resil.

[TLM14] Tri Tran, K-V. Linga, and Jan M. Maciejowski, « Economic Model Predictive Control - A Review », *in*: *Proceedings of the 31st International Symposium on Automation and Robotics in Construction and Mining (ISARC)*, International Association for Automation and Robotics in Construction (IAARC), July 2014.

[Tut+13] David P. Tuttle et al., « Plug-In Vehicle to Home (V2H) duration and power output capability », *in*: *2013 IEEE Transportation Electrification Conference and Expo (ITEC)*, IEEE, June 2013.

[Wal+14] J. Walsh et al., *Ch. 2: Our Changing Climate. Climate Change Impacts in the United States: The Third National Climate Assessment*, tech. rep., 2014, DOI: 10.7930/j0kw5cxt.

[Wet02] Roger J-B. Wets, « Stochastic Programming Models: Wait-and-See Versus Here-and-Now », *in*: *Decision Making Under Uncertainty*, ed. by Claude

Greengard and Andrzej Ruszczynski, New York, NY: Springer New York, 2002, pp. 1–15, ISBN: 978-1-4684-9256-9.

[Xin17] Elisa Ferrario & Enrico Zio Xing Liu, « Resilience analysis framework for interconnected critical infrastructures », *in*: *ASCE-ASME Journal of Risk and Uncertainty in Engineering Systems Part B: Mechanical Engineering* 3 (2017), pp. 1–10.

[YLD71] Haimes YY, Lasdon LS, and Wismer DA, « On a Bicriterion Formulation of the Problems of Integrated System Identification and System Optimization », *in*: *IEEE Transactions on Systems, Man, and Cybernetics* SMC-1.*3* (1971), pp. 296–297.

[Zha+19] Fangfei Zhang et al., « Resilient Energy Management for Residential Communities under Grid Outages », *in*: *2019 9th International Conference on Power and Energy Systems (ICPES)*, IEEE, Dec. 2019.

[Zha+20] Fangfei Zhang et al., « Hierarchical energy management scheme for residential communities under grid outage event », *in*: *IET Smart Grid* 3.*2* (Apr. 2020), pp. 174–181.

[ZL15] Jing Zeng and Jinfeng Liu, « Economic Model Predictive Control of Wastewater Treatment Processes », *in*: *Industrial & Engineering Chemistry Research* 54.*21* (May 2015), pp. 5710–5721.

DOCTORAT BRETAGNE LOIRE / MATHSTIC

CentraleSupélec

Titre : Conception de contrôleurs résilients pour la gestion d'énergie dans les bâtiments.

Mot clés : Contrôle prédictif ; Système de gestion d'énergie dans les bâtiments ; Optimisation multi objectifs ; Résilience ; Panne de réseau électrique ; Commande prédictive stochastique

Résumé : L'une des conséquences les plus apparentes du réchauffement climatique, est la rapide augmentation de la fréquence et des amplitudes des événements météorologiques extrêmes. Ceux-ci entraînent des pannes de réseau électrique souvent de longue durée. De nos jours, plusieurs fournisseurs d'électricité implémentent des stratégies résilientes afin de fournir un tant soit peu de l'électricité aux consommateurs durant ces périodes de pannes. Cependant, la résilience du réseau ne serait pas suffisante si le système de gestion d'énergie du bâtiment des utilisateurs n'est pas également résilient. Par conséquent, les travaux effectués dans cette thèse se réfèrent à l'intégration de résilience aux pannes du réseau électrique dans le système de gestion de l'énergie des bâtiments. Nous proposons un contrôleur résilient prédictif en cas de pannes déterministes. Lorsque l'information associée à la panne devient incertaine, il en résulte un problème d'optimisation dont certaines contraintes sont stochastiques discrètes. L'une des méthodes de résolution de ces problèmes est la programmation stochastique multi-étapes dont le principal inconvénient est l'explosion combinatoire. Nous proposons une solution pour pallier cet obstacle en reformulant le problème d'optimisation sous-jacent. La méthode proposée est utilisée pour concevoir le contrôleur résilient stochastique, dont les performances sont comparées à celle d'un contrôleur basé sur la programmation stochastique multi étapes.

DOCTORAT BRETAGNE LOIRE / MATHSTIC

CentraleSupélec

Title: Design of resilient controllers for Buildings Energy Management

Keywords: Model predictive control; Building energy management system; Multi objective optimisation; Resilience; Grid power outage; Stochastic model predictive control

Abstract: Extreme weather events linked to climate change are getting worse while becoming more frequent worldwide. One of their consequence is the loss of electricity supply for long-lasting periods. Nowadays, many electricity providers often implement resilience in their network in case of these blackouts to provide the customers with electricity at least partially until the network is completely repaired. However, the network resilience would not be sufficient if the user's building energy management system is not itself resilient. Therefore, the work we present in this thesis is to implement resilience to grid power outages, an example of an extreme event in building energy management system. We proposed the resilient controller based on the predictive control framework in case of deterministic grid power outages. When the outage information becomes uncertain, it leads to solving an optimisation problem with discrete stochastic constraints. One way to solve this problem is the multi-stage stochastic programming which main drawback is the combinatorial explosion. We propose a solution that avoids this inconvenience by reformulating the underlying optimisation problem. The proposed method is utilised to design the stochastic resilient controller, which performances we compare to a multi stage stochastic based controller